

# Decentralized congestion control for reliable vehicular communication

**Citation for published version (APA):**

Belagal Math, C. (2019). *Decentralized congestion control for reliable vehicular communication*. [Phd Thesis 1 (Research TU/e / Graduation TU/e), Electrical Engineering]. Technische Universiteit Eindhoven.

**Document status and date:**

Published: 25/02/2019

**Document Version:**

Publisher's PDF, also known as Version of Record (includes final page, issue and volume numbers)

**Please check the document version of this publication:**

- A submitted manuscript is the version of the article upon submission and before peer-review. There can be important differences between the submitted version and the official published version of record. People interested in the research are advised to contact the author for the final version of the publication, or visit the DOI to the publisher's website.
- The final author version and the galley proof are versions of the publication after peer review.
- The final published version features the final layout of the paper including the volume, issue and page numbers.

[Link to publication](#)

**General rights**

Copyright and moral rights for the publications made accessible in the public portal are retained by the authors and/or other copyright owners and it is a condition of accessing publications that users recognise and abide by the legal requirements associated with these rights.

- Users may download and print one copy of any publication from the public portal for the purpose of private study or research.
- You may not further distribute the material or use it for any profit-making activity or commercial gain
- You may freely distribute the URL identifying the publication in the public portal.

If the publication is distributed under the terms of Article 25fa of the Dutch Copyright Act, indicated by the "Taverne" license above, please follow below link for the End User Agreement:

[www.tue.nl/taverne](http://www.tue.nl/taverne)

**Take down policy**

If you believe that this document breaches copyright please contact us at:

[openaccess@tue.nl](mailto:openaccess@tue.nl)

providing details and we will investigate your claim.

# Decentralized Congestion Control for Reliable Vehicular Communication

PROEFSCHRIFT

ter verkrijging van de graad van doctor aan de  
Technische Universiteit Eindhoven, op gezag van de  
rector magnificus, prof.dr.ir. F.P.T. Baaijens, voor een  
commissie aangewezen door het College voor  
Promoties in het openbaar te verdedigen  
op maandag 25 februari 2019 om 16.00 uur

door

Chetan Belagal Math

geboren te Karnataka, India

Dit proefschrift is goedgekeurd door de promotoren en de samenstelling van de promotiecommissie is als volgt:

Voorzitter: prof.dr.ir. J. H. Blom  
Promotor: prof.dr.ir. S. M. Heemstra de Groot  
Co-promotor: dr.ir. H. Li  
                  prof.dr.ir. I. G. M. M. Niemegeers  
Leden: prof.dr. R. Lo Cigno (University of Trento)  
          prof.dr.ir. G. Heijenk (Universiteit Twente)  
          prof.dr.ir. T. Basten  
          dr.ir. J. Hoebeke (Ghent University)

Het onderzoek of ontwerp dat in dit proefschrift wordt beschreven is uitgevoerd in overeenstemming met de TU/e Gedragscode Wetenschapsbeoefening.

A catalogue record is available from the Eindhoven University of Technology Library.

ISBN: 978-90-386-4703-6

Title: Decentralized Congestion Control for Reliable Vehicular Communication

Author: Chetan Belagal Math

Eindhoven University of Technology, 2019.

Copyright © 2019 Chetan Belagal Math, Eindhoven, the Netherlands

All rights reserved. No part of this publication may be reproduced or transmitted in any form or by any means, electronic, mechanical, including photocopy, recording, or any information storage and retrieval system, without the prior written permission of the copyright owner.

Typeset using L<sup>A</sup>T<sub>E</sub>X, printed in The Netherlands.





“Mistake increases your experience & experience decreases your mistakes. if you learn from your mistakes then others learn from your success.”

by A.P.J. Abdul Kalam



## Summary

Vehicular communication enables various safety applications aimed at reducing road hazard situations, enhancing traffic efficiency, road capacity, improving individual driving comfort, and expanding the boundaries of ADAS (Advanced Driver Assistance Systems) and automation systems. IEEE 802.11p, a WiFi (Wireless Fidelity) standard adapted for the highly dynamic vehicular environment, is a basis for such vehicular communication, which is known as DSRC (Dedicated Short-Range Communication) and ITS-G5 (Intelligent Transportation System- 5 GHz) in the US and Europe respectively. The US NHTSA (National Highway Traffic Safety Administration) reports that vehicular communication may avoid up to 82% of the crashes, preventing tens of thousands of fatalities every year.

Safety applications rely on the periodic broadcasting of beacon messages on a control channel by all traffic participants to inform their environment, and, foresee and avoid hazardous situations. Thus, the performance of these safety applications directly depends on the performance of this broadcasting. Examples of safety applications are forward collision warning, lane change warning and intersection collision warning.

The density of IEEE 802.11p devices (nodes) sharing the channel depends on the road topology and changes over time due to changing traffic. The introduction of new IEEE 802.11p devices by vulnerable road users such as pedestrians and cyclists will further increase the node density. As the node density increases the channel load also increases. This may cause channel congestion, leading to a degradation of the communication performance, e.g., messages get lost, thus, decreasing the effectiveness of the safety applications.

DSRC and ITS-G5 are designed to function without any infrastructure. They require a Decentralized Congestion Control (DCC) to regulate the channel load. In a DCC, each node independently estimates the congestion level and adjusts one or more parameters such as message-rate, data-rate, transmit power or carrier sensing threshold. However, changing these parameters may affect the effectiveness of the application performance, e.g., lowering the message rate beyond a particular

value may jeopardize the timeliness of the information broadcast by a vehicle to its neighbors.

In this dissertation, we focus on ensuring reliable safety application performance at high node densities, by means of DCC algorithms. The capacity of the control channel, in terms of the number of beacon messages from different vehicles it can handle, is the major challenge for DCC algorithms at high node densities. One way to increase the channel capacity is to increase the data-rate at which beacon messages are sent. This is what is done by data-rate DCC algorithms.

We analyze the effect of the communication parameters, message-rate, data-rate, transmission power and carrier sensing threshold, on the application performance. We specifically identify the restrictions imposed on these parameters for having an acceptable performance of the safety applications.

We formulate the design goals and requirements of DCC algorithms. After a state-of-the-art analysis, we propose a data-rate DCC algorithm, PDR-DCC. Simulation studies show that PDR-DCC performs better than other DCC algorithms for a wide range of application requirements and densities. However, the maximum node density at which the control channel becomes congested is similar to other DCC algorithms.

To create a DCC which is also scalable to large node densities, we propose a combined message-rate and data-rate DCC algorithm, MD-DCC. Simulation studies show that MD-DCC leads to superior application performance with respect to other DCC algorithms for various application requirements and densities. As intended, MD-DCC supports higher node densities than other DCC algorithms. Specifically, it supports at least a 2.7 times higher node density than the standards-recommended message-rate algorithm, LIMERIC, and a 10 times higher density than the pure data-rate, PDR-DCC.

We implemented MD-DCC on a limited IEEE 802.11p testbed. Through emulations, we demonstrate that MD-DCC avoids congestion at higher node densities than LIMERIC and PDR-DCC.

New DCC algorithms such as MD-DCC should coexist with the already deployed algorithms. Through simulations, we quantify the effect of the coexistence of MD-DCC with the message-rate DCC algorithm, LIMERIC, for different mixes. The results show that there is no significant degradation of the application performance when MD-DCC coexists with LIMERIC.

Finally, we point out the remaining issues to be addressed before the deployment of MD-DCC and PDR-DCC should take place, as well as interesting research directions we foresee based on our studies.

# Contents

Summary .....	vii
1. Introduction .....	1
1.1. Connected vehicles .....	2
1.2. Challenges .....	5
1.3. Congestion control algorithms .....	7
1.4. Research questions to be addressed .....	8
1.5. Research methods .....	8
1.6. Main contribution and outline of the thesis .....	9
1.7. List of publications .....	11
2. Key technical aspects of DSRC and ITS-G5 .....	15
2.1. Introduction .....	15
2.2. State of standardization .....	15
2.2.1. Spectrum allocation .....	15
2.2.2. Safety application messages .....	16
2.2.3. Protocol stack .....	17
2.2.4. IEEE 802.11p .....	19
2.3. Connected vehicles activities in US and Europe .....	21
2.3.1. US .....	22
2.3.2. Europe .....	23
2.4. Summary .....	24
3. Safety application communication and application reliability .....	25
3.1. Introduction .....	25
3.2. Safety application requirements .....	27
3.2.1. Positioning accuracy .....	28
3.2.2. Timeliness of information updates .....	29
3.3. Application reliability .....	29
3.4. Application reliability assessment .....	30
3.4.1. Inter reception time .....	31
3.4.2. T-window application reliability .....	31

3.5.	Relation between communication and application reliability .....	32
3.6.	Communication parameter requirements of safety applications.....	35
3.6.1.	Minimum application reliability.....	35
3.6.2.	Awareness range.....	35
3.7.	Conclusion.....	36
4.	Decentralized congestion control for vehicular communications.....	37
4.1.	Introduction.....	37
4.2.	Effect of DCC tuning parameters .....	38
4.2.1.	Channel load.....	38
4.2.2.	Application performance.....	40
4.3.	Design goals of DCC algorithms .....	40
4.4.	Metrics to assess DCC performance.....	41
4.5.	Overview of proposed DCC algorithms.....	44
4.5.1.	DCC proposed by academics.....	44
4.5.2.	DCC in standardization .....	47
4.6.	Conclusion.....	48
5.	Data-rate adaptation for congestion control .....	49
5.1.	Introduction.....	49
5.2.	Effects of data-rate on channel capacity and application performance	50
5.2.1.	Channel capacity.....	50
5.2.2.	Application performance.....	52
5.3.	Packet count based data-rate DCC.....	52
5.3.1.	PDR-DCC algorithm.....	52
5.3.2.	Packet count .....	53
5.3.3.	Evaluation of DCC design goals .....	54
5.4.	Performance evaluation .....	55
5.4.1.	Simulation setup .....	55
5.4.2.	Channel load observations .....	59
5.4.3.	Fairness observations.....	61
5.4.4.	Application performance observations.....	63
5.5.	Conclusion.....	66
6.	Combined message-rate and data-rate decentralized congestion control ..	67
6.1.	Introduction.....	67
6.2.	Combined message-rate and data-rate DCC.....	68
6.2.1.	MD-DCC algorithm.....	68
6.2.2.	Modification for stability .....	70

---

6.2.3.	Evaluation of DCC design goals .....	71
6.3.	MD-DCC parameter selection.....	71
6.4.	Analytical performance evaluation .....	72
6.5.	Simulation performance evaluation .....	76
6.5.1.	Simulation setup .....	76
6.5.2.	Channel load observations.....	78
6.5.3.	Fairness observations .....	82
6.5.4.	Application performance observations.....	86
6.6.	Conclusion.....	90
7.	Coexistence of MD-DCC with LIMERIC .....	91
7.1.	Introduction .....	91
7.2.	Coexistence performance evaluation.....	92
7.2.1.	Simulation setup .....	92
7.2.2.	Channel load observations.....	93
7.2.3.	Fairness observations .....	97
7.2.4.	Application performance observations.....	101
7.3.	Conclusion.....	103
8.	Experimental evaluation of MD-DCC .....	105
8.1.	Introduction .....	105
8.2.	Emulation platform.....	105
8.2.1.	DCC implementation in MK5 .....	106
8.2.2.	Shortcomings of the present emulation platform .....	108
8.3.	Experimental evaluations .....	111
8.3.1.	Emulation setup.....	111
8.3.2.	Congestion point .....	113
8.3.3.	Fairness of MD-DCC .....	115
8.3.4.	MD-DCC adaptation to abrupt changes in vehicle density .....	117
8.3.5.	Effect of dynamic density changes on the coexistence of MD-DCC and LIMERIC.....	119
8.4.	Conclusion.....	121
9.	Conclusion and future work.....	123
9.1.	Conclusion.....	123
9.2.	Future work .....	126
Appendix A	Stability analysis of MD-DCC.....	129
Appendix B	Description of DCC algorithms.....	133



B.1. LIMERIC .....	133
B.2. DR-DCC .....	134
B.3. SUPRA .....	134
B.4. SAE-DCC .....	135
B.4.1. Basic packet generation .....	136
B.4.2. Packet generation based on vehicle dynamics .....	137
Appendix C C-ITS simulation platform .....	139
C.1. Network simulator .....	139
C.1.1. Congestion control implementation in ns-3 .....	139
C.2. Traffic simulator .....	140
C.3. C-ITS simulator .....	141
Bibliography .....	143
Abbreviations .....	153
Acknowledgment .....	157
Curriculum vitae .....	159

## CHAPTER 1

# Introduction

Every year, road traffic accidents kill about 1.3 million people worldwide, and severely injure another 50 million [1]. Nearly 33,000 [2] and 27,000 [3, 4] deaths happen every year due to road traffic accidents in US and Europe respectively. There were around 3500 road fatalities in Germany in 2015 [5]. The estimated economic loss due to road traffic accidents for the Netherlands and Germany is over 12 and 43 billion euros every year respectively [6].

Human error is the major cause of traffic accidents. In Europe, 95% of all traffic accidents involve human errors [7]. Furthermore, with increasing road traffic worldwide the challenges that a driver faces are growing considerably. Thus, driving requires a high level of concentration and quick reactions.

Advanced Driver Assistance Systems (ADAS) have been developed, to alleviate the burden on drivers and improve driving safety. ADAS makes the driver aware of potentially hazardous situations in the environment and instruct the driver to take corrective actions. In some cases, corrective actions are taken automatically, i.e., without any assistance from the driver. These are known as automation systems.

The self-driving car is one obvious example of automation systems. Self-driving cars are envisioned in the near future [8]. A self-driving car is a vehicle that is capable of sensing its environment and driving without human input. Sensing can be performed using on-board sensors such as radars, cameras, and LiDARs [9]. Connected vehicles can also sense their surrounding environment by exchanging information, such as position and velocity, between various traffic participants such as vehicles and pedestrians, using wireless communication. Connected vehicles enhance the reliability of self-driving cars by providing beyond-line-of-sight information of the surrounding environment, which is not possible with on-board sensors alone. The US National Highway Traffic Safety Administration (NHTSA) has reported that connected vehicles can improve the reliability of ADAS and automation systems and may potentially avoid up to 82% of crash scenarios, preventing tens of thousands of fatalities every year [10, 11]. In this thesis, we focus on connected vehicles.

Connected vehicles exchange information, such as the position, speed, heading direction and acceleration, among neighbors to create a dynamic map of the surrounding environment. Safety applications rely on the dynamic map to foresee and avoid hazardous situations. This dynamic map should, as much as possible, reflect the real-time traffic changes around the vehicle. To achieve this we need reliable exchange of information through a wireless channel. In this thesis, we focus on ensuring reliable exchange of information.

In the rest of this chapter, we provide a general introduction of connected vehicles. Following this, in this thesis we discuss the challenges that concern us, formulate the research questions and discuss the research methods followed to address them in this thesis. Lastly, we present the contributions, outline of the thesis and list of publications obtained during this Ph.D.

### 1.1. Connected vehicles

Connected vehicles exchange information among e-neighbors to support various safety and traffic efficiency applications. E-neighbors of a vehicle refer to the vehicles, infrastructure and pedestrians that can communicate with the vehicle using wireless communication. Safety and traffic efficiency applications such as intersection collision warning, lane change warning, forward collision warning and speed limit advisory are illustrated in Figure 1.1. For instance, the intersection collision warning application relies on information exchange between vehicles to warn the driver about approaching vehicles at an intersection even when they cannot see each other. Connected vehicles use Vehicle-to-Everything (V2X) communication to exchange information. V2X communication which includes Vehicle-to-Vehicle (V2V), Vehicle-to-Infrastructure (V2I) and Infrastructure-to-Vehicle (I2V) communication are the key components of the connected vehicles. Furthermore, information is exchanged between vehicles and various receivers such as Vehicle-to-Device (V2D), and Vehicle-to-vulnerable road users such as pedestrians, bicycles and motorbikes [12, 13].

ADAS and self-driving cars can use the surrounding connected vehicles to sense the environment. On-board sensors [9] have a limited operating range and require a line-of-sight to detect objects. The operating range of camera, radar and LiDAR sensors are shown in Figure 1.2. Connected vehicles add the following benefits to systems that only rely on sensors:

- Connected vehicles provide an extended field of perception, beyond line-of-sight, and hence, allow the detection of threats invisible to on-board sensors.

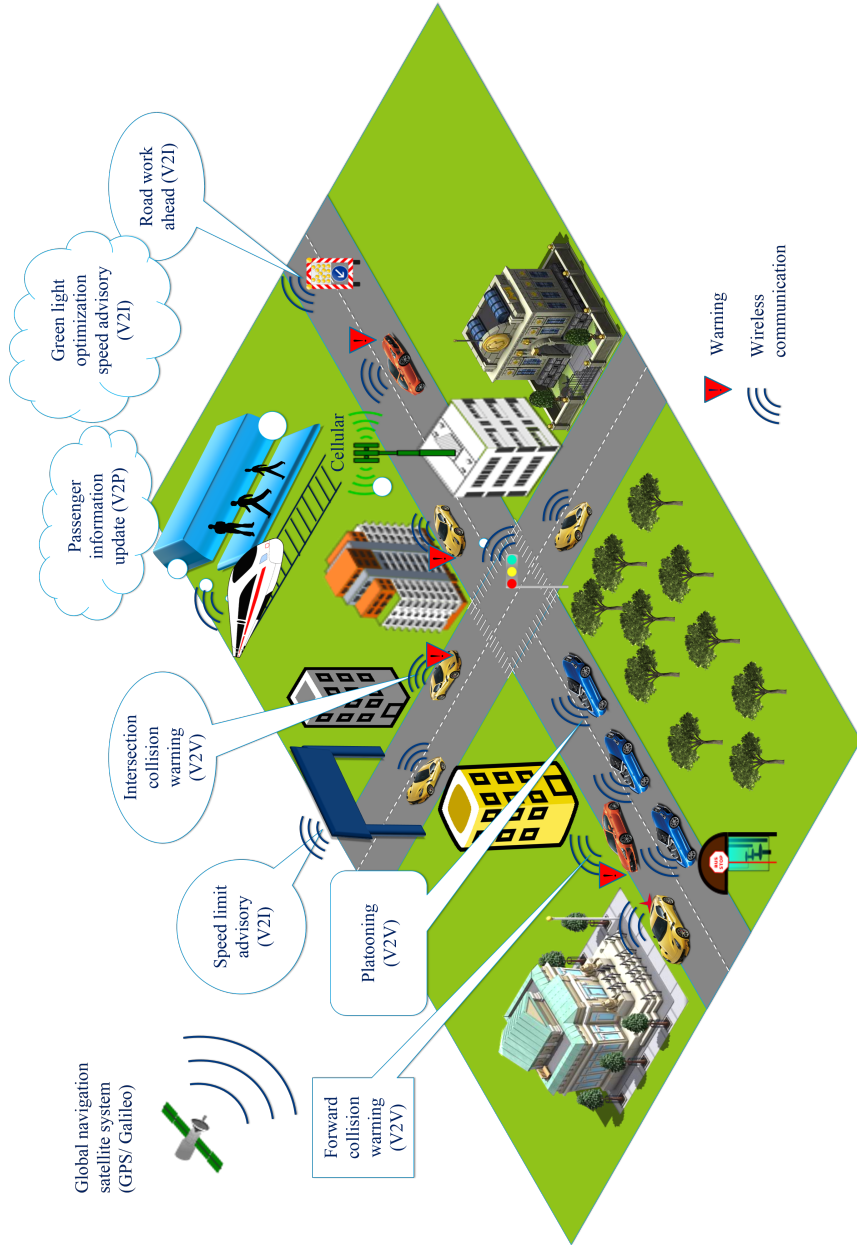
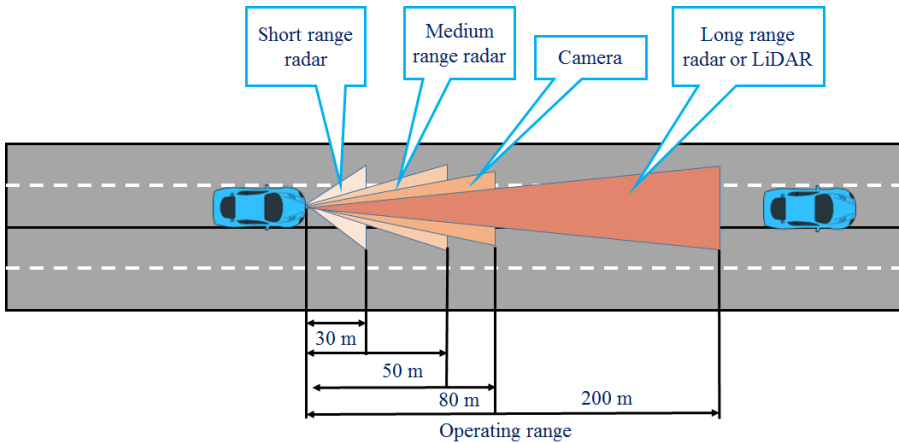


Figure 1.1 – Overview of connected vehicle applications [14]

- Connected vehicles provide important information to each other such as position, speed, heading, acceleration, and deceleration, which are usually more accurate and reliable than those remotely measured by sensors.
- Connected vehicles can take cooperative decisions to reduce the severity of the maneuvers required by each vehicle to avoid a collision.

The additional information and redundancy provided by connected vehicles result in better accuracy and reliability of ADAS and self-driving cars.



**Figure 1.2** – Sensor operation range and line-of-sight detection [9]

Currently, LTE (Long Term Evolution) and WiFi (Wireless Fidelity) are enablers of the connected vehicle technology. Cellular based LTE-V2X was standardized by the 3GPP (3<sup>rd</sup> Generation Partnership Project) in 2016 under the umbrella of LTE release 14 [15]. WiFi based IEEE 802.11p was standardized by the IEEE in 2009 [16]. IEEE 802.11p is more mature than LTE-V2X as IEEE 802.11p has been the subject of extensive standardization, product development and field trials [11, 17–20]. Hence, in this thesis, we limit ourselves to IEEE 802.11p based architectures.

IEEE 802.11p based connected vehicle technology is known as DSRC (Dedicated Short-Range Communication) in the US and ITS-G5 (Intelligent Transportation System - 5 GHz) in Europe. IEEE 802.11p specifies the physical (PHY) and medium access control (MAC) layer of DSRC and ITS-G5 systems. The PHY layer of IEEE 802.11p is inherited from IEEE 802.11a [21]. IEEE 802.11p utilizes the carrier sense multiple access with collision avoidance (CSMA/CA) scheme, similar to those of other IEEE 802.11 family protocols [22].

Both DSRC and ITS-G5 standards have defined beacon messages, which each connected vehicle is mandatory to broadcast periodically to all neighbors. Safety applications rely on beacon messages to track and predict dangerous situations, so that each connected vehicle can react accordingly in time to assure safety. Typical beacon message based safety applications such as forward collision warning and intersection collision warning are shown in Figure 1.1.

## 1.2. Challenges

A number of challenges need to be addressed for reliable V2X communication. The challenges include:

### **The effects of unreliable communication on application reliability**

Safety applications track the neighbor vehicles to predict and avoid dangerous situations. Thus, they require timely updates of information from the neighbor vehicles. To track a neighbor reliably a particular safety application requires the reception of at least  $N$  messages within a tolerance period of  $T$  seconds [23]. These requirements have to be satisfied by the underlying IEEE 802.11p based communication system. Thus, the safety application reliability is heavily dependent on the performance of the underlying communication system. However, it is not clear yet how and to what extent communication parameters such as message-rate, data-rate, transmit power or carrier sensing threshold, affect the application reliability. This we intend to clarify in this thesis.

### **Limited channel capacity**

A fixed 10 MHz bandwidth of the channel limits the channel capacity, in terms of the number of beacon messages from different vehicles it can handle. CSMA/CA imposes further channel capacity limitation. CSMA/CA uses channel sensing and a backoff procedure to avoid beacon message collisions. However, as the channel load increases beyond a specific value congestion occurs, i.e., the incidence of beacon message collisions becomes too high, degrading application reliability significantly [11, 24]. Therefore, one needs to avoid congestion by keeping the channel load below a threshold. However, channel load increases as vehicular density increases. Since the vehicular density is beyond our control, the challenge is how to ensure that at high vehicular densities the channel load stays below a target value.

### **Dynamic vehicular environment**

The mobility of vehicles leads to time-varying shadowing, changing number of vehicles and different road topology. Relative motion between neighbor vehicles and roadside structures will yield to Doppler spread and increases multipath fading of the channel. These time-varying characteristics of the vehicular environment are much more dynamic than for a quasi-static indoor environment and are a major challenge as they significantly impact the application reliability.

### **Broadcast transmission**

Vehicles broadcast beacon messages to their neighbors to notify their presence. Timely beacon messages from neighbor vehicles are necessary for the reliable application. Broadcast transmissions do not receive any acknowledgments, thus, there is no direct possibility to guarantee successful delivery of beacon messages. Furthermore, the probability of beacon message delivery to a neighbor decreases as the distance between the vehicle and the neighbor increases. The challenge for the vehicle is to reliably deliver its current state information to all its neighbors within a defined range and within a specific time frame using the same beacon message.

### **Hidden nodes**

The sensing range of a vehicle is defined as the range around a vehicle within which the vehicle senses the channel busy if other vehicles in the range transmit the message. Vehicles sense each other message transmissions to avoid message collisions. Hidden nodes of a vehicle (node) are vehicles that do not sense each other message transmissions but they can sense the transmissions of the vehicle. Hidden nodes may lead to message collisions, as they cannot sense each other's transmissions. The hidden node problem is common in carrier sensing mechanism based wireless networks. Capture effect can reduce the hidden node problem in V2X communication [25].

Capture effect occurs when two vehicles transmit a message that overlaps at a specific receiver vehicle. Capture effect is a phenomenon where the receiver can capture the stronger of the two messages during simultaneous message transmissions. However, the behavior of capture effect is vendor specific and depends mostly on the arrival time difference between the messages [25]. We do not consider the capture effect in our thesis. The challenge is to minimize the beacon message collisions due to hidden nodes [26].

In this thesis, we address the above mentioned challenges as they predominantly hamper the application performance. We do this by means of congestion control algorithms.

### 1.3. Congestion control algorithms

Safety applications rely on the exchange of information through a wireless channel. Due to the mobility of vehicles, the vehicular density changes over time and road topology. Typically, the vehicles transmit using default communication parameters, such as 10 Hz message-rate, which do not change with vehicle density. Thus, the channel load increases as the vehicle density increases. This may cause channel congestion, and lead to a degradation of the application reliability. Note that congestion in this thesis refers to congestion of the communication channel.

Congestion control algorithms tune one or more communication parameters such as message-rate, data-rate, transmit power or carrier sensing threshold to control channel load and avoid channel congestion. However, changing these parameters may have an effect on the effectiveness of the application performance, e.g., lowering the message-rate beyond a certain value may jeopardize the timeliness of the information broadcast by a vehicle to its neighbors.

Congestion control algorithms can be implemented in a centralized or decentralized way. DSRC and ITS-G5 are designed to function without any centralized infrastructure. So Decentralized Congestion Control (DCC) is mandatory in DSRC and ITS-G5. In DCC, each vehicle independently adjusts one or more communication parameters.

DCC algorithms should be fair. Fairness in this context means that all vehicles sharing the channel should be entitled to the same channel use time. Channel use time is defined as the amount of time occupied by a vehicle for beacon message transmission over a one second period. Note that vehicles may have different applications with different requirements. Some (more important) applications have higher priority than others. This implies that fairness is not always desirable. However, at this moment, the applications and their requirements are not standardized yet. Therefore we assume that the applications running in all the vehicles are equally important, and the channel use time allocation should be fair.

Existing DCC algorithms in literature are designed only to control channel load; the effect of DCC algorithms on application performance has not been sufficiently considered [27–43]. In this thesis, we focus on designing DCC algorithms that avoid congestion in a fair manner with satisfactory application performance.



The channel capacity is limited, in terms of the maximum number of beacon messages supported by the channel. Channel capacity is a major challenge at high vehicular densities. One way to increase the channel capacity is to increase the data-rate at which beacon messages are sent. This is what is done by data-rate DCC algorithms. However, the effect of data-rate DCC on application performance and maximum supported vehicular densities should be further studied.

New DCC algorithms should coexist with the already deployed algorithms. However, the coexistence may lead to unfair channel use time for DCC algorithms leading to degradation of the application performance [44, 45]. Thus, the effect of coexistence of DCC algorithms on application performance needs to be further studied.

#### 1.4. Research questions to be addressed

Optimizing the usage of the channel so that safety applications are sustained even at large vehicular densities, is crucial. The objective of this thesis is to ensure reliable safety application performance at high vehicular densities by means of DCC algorithms. Specifically, data-rate adaptation techniques are explored to make DCC algorithms scalable to high vehicular densities. The specific questions we address in this thesis are the following:

- R1:** To what extent communication parameters influence application performance?
- R2:** To what extent various DCC algorithms influence application performance?
- R3:** To what extent does the data-rate DCC improve the application performance compared to DCC algorithms reported in the literature?
- R4:** Can a combined message-rate and data-rate DCC support larger vehicular densities with reliable application performance than DCC algorithms reported in the literature?
- R5:** To what extent coexistence of new DCC algorithms with the already deployed DCCs affects the application performance?
- R6:** Can we experimentally validate the theoretical results of DCC algorithms?

#### 1.5. Research methods

In this section, we discuss the research methods followed to address the above-mentioned research questions. The effect of the communication parameters and DCC algorithms on the application performance is investigated initially using analytical models. The inferences from the analysis are then used to

design a data-rate DCC algorithm and a combined message-rate and data-rate DCC algorithm. To evaluate and compare the performance and coexistence of the proposed DCC algorithms for high vehicular densities, we have mainly used simulations. An experimental study on real roads could not have been practical and too expensive since it would require a very large number of On-Board Units (OBUs), the hardware communication and processing units that each car in the future will eventually be equipped with. For our simulations we use a combination of network and traffic simulators. The network simulator ns-3 [46] is used to simulate V2X communications. The traffic simulator SUMO [47] is used to simulate realistic road traffic scenarios. Furthermore, an experimental evaluation of the proposed DCC algorithms was performed using a small number of commercial off-the-shelf IEEE 802.11p OBUs [48] to validate our simulation results, under specific laboratory conditions.

### 1.6. Main contribution and outline of the thesis

In this section, we give an overview of the remainder of this thesis and discuss the contributions of the individual chapters. The organization of this thesis and research questions tackled by each chapter is shown in Figure 1.3.

**Chapter 2** provides the technical details of the spectrum allocation, the protocol stack and discusses the state of the research and highlights key activities of DSRC and ITS-G5.

**Chapter 3** quantifies the effect of the communication parameters, message-rate, data-rate, transmission power and carrier sensing threshold, on the application performance. It discusses ways to measure application performance, which reflects the effect of unreliable wireless communication on the reliability of the application. We specifically identify the restrictions imposed on the above mentioned communication parameters for having an acceptable performance of the safety applications.

**Chapter 4** conducts a review of decentralized congestion control mechanisms proposed in the literature as well as those advocated in standardization bodies. Based on the conclusions of this review, we formulate the design goals and requirements of improved DCC algorithms.

**Chapter 5** proposes a data-rate based decentralized congestion control algorithm (PDR-DCC) to improve application performance than reported DCC algorithms. To avoid congestion PDR-DCC increases the data-rate as density increases. PDR-DCC adapts data-rate based on a packet count to assure fairness. We discuss various implementation aspects of the algorithm. Simulation

studies show that PDR-DCC has better application performance than other DCC algorithms for a wide range of applications and vehicle densities.

**Chapter 6** proposes a combined message-rate and data-rate DCC, MD-DCC, which is scalable to very large vehicular densities. MD-DCC adapts message-rate and data-rate based on the application requirements to support the reliable functioning of safety applications. We discuss various implementation aspects of MD-DCC and its adaptation to the application requirements. Through simulations, we show that MD-DCC can support application reliably for much higher vehicular densities than reported DCC algorithms.

**Chapter 7** quantifies the effect of coexistence of MD-DCC with LIMERIC on safety application performance. New DCC algorithms such as MD-DCC should coexist with already deployed algorithms such as ETSI proposed LIMERIC. Thus, through simulations, we quantify the effect of the coexistence of MD-DCC with LIMERIC. The results show that there is no significant degradation of the application performance when MD-DCC coexists with LIMERIC. Furthermore, coexistence with MD-DCC can improve the application performance of LIMERIC.

**Chapter 8** presents experimental analysis of MD-DCC. We implement MD-DCC on industry-proven IEEE 802.11p OBUs [48]. Using a small number of OBUs, we perform emulations to evaluate coexistence of MD-DCC with LIMERIC and fairness performance of MD-DCC. In addition, we analyze the effect of dynamic vehicular density changes on MD-DCC. Furthermore, our results have shown that MD-DCC indeed supports higher vehicular densities than LIMERIC and PDR-DCC.

**Chapter 9** draws conclusions from our work and presents future research topics that ought to be solved for making V2X based safety applications reliable at high vehicular densities.

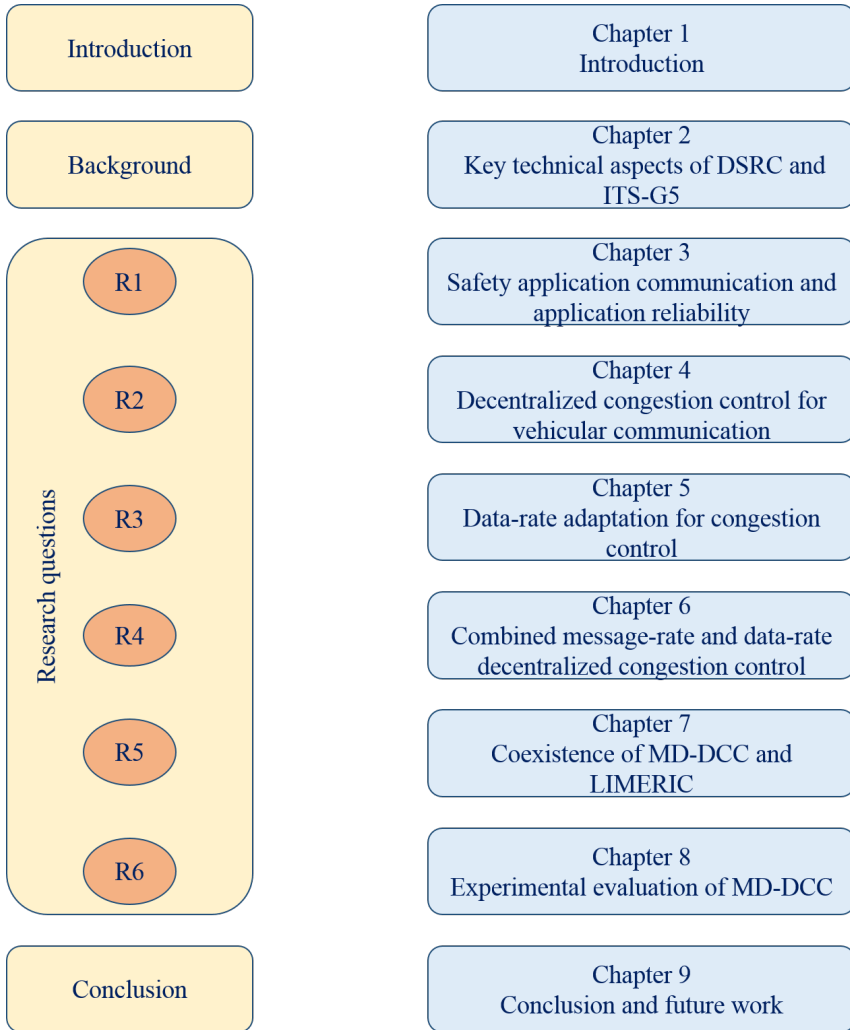


Figure 1.3 – Organization of the thesis

### 1.7. List of publications

The research that led to this Ph.D. thesis has generated several publications in peer-reviewed scientific journals, proceedings of international conferences, and patents. Table 1.1 shows which chapters led to which publications. A complete list of publications is provided below.

#### Journal and conference publications

- (1) **C. Belagal Math**, H. Li, L. F. Abanto-Leon, Sonia M. Heemstra de Groot, and Ignas Niemegeers, “Coexistence of Decentralized Congestion

- Control Algorithms for V2V Communication,” *2018 IEEE 87th Vehicular Technology Conference (VTC Spring)*, Porto, 2018, pp. 1-6.
- (2) Y. Wei, **C. Belagal Math**, H. Li and Sonia M. Heemstra de Groot, “SAE-DCC Evaluation and Comparison with Message Rate and Data Rate Based Congestion Control Algorithms of V2X Communication,” *2018 IEEE 87th Vehicular Technology Conference (VTC Spring)*, Porto, 2018, pp. 1-7.
- (3) L. F. Abanto-Leon, A. Koppelaar, **C. Belagal Math**, Sonia M. Heemstra de Groot “Impact of Quantized Side Information on Subchannel Scheduling for Cellular V2X,” *2018 IEEE 87th Vehicular Technology Conference (VTC Spring)*, Porto, 2018, pp. 1-5.
- (4) A. Ibrahim, **C. Belagal Math**, D. Goswami, T. Basten and H. Li, “Co-simulation Framework of Control, Communication and Traffic for Vehicle Platoons,” *21st Euromicro Conference on Digital System Design (DSD)*, Prague, 2018, pp. 352-356.
- (5) A. Choudhury, T. Maszczyk, **C. Belagal Math**, H. Li, J. Dauwels, “Analysis of the benefits of GLOSA through comprehensive simulations,” *IEEE Transaction of Intelligent Transportation System* (submitted).
- (6) **C. Belagal Math**, H. Li, Sonia M. Heemstra de Groot, and Ignas Niemegeers, “A combined fair decentralized message-rate and data-rate congestion control for V2V communication,” *2017 IEEE Vehicular Networking Conference (VNC)*, Torino, 2017, pp. 271-278.
- (7) **C. Belagal Math**, H. Li, Sonia M. Heemstra de Groot, and Ignas Niemegeers, “V2X Application-Reliability Analysis of Data-Rate and Message-Rate Congestion Control Algorithms,” *IEEE Communications Letters*, vol. 21, no. 6, pp. 1285-1288, June 2017.
- (8) **C. Belagal Math**, H. Li, Sonia M. Heemstra de Groot, and Ignas Niemegeers, “Fair decentralized data-rate congestion control for V2V communications,” *2017 24th International Conference on Telecommunications (ICT)*, Limassol, 2017, pp. 1-7.
- (9) A. Saxena, Hong Li, D. Goswami and **C. Belagal Math**, “Design and analysis of control strategies for vehicle platooning,” *2016 IEEE 19th International Conference on Intelligent Transportation Systems (ITSC)*, Rio de Janeiro, 2016, pp. 1805-1812.
- (10) A. Choudhury, T. Maszczyk, M. T. Asif, N. Mitrovic, **C. Belagal Math**, H. Li, J. Dauwels, “An integrated V2X simulator with applications in vehicle platooning,” *2016 IEEE 19th International Conference on*

- Intelligent Transportation Systems (ITSC)*, Rio de Janeiro, 2016, pp. 1017-1022.
- (11) A. Choudhury, T. Maszczyk, **C. Belagal Math**, H. Li, J. Dauwels, “An Integrated Simulation Environment for Testing V2X Protocols and Applications,” *Procedia Computer Science*, vol. 80, pp. 2042-2052, 2016.
- (12) **C. Belagal Math**, H. Li and Sonia M. Heemstra de Groot, “Risk Assessment for Traffic Safety Applications with V2V Communications,” *2016 IEEE 84th Vehicular Technology Conference (VTC-Fall)*, Montreal, QC, 2016, pp. 1-6.
- (13) G. Pathak, H. Li, **C. Belagal Math** and Sonia M. Heemstra de Groot, “Modelling of Communication Reliability for Platooning Applications for Intelligent Transport System,” *2016 IEEE 84th Vehicular Technology Conference (VTC-Fall)*, Montreal, QC, 2016, pp. 1-6.
- (14) **C. Belagal Math**, H. Li and Sonia M. Heemstra de Groot, “Data Rate based Congestion Control in V2V communication for traffic safety applications,” *2015 IEEE Symposium on Communications and Vehicular Technology in the Benelux (SCVT)*, Luxembourg City, 2015, pp. 1-6.
- (15) D. DebBarma, Q. Wang, **C. Belagal Math**, Ignas Niemegeers and Sonia M. Heemstra de Groot, “Energy efficient Fi-Wi LAN with performance optimization,” *2015 IEEE Symposium on Communications and Vehicular Technology in the Benelux (SCVT)*, Luxembourg City, 2015, pp. 1-6.
- (16) D. DebBarma, Q. Wang, **C. Belagal Math**, Ignas Niemegeers and Sonia M. Heemstra de Groot, “Channel Utilization Based Energy Efficient RoF Centralized Enterprise WLAN,” *2015 IEEE Symposium on Communications and Vehicular Technology in the Benelux (SCVT)*, Luxembourg City, 2015, pp. 1-6.

### Patents

- (17) **C. Belagal Math**, H. Li and Sonia M. Heemstra de Groot, “A combined message-rate and data-rate congestion control,” *US patent office, US82095344*, Feb 2018 (Filed).
- (18) **C. Belagal Math**, H. Li and Sonia M. Heemstra de Groot, “A packet count based channel load measurement,” *US patent office, US82074318*, Feb 2018 (Filed).
- (19) **C. Belagal Math**, H. Li and Sonia M. Heemstra de Groot, “A combined message-rate and data-rate congestion control,” *European Patent Office, EP17203396*, Nov 2017 (Filed).

- (20) **C. Belagal Math**, H. Li and Sonia M. Heemstra de Groot, “A packet count based channel load measurement,” *European Patent Office*, *EP17169091*, May 2017 (Filed).

**Table 1.1** – Publication and Chapter (Chap) relation: ● (Strong relation), ○ (Weak relation)

Publication number	Chap-3	Chap-4	Chap-5	Chap-6	Chap-7	Chap-8
(1)					●	○
(2)				○		
(6)				●	○	○
(7)	○	○	○	○		
(8)			●			○
(12)	●	○				
(14)		○	○	○		
(17)			●			
(18)			●			
(19)			○	●		
(20)			○	●		

## Key technical aspects of DSRC and ITS-G5

### 2.1. Introduction

Connected vehicle technology is also known as Cooperative Intelligent Transportation Systems (C-ITS) [49]. DSRC, ITS-G5 and LTE-V2X technologies are key enablers for C-ITS. This chapter addresses the aspects of DSRC and ITS-G5 systems that are relevant for this thesis. Furthermore, it provides an overview of the research initiatives and activities in this field.

This chapter is organized as follows. Section 2.2 provides a technical introduction to the spectrum allocation, safety application messages, the protocol stack of C-ITS utilized in the US and Europe and details of the IEEE 802.11p PHY and MAC layers. Section 2.3 discusses the key DSRC and ITS-G5 research activities. Finally, Section 2.4 summarizes the key insights presented in this chapter.

### 2.2. State of standardization

#### 2.2.1. Spectrum allocation

The US Federal Communication Commission (FCC) allocated in 1999 a dedicated 75 *MHz* frequency band between 5.850 to 5.925 *GHz* for DSRC. The spectrum is divided into seven 10 *MHz* channels with a 5 *MHz* guard band (GB) at the low end, as illustrated in Figure 2.1. Each channel is designated as either a service channel (SCH) or the control channel (CCH) with specific rules for usage [50, 51]. More specifically, the CCH is reserved for the exchange of safety application messages and announcements of services provided on other channels. The data of non-safety applications will be conveyed on the service channels.

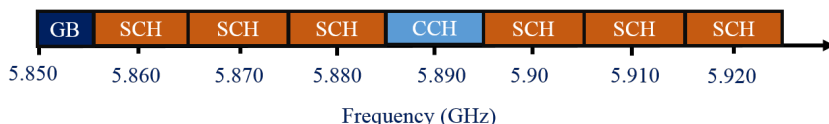
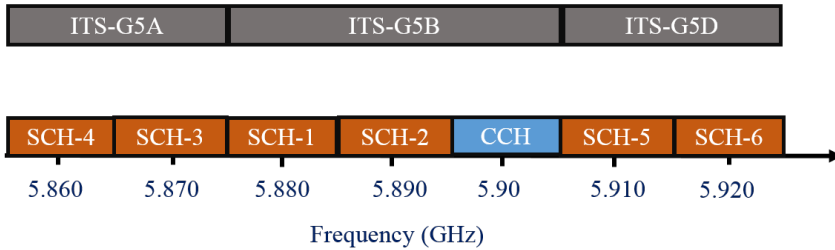


Figure 2.1 – C-ITS spectrum in the US [52]



A slightly different spectrum was allocated for C-ITS in Europe [22]. The spectrum lying between 5.855 *GHz* to 5.925 *GHz* is split into three frequency ranges labeled ITS-G5B, ITS-G5A, and ITS-G5D. Each of them is further divided into one or more 10 *MHz* channels, as shown in Figure 2.2. The channels CCH, SCH1 and SCH2 are dedicated to C-ITS safety applications. Non-safety application communication are confined to SCH3 and SCH4. SCH5 and SCH6 are reserved for future C-ITS applications.



**Figure 2.2** – C-ITS spectrum in Europe [52]

Note that the CCH in Europe centers at 5.9 *GHz*, which is different from the CCH frequency in the US. This incompatibility may lead to interoperability issues. Discussions are underway between the two sides in an attempt to harmonize the bands [53]. The spectrum allocation and standards for DSRC in Singapore are the same as in the US [54]. At the time of writing this thesis, there was no defined spectrum allocated for IEEE 802.11p systems in China, although the Ministry of Industry and Information Technology (MIIT) of China has proposed the 5.905-5.925 *GHz* band for LTE-V2X communication [55].

### 2.2.2. Safety application messages

Safety applications rely on beacon and event-driven messages [56, 57]. Beacon messages are broadcast periodically. The beacon messages include information about the behavior of the vehicles such as the location, speed, heading, and acceleration, which helps to create a dynamic map of the surrounding environment. Beacon messages are referred to as Basic Safety Messages (BSMs) [58] in the US and Cooperative Awareness Messages (CAMs) [59] in Europe. In Europe, event-driven messages, known as Decentralized Environmental Notification Messages (DENMs), are generated in case of an event such as sudden braking, and to convey accident and post-crash information [60]. In the US, similar

event-driven information is appended to a BSM [58]. A list of such events can be found in [61].

### 2.2.3. Protocol stack

#### DSRC

The DSRC technology is composed of a set of standards as shown in Figure 2.3 [14]. At the top of the stack, the SAE (Society of Automotive Engineers) standards

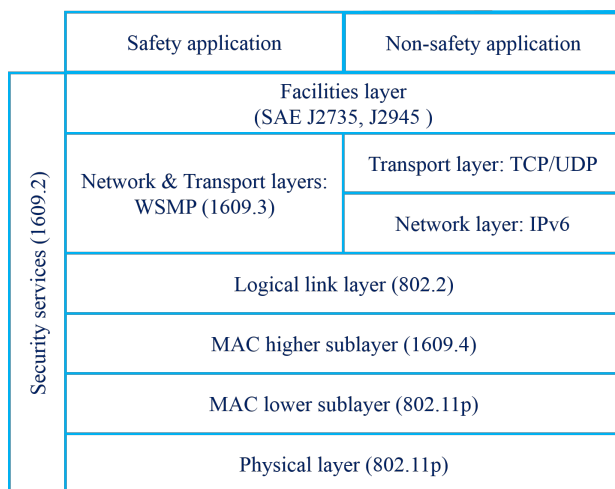


**Figure 2.3** – DSRC protocol stack [14]

SAE J2735 and SAE J2945 are used. SAE J2735 [62] defines numerous message formats considering safety requirements for a wide range of application scenarios. SAE J2945 [63] on the other hand specifies the system requirements of DSRC On-Board Units (OBUs) for V2V communications such as the means to utilize those messages, communication performance requirements, and channel congestion control strategy. The WAVE (Wireless Access for Vehicular Environment), which is defined under IEEE 1609 [64] forms the key part of the DSRC protocol stack. IEEE 1609.2 [65] provides security services for applications and management packets, protecting communications from attacks and protecting user's privacy. IEEE 1609.3 [66] concerns the WAVE Short Message Protocol (WSMP), which provides safety and management message delivery services between DSRC devices. Non-safety messages use Internet protocols for the network and transport layers, such as Internet Protocol version 6 (IPv6), User Datagram Protocol (UDP) and Transmission Control Protocol (TCP). IEEE 1609.4 [67] specifies the channel switching functionality for DSRC devices to alternate between the use of CCH

and SCH. DSRC uses the IEEE 802.2 [68] Logical Link Control (LLC). At the bottom of the stack is the IEEE 802.11p [16] standard for MAC and PHY layers.

### ETSI C-ITS

The protocol stack of C-ITS in Europe is developed by the European Telecommunication Standardization Institute Technical Committee on Intelligent Transport System (ETSI TC ITS) to support C-ITS and is illustrated in Figure 2.4. The specification and requirements of certain safety applications such as Road Hazard Signaling (RHS) [69] and Longitudinal Collision Risk Warning (LCRW) [70] are standardized. The facilities layer standardizes the message format of CAM [59], DENM [60] and other messages. ITS-G5 uses the ETSI GeoNetworking protocol [71] and the Basic Transport Protocol (BTP) at network and transport layer respectively [72]. However, other network protocols, e.g., IPv6, or transport protocols, e.g., UDP or TCP can also be used. The choice of the communication profile, whether GeoNetworking protocol or IPv6, depends on the application. IPv6 packets can also be transmitted over GeoNetworking protocol, for which the adaptation sublayer GN6 [73] has been designed. Security and privacy services are provided by standards such as ETSI TS 102 940 [74, 75] and ETSI TS 102 941 [76] respectively. An architecture to implement various management services such as DCC [36] is also specified. C-ITS in Europe supports various access technologies such as ITS-G5, cellular, and WiMAX.

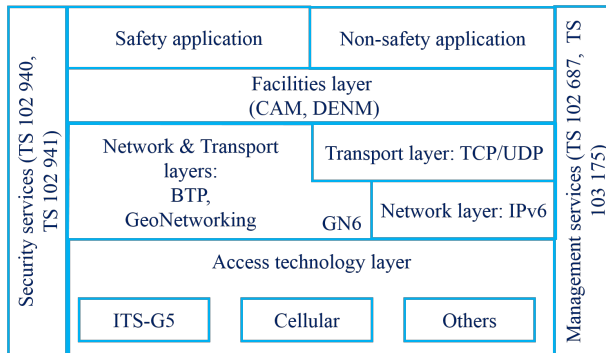


**Figure 2.4** – Protocol stack of C-ITS in Europe [77]

Cellular LTE-V2X was standardized in LTE release 14 [15]. LTE-V2X supports direct V2V communications using mode-3 and mode-4. In mode-3 the scheduling and interference management of V2V communication is performed by a centralized infrastructure (eNodeBs). Mode-4 does not require a centralized

infrastructure similar to IEEE 802.11p systems, and each vehicle selects their radio resources independently using a distributed scheduling schemes.

ITS-G5 is derived from WAVE and adapted to the European requirements. ITS-G5 uses IEEE 802.11p for PHY, MAC and a modification of IEEE 1609.4 for channel switching. There exist many similarities between ITS-G5 and DSRC systems. Both ITS-G5 and DSRC use IEEE 802.11p based MAC and PHY which is discussed in the next section. Other access technologies, such as LTE-V2X and WiMAX are not excluded but are out of the scope of this thesis.

#### 2.2.4. IEEE 802.11p

##### Physical layer

IEEE 802.11p PHY is inherited from IEEE 802.11a [21]. It utilizes an Orthogonal Frequency Division Multiplexing (OFDM) modulation scheme and uses a reduced channel bandwidth of 10 *MHz*, instead of the usual 20 *MHz* used in IEEE 802.11a. Furthermore, parameters such as symbol duration and carrier spacing of 802.11a are modified to compensate the time and frequency selective fading effects in the connected vehicle environment. Table 2.1 compares the physical layer implementations in IEEE 802.11a and IEEE 802.11p [78]. IEEE 802.11p permits dynamic change of transmit power, data-rate, and carrier sensing threshold for each message if it is requested by the upper layers. This feature will be used for the implementation of congestion control.

##### Medium access control layer

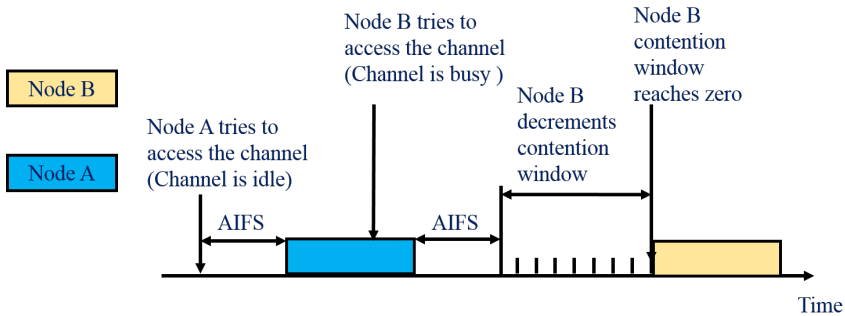
The MAC layer coordinates the access to the channel, which is shared between all the vehicles (nodes). The goal is to minimize message collisions and increase the reception probability of messages. IEEE 802.11p utilizes the CSMA/CA scheme, similar to those for other IEEE 802.11 family protocols.

CSMA/CA uses channel sensing and backoff to avoid simultaneous message transmissions on the channel. The CSMA/CA channel access scheme is shown in Figure 2.5. A vehicle senses the wireless channel before sending a message. The channel is sensed idle if the received signal strength is lower than the carrier sensing threshold. In this case, the sensing MAC entity concludes that there is no message transmission on the channel. In CSMA/CA, each node is listening to the channel, and if it is sensed idle for a predetermined time interval, the so-called Arbitration Inter-Frame Space (AIFS), the node transmits a message. If the channel is sensed busy or becomes busy during the AIFS, the node has to perform a backoff procedure: delay its channel access according to a random time interval.

**Table 2.1** – Comparison of IEEE 802.11p and IEEE 802.11a physical layer [78]

Parameter	IEEE 802.11a	IEEE 802.11p	Changes
Data-rate	6, 9, 12, 18, 24, 36, 48 and 54 <i>Mbps</i>	3, 4.5, 6, 9, 12, 18, 24 and 27 <i>Mbps</i>	Half
Modulation mode	BPSK, QPSK, 16 QAM and 64 QAM	BPSK, QPSK, 16 QAM and 64 QAM	No change
Code rate	1/2, 2/3, and 3/4	1/2, 2/3, and 3/4	No change
Number of subcarriers	52	52	No change
Symbol duration	4 $\mu s$	8 $\mu s$	Double
Guard time	0.8 $\mu s$	1.6 $\mu s$	Double
FFT period	3.2 $\mu s$	6.4 $\mu s$	Double
Preamble duration	16 $\mu s$	32 $\mu s$	Double
Subcarrier spacing	0.3125 <i>MHz</i>	0.15625 <i>MHz</i>	Half

In this case, the node randomly chooses an integer from the uniformly distributed  $[0, CW]$  interval, where  $CW$  is the current size of the contention window. The resultant value is then set as a backoff counter value and will be decremented per slot time ( $13 \mu s$  [22]) after the channel is idle for an AIFS period. The node will be allowed to perform a message transmission immediately after the backoff counter reaches zero, as shown in Figure 2.5.

**Figure 2.5** – Generalized CSMA/CA channel access scheme [52]

In unicast transmissions the MAC adapts the contention window size based on the acknowledgments to decrease the probability of message collisions. The MAC starts with the minimum contention window size ( $CW_{min}$ ), which is increased until it reaches the maximum contention window ( $CW_{max}$ ) size if an acknowledgment for the transmitted message is not received. However, broadcast transmissions do not receive acknowledgments thus the contention window size adaptation is disabled and the maximum contention window ( $CW_{max}$ ) size is used.

IEEE 802.11p categorizes the data traffic based on the priority. It uses the Enhanced Distributed Channel Access (EDCA) functionality originally proposed for IEEE 802.11e [22]. EDCA provides four different priority queues or Access Categories (ACs). The parameters that are controlled by the priority are the contention window size and the AIFS. The higher priority data traffic uses smaller contention window size and AIFS. Hence, less delay, on average, will be experienced by a high priority message to gain access to the wireless medium. Therefore, on average high priority traffic has quicker channel access than the low priority traffic.

The ACs include AC\_VO (voice), AC\_VI (video), AC\_BE (best effort) and AC\_BK (background), where AC\_VO has the highest priority and AC\_BK the lowest priority. The values of CW and AIFS of these ACs are shown in Table 2.2.

The beacon messages (CAM and BSM) utilize the AC\_VI access category. Beacon messages do not receive any acknowledgment, hence a fixed contention window size of 7 [22] is utilized. Event-driven messages (DENM) have higher priority than beacon messages (CAM) as they utilize AC\_VO access category.

**Table 2.2** – AIFS and CW sizes for IEEE 802.11p's access categories [22]

Access category	Minimum contention window size ( $CW_{min}$ )	Maximum contention window size ( $CW_{max}$ )	AIFS ( $\mu s$ )
AC_VO	3	7	58
AC_VI	7	15	71
AC_BE	15	1023	110
AC_BK	15	1023	149

### 2.3. Connected vehicles activities in US and Europe

Currently, a number of DSRC and ITS-G5 research and development projects are going on and more are being planned worldwide. The most significant of

these contributions come primarily from the US and Europe. Cars such as Mercedes-Benz E and S-class [79] and Cadillac CTS [80] are already equipped with IEEE 802.11p based systems.

### 2.3.1. US

The US Department of Transportation (USDOT) and NHTSA have initiated and promoted a vast range of projects.

Already completed-projects such as Vehicle Safety Communication (VSC) [18] and Vehicle Safety Communication-Applications (VSC-A) [11] have made a significant contribution to the connected vehicle technology. The objective of VSC was to investigate the benefits and potential applications enabled or enhanced by the connected vehicle technology. The study resulted in 34 safety and 11 non-safety application scenarios. Among them, eight safety applications were prioritized based on their benefits. Field tests were performed on the prioritized applications, and the proof of concept and capability of DSRC systems were demonstrated by VSC-A. Furthermore, the VSC-A project developed a common communication architecture for safety applications as well as the required protocols and messaging frameworks for achieving the interoperability between different vehicle manufacturers, contributing and validating proposals of SAE [62], IEEE 1609 [64], and IEEE 802.11p [16] standards groups.

The connected vehicle safety pilot [81] project was conducted by the USDOT to analyze the effectiveness of DSRC based technology to reduce accidents. The analysis was performed by equipping around 3000 vehicles with DSRC devices enabling various safety applications such as forward collision warning, lane change warning, emergency electronic brake light warning, and blind spot warning. The safety pilot ran from 2011 to 2013. In 2014, USDOT published a technical report to discuss the readiness of DSRC based technology for deployment [82]. It states that the DSRC technology is ready for deployment and would on an annual basis potentially prevent 25,000 to 592,000 crashes and save 49 to 1,083 lives [82].

USDOT in 2015 initiated a large-scale connected vehicle pilot deployment program [83] to demonstrate the benefits of connected vehicle technology in New York [84], Wyoming [85] and Tampa [86]. The New York deployment is primarily focused on safety applications, which rely on V2V, V2I, and Infrastructure-to-Pedestrian (I2P) communications. These applications provide drivers with alerts so that the driver can take actions to avoid a crash. The New York city plans to install the DSRC devices on approximately 8,000 vehicles and 300 Roadside Units (RSUs) on the streets of Manhattan. Contrary to the city

scenario of New York, Wyoming is investigating the benefits of connected vehicle technology on the I-80 highway. Wyoming plans to deploy 400 DSRC devices on fleet vehicles and 75 RSUs. The primary focus of Tampa is to alleviate traffic congestion and improve safety during morning commuting hours. The projects will be completed in 2019.

### 2.3.2. Europe

In Europe, the European Commission, the European member states and the Car 2 Car Communication Consortium (C2C-CC) are key players that initiate various connected vehicle technology projects. The C2C-CC is a group of C-ITS manufactures, suppliers, universities and research institutes in Europe.

Projects such as PReVENT [87], SAFESPOT [19], and CVIS [20] have proven the feasibility of safety and traffic efficiency applications based on vehicular communication. The DRIVE C2X [88] project performed large-scale field trials. The field trials, involving seven test sites all across Europe proved the safety and efficiency benefits of C-ITS. More than 750 drivers successfully tested eight safety-related applications all over Europe. The evaluation of field trials across Europe verifies the proper functioning of the C-ITS under real-life conditions and proves European-wide interoperability. The user acceptance measurements show that in nine out of ten tests users were enthusiastic about the C-ITS and that they would use it if it was available on their vehicles.

C-Roads [89] platform is a joint initiative of European member states such as the Netherlands, Germany, France, Austria, Belgium, the United Kingdom and road operators for testing and implementing C-ITS services. The project focuses on the current and future C-ITS services, specifically on the definition and implementation of a harmonized communication profile for C-ITS services on road infrastructures all across Europe. Pilot services such as road work-ahead warning, speed-limit advisory, traffic-jam ahead, and green-light-optimization-speed advisory are already implemented in specific regions in Europe [90].

Similar to C-Road, the C-ITS mobility innovation and deployment in Europe (C-MoBILE) [91] project is deploying C-ITS services designed to deal with mobility challenges across Europe. The project aims to help local authorities deploy the C-ITS services they need. The focus of the project is on urban areas. A total of eight C-ITS equipped cities and regions across Europe are involved in the project.

InterCor (Interoperable corridors) [92] is another European project which aims to connect the C-ITS corridor initiatives from various European member states



such as the Netherlands C-ITS Corridor [84] (Netherlands-Germany-Austria), the French corridor defined in the SCOOP project [93], and the United Kingdom and Belgian C-ITS initiatives. The project aims to enable vehicles and related road infrastructure to communicate through cellular, ITS-G5 or a combination of both networks on road corridors running through the Netherlands, Belgium, United Kingdom and France. The overall goal is to achieve safer, more efficient and more convenient mobility of people and goods. The focus of the project is on the highways.

European projects such as CoEXist [94] and Transition areas for infrastructure-assisted driving (TransAID) [95] focus on the smooth coexistence of automated, connected and conventional vehicles.

## 2.4. Summary

In this chapter, we have presented an overview of the key technical aspects of DSRC and ITS-G5. We have discussed the safety application specific messages that are used in Europe (CAM, DENM) and the US (BSM). We observed that US and Europe have allocated spectrum for DSRC and ITS-G5 respectively. Furthermore, we have given the basics of DSRC and ITS-G5 protocol stacks and discussed their IEEE 802.11p based PHY and MAC layers. Finally, we have presented a survey of the related research projects and industrial activities in the US and Europe that aim to investigate different aspects of DSRC and ITS-G5 systems.

# Safety application communication and application reliability

## 3.1. Introduction

Connected vehicles enable various safety applications. In its VSC project, USDOT investigated various safety applications [18]. Among them, the project recommends eight high-potential safety applications that would reduce the vehicular accidents by more than 80% [11]. These are: Traffic Signal Violation Warning (TSVW), Curve Speed Warning (CSW), Emergency Electronic Brake Lights (EEBL), Pre-Crash Warning (PCW), Forward Collision Warning (FCW), Left Turn Assistant (LTA), Lane Change Warning (LCW) and Stop Sign Movement Assistance (SSMA). A brief description of each of these applications is given in Table 3.1. The applications are based on I2V and V2V communications. The reliability of safety applications is heavily dependent on the communication link quality with the neighbors as they rely on beacon message exchange among neighbors to predict accidents.

In this chapter, we discuss the safety applications and their communication requirements. We examine the effect of unreliable wireless communication on the safety application reliability. We further analyze the relation between the communication reliability, i.e., the probability of successfully delivering a message, and application reliability. The analysis is used to present a framework for mapping the application requirements to various communication parameters such as message-rate, data-rate, carrier sensing threshold, and transmit power required to ensure reliable safety applications.

The rest of the chapter is organized as follows. In Section 3.2, we discuss the requirements of the safety applications. Section 3.3 introduces application reliability. Section 3.4 discusses how to assess application reliability. Section 3.5 explores the relation between communication and application reliability. Section 3.6 relates the application reliability requirements to various communication parameters. Finally, Section 3.7 presents conclusions.

Table 3.1 – Safety applications [18]

Application	Communication	Description
Traffic signal violation warning	I2V	Warns the driver to stop if it predicts a stop signal violation.
Curve speed warning	I2V	Application warns the driver if the vehicle speed through the curve exceeds the recommended speed.
Emergency electronic brake lights	V2V	When a vehicle brakes hard its emergency electronic brake lights application warns other vehicles following behind to take appropriate actions to avoid accidents.
Pre-crash sensing	V2V	Pre-crash sensing prepares the driver for imminent, unavoidable collisions by activating passive safety systems.
Forward collision warning	V2V	Application aids the driver in avoiding or mitigating collisions with the rear end of vehicles in the forward path of travel.
Left turn assistant	V2V or I2V	Informs the driver about oncoming traffic to assist him in taking a safe left turn at an intersection.
Lane change warning	V2V	Warns the driver if an intended lane change may cause a crash with a neighbor vehicle.
Stop sign movement assistance	I2V	Application warns the driver about the oncoming traffic to avoid collisions at the stop signs.

V2V= Vehicle-to-Vehicle communication, I2V= Infrastructure-to-Vehicle communication

### 3.2. Safety application requirements

The general principle of V2X safety applications, e.g. V2V applications suggested by the USDOT VSC project as shown in Figure 3.1 [18], is to use the

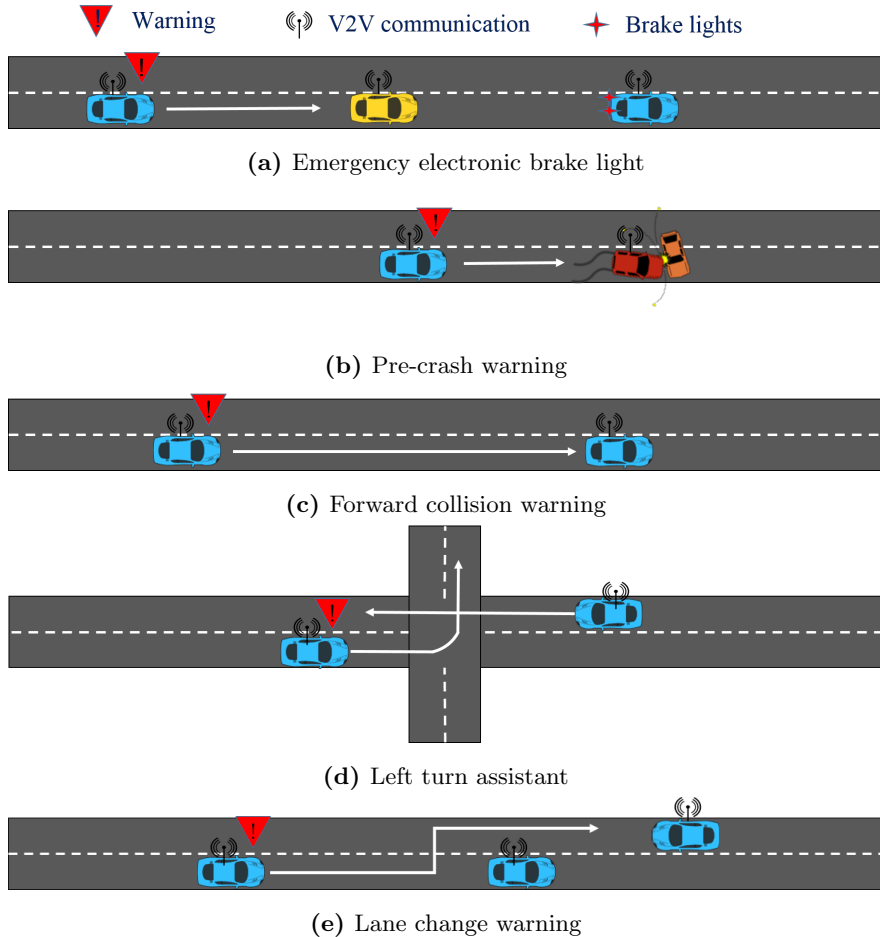


**Figure 3.1** – Vehicle-to-Vehicle safety applications

exchanged information among vehicles to compute a safety metric, in particular the time-to-collision (TTC), to determine what action needs to be taken, e.g., to warn the driver or brake the vehicle. The collision probability increases with the decrease of TTC. According to this, three notification levels are defined: no-warning, awareness warning and automatic pre/post-crash as shown in Figure 3.2. Notifications are not issued for the no-warning level. In the event of triggering awareness warning level, the driver will be notified by graphics or an acoustic warning, or the activation of several LED band segments or other technologies. If

there is no reaction of the driver and TTC continues to decrease leading to the expiration of the awareness warning level time threshold, the notification may be taken over by a direct intervention of the active safety systems such as automatic braking and steering (automatic pre/post-crash level). For example, the awareness warning level should notify the driver 3 s before a plausible collision [96] and the automatic pre/post-crash level should activate safety systems at least 1 s before the impact.



**Figure 3.2** – Notification levels for safety application

Beacon message exchanges should support timely reliable tracking of vehicles and TTC computation. The estimated TTC should issue a reliable notification. The accuracy of TTC mainly depends on the positioning accuracy and timely information updates from the neighbors.

### 3.2.1. Positioning accuracy

The positioning of vehicles is performed using Global Navigation Satellite Systems (GNSS) such as GPS (Global Positioning System) and Galileo. Accurate positioning of the vehicles is necessary for reliable TTC estimation. The VSC-A project [11] by USDOT identified two different levels of GPS accuracy, for different classes of safety applications: road-level and lane-level. Applications such as EEBL require a road-level accuracy of less than 5 m and applications such as FCW require a lane-level accuracy of less than 1.5 m. VSC-A has investigated GPS accuracy and availability at various urban, rural, and highway environments. It concluded that GPS is adequate in most of the environments. Although GPS outage may appear in deep urban environments [11], techniques that estimate the position of a vehicle based on in-vehicle sensors information such as speed and yaw rate can be utilized. Research is ongoing to improve the availability [97–101] and accuracy of GPS [102–108].

### 3.2.2. Timeliness of information updates

For a reliable safety application, certain information update requirements need to be met. These requirements can be formulated as the mandatory reception of at least  $N$  messages within a tolerance period of  $T$  seconds, from each neighbor [23]. Not satisfying information update requirements may result in large errors in TTC estimations. This could lead to false notifications about hazardous situations. The information update requirements vary depending on the application. For example, a FCW application requires a single ( $N = 1$ ) message to be received within one second ( $T = 1$  s) [23]. Similarly, a LCW application requires at least two messages ( $N = 2$ ) within one second ( $T = 1$  s).

The information update requirement of a particular application running in a particular vehicle, i.e., ( $N, T$ ), should be satisfied by all the vehicles within their awareness range. The awareness range of an application for a vehicle is defined as the range within which all vehicles that may constitute a potential hazard for the vehicle are present. Let us consider an FCW application (Figure 3.1c). A vehicle moving at a speed of 125 km/h (35 m/s) with a mean (driver) reaction time of 1.1 s [109] and deceleration (braking) capability of 6.8 m/s<sup>2</sup> [109] requires an awareness range of 125 m to issue an awareness warning [23]. In this case, we assume a worst case scenario where the leading vehicle stops abruptly. Similar requirements hold for the LCW application (Figure 3.1e). If we consider a car moving at 125 km/h (35 m/s) overtaking a car driving at 100 km/h (28 m/s) with a reaction time of 1.1 s, the application has to give a warning at the latest, at a distance (awareness range) of 50 m to avoid a collision [23]. The awareness range thus depends on various factors such as the speed of the vehicles, the reaction time of the driver and the application. Nevertheless, for reliable functioning of the application, all vehicles within the awareness range of the vehicle running the application should satisfy the information update requirements ( $N, T$ ) of the application.

### 3.3. Application reliability

V2X safety application reliability is determined by several subsystems as shown in Figure 3.3. The sensor subsystem gathers sensor information such as position, velocity and acceleration. The communication subsystem transmits its neighbor vehicles sensor information to the application controller using V2X communication. The application controller computes the safety metric such as TTC to decide the necessary actions, which are then performed by the actuator subsystem. In awareness warning phase the warnings are provided to the driver

to decide the necessary actions; however, in automatic pre/post-crash the system decides the necessary actions such as automatic braking, steering and safety system deployment such as air bags.

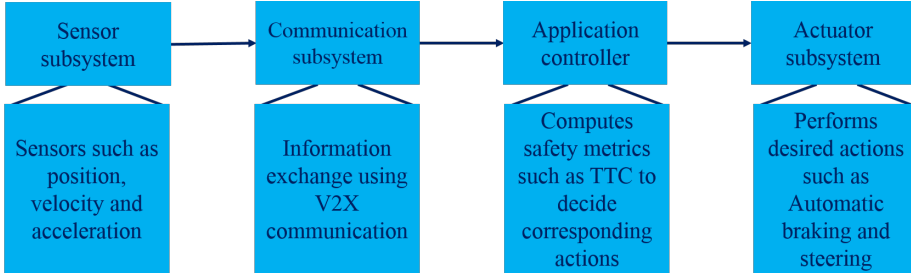


**Figure 3.3** – Function sequence of V2X safety application

The reliability of a system is defined as the probability of the system to perform its required function without failure. The safety application can function reliably only when all the subsystems are reliable. The application reliability is defined as the probability that the safety application performs the necessary function in time to assure safety, e.g., to avoid accidents. In our study, we consider a simple reliability model for V2X safety application. The application reliability  $R_{app}$ , is given by:

$$R_{app} = R_{se} \times R_{com} \times R_{cn} \times R_{au} \quad (3.1)$$

where  $R_{se}$  is the probability of reliable sensor information,  $R_{com}$  is the probability of timely information updates from the neighbors,  $R_{cn}$  is the probability of taking the right decision by the controller,  $R_{au}$  is the probability the actuator performs the desired action. The derivation of  $R_{app}$  is based on the assumption that the  $R_{se}$ ,  $R_{com}$ ,  $R_{cn}$  and  $R_{au}$  are statistically independent.

In this thesis, we focus on the probability of timely information updates from the neighbors  $R_{com}$ . Thus, we assume reliable sensors, application controller and actuators, i.e.,  $R_{se} = 1$ ,  $R_{cn} = 1$  and  $R_{au} = 1$  and  $R_{app}$ , in our study is calculated based on the  $R_{com}$ . Note that the computation of  $R_{se}$ ,  $R_{cn}$  and  $R_{au}$  can be complicated. For instance,  $R_{se}$  is dependent on the reliability of multiple sensors such as velocity and acceleration sensors in such case a more detailed model for  $R_{se}$  may be necessary.

### 3.4. Application reliability assessment

Safety applications information update requirements are to be satisfied by the underlying wireless communication technology. However, the communication

link quality depends on various factors such as the speed of the vehicle, distance, vehicular density, and the characteristics of the wireless channel (e.g., obstacles in line-of-sight and reflecting objects around). Therefore, the effectiveness of safety applications on the vehicle directly depends on the quality of the communication links with the neighbors. Thus, it is vital to define an assessment approach to determine if the link quality is sufficient to support reliable operation of a safety application, which would take both the underlying communication quality and the application requirements of the applications into account. In this section, we discuss ways to assess the application reliability.

The packet reception ratio (PRR) is one of the most commonly used metrics for communication reliability. PRR is defined as the probability of successful delivery of a packet over a link. A link is defined as a sender-receiver pair. Beacon messages are broadcast to all the e-neighbors. Thus all links of a vehicle should receive all the beacon messages broadcast by the vehicle. The PRR of a link is calculated based on this principle. It is calculated as the ratio of the number of packets (messages) received to the number of beacon packets transmitted. The PRR provides the probability of delivering a beacon message over the link but does not capture the timeliness of the information which determines the application reliability.

Suitable and commonly used metrics to assess the application reliability are inter reception time [110] and T-window application reliability [111]. These are discussed below.

#### 3.4.1. Inter reception time

The Inter Reception Time (IRT) between a sending and a receiving vehicle, is defined as the average time between two subsequent successfully received messages [110]. It is a measure of the frequency of information updating of the sending vehicle. The IRT value represents the timeliness of the information. However, the information update requirements ( $N, T$ ) of the application are not considered.

#### 3.4.2. T-window application reliability

The sporadic loss of messages that are periodically broadcast may not be detrimental to the application reliability. The application can still reliably track the vehicles, as long as the information update requirements ( $N, T$ ) of the application are satisfied. This is the rationale for the T-window application reliability  $T_{AR}$  [111].



$T_{AR}$  is defined as the probability of successfully receiving  $N$  messages over a tolerance time  $T$  for a particular application. This probability is determined by the communication reliability or PRR [23] and is expressed as shown below:

$$T_{AR} = \sum_N^k \binom{k}{N} \times p^N \times (1-p)^{k-N} \quad (3.2)$$

where  $p$  is the PRR between sender and receiver, and  $k$  is the number of messages that are sent by the sender in the time window  $T$ . Note that  $k$  and  $N$  are positive integers and  $k \geq N$ .

The message-rate  $R$  of the sender vehicle can be expressed as follows:

$$R = \frac{k}{T} \quad (3.3)$$

From Eq.(3.2) and Eq.(3.3), the  $T_{AR}$  is given by:

$$T_{AR} = \sum_N^{R \times T} \binom{R \times T}{N} \times p^N \times (1-p)^{(R \times T) - N} \quad (3.4)$$

Eq.(3.2) is based on the assumption that message drops are independent. The assumption is further verified through simulations and field trials for various urban and highway scenarios in [112]. In [112, 113] Neighbor Awareness Ratio (NAR) is proposed to measure the application reliability, this is similar to  $T_{AR}$  with  $N = 1$  and  $T = 1$  s information update requirements.

$T_{AR}$  considers both freshness of information and information update requirements of the application. The higher the value of  $T_{AR}$ , the better the accuracy of TTC estimation is. Thus,  $T_{AR}$  is an estimate of the probability that a safety application is supported reliably by the underlying communication system. Therefore, throughout our thesis, we utilize  $T_{AR}$  to quantify the application reliability.

Note that the analysis of  $T_{AR}$  assumes independent message drops. However, there are studies [114] that suggest a correlation between successive beacon message collisions. Furthermore, we assume that the message-rate and PRR are independent which does not hold in all cases. Hence, a more detailed model and experimental analysis of  $T_{AR}$  would be needed to quantify the impact of the assumptions.

### 3.5. Relation between communication and application reliability

From Eq.(3.4), we observe that the information update requirements ( $N$ ,  $T$ ), message-rate, and communication reliability (PRR) influence the application reliability ( $T_{AR}$ ). The PRR varies due to mobility, shadowing, the distance between sender and receiver, and traffic density. The message-rate of vehicles

may change due to congestion control algorithms, and vehicular dynamics such as speed and heading [36]. To get more insights, in this section, we analyze the effect of message-rate and PRR on the application reliability for different information update requirements.

Typically, as long as (at least) one message from the neighbor vehicle is successfully received within a tolerance time window  $T$ , the receiver vehicle should be able to avoid hazard situations reliably. Most of the applications, e.g., FCW, require one message every second ( $N = 1$  and  $T = 1$  s) [23]. However, more demanding applications such as LCW and platooning require more than one message ( $N > 1$ ) in one second ( $T = 1$  s). The LCW application requires two messages every second ( $N = 2$  and  $T = 1$  s) [23].

In this thesis, we analyze the application reliability and awareness range performance of FCW and LCW applications. These applications are selected as they are amongst the high priority applications suggested by the VSC-A [11] project and have varied information update requirements. The analysis can be extended to applications such as platooning which have higher information update requirements than the LCW.

Figure 3.4 and Figure 3.5 show the  $T_{AR}$  of FCW and LCW application respectively. We observe that for a given PRR, the  $T_{AR}$  of LCW and FCW increases as the message-rate increases. For a fixed message-rate and PRR, the  $T_{AR}$  of LCW (Figure 3.5) is lower than FCW (Figure 3.4) as the LCW application has higher information update requirements ( $N = 2$ ) than the FCW application ( $N = 1$ ). From Figure 3.4 and Figure 3.5, we observe that to maintain a fixed  $T_{AR}$  of the application we need to increase the message-rate as the PRR decreases.

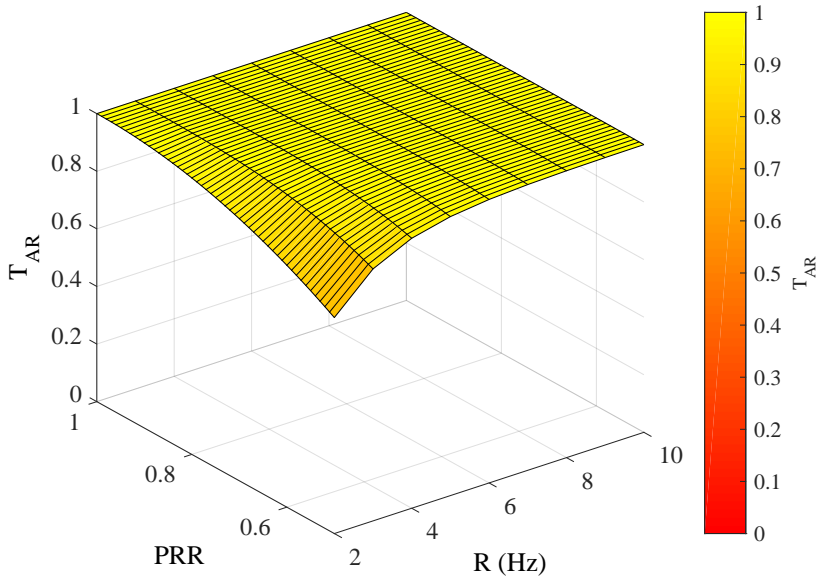


**Figure 3.4** – Application reliability ( $T_{AR}$ ) of the forward collision warning (FCW) application for different packet reception ratios (PRR) and message-rates ( $R$ )

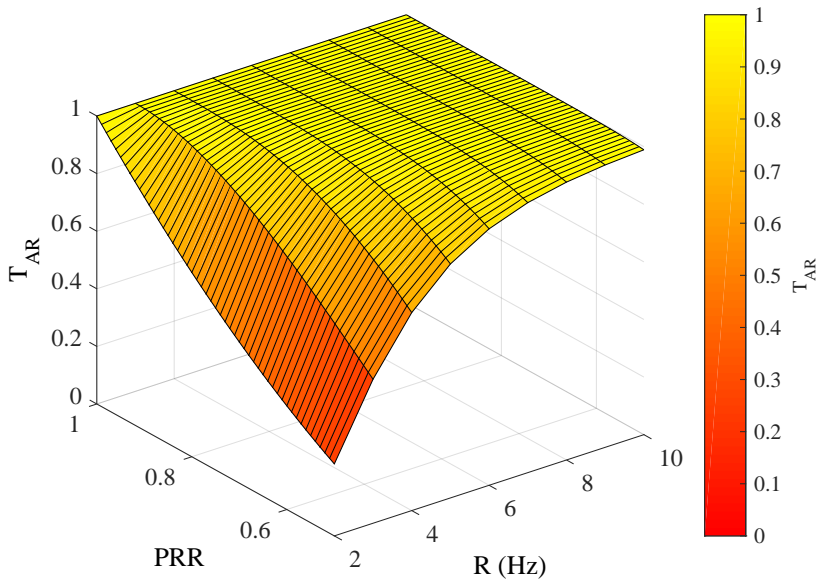


**Figure 3.5** – Application reliability ( $T_{AR}$ ) of the lane change warning (LCW) application for different packet reception ratios (PRR) and message-rates ( $R$ )

### 3.6. Communication parameter requirements of safety applications

The application has requirements on minimum application reliability and awareness range. In this section, we discuss how the reliability and awareness range requirements of the application, should drive the selection of the communication parameters: message-rate, data-rate, transmit power, and carrier sensing threshold.

#### 3.6.1. Minimum application reliability

Application reliability should be greater than or equal to the desired minimum application reliability  $T_{AR_{min}}$ , to ensure reliable tracking of the neighbors. The minimum message-rate  $r_{min}$ , required to maintain application reliability greater than or equal to  $T_{AR_{min}}$  is calculated as shown below:

$$T_{AR_{min}} \geq \sum_N^{r_{min} \times T} \binom{r_{min} \times T}{N} \times p^N \times (1-p)^{(r_{min} \times T) - N} \quad (3.5)$$

where  $r_{min}$  is the least positive integer in the range from 2 to 10 that satisfies the Eq.(3.5), 10 Hz is the maximum message-rate permitted in the standards [22], and 2 Hz is the minimum message-rate for which the equation is valid [112].

The required minimum message-rate  $r_{min}$  should be adapted based on  $p$ ,  $T_{AR_{min}}$  and the information update requirements of the application. For example, let us consider a  $T_{AR_{min}}$  of 0.99 as in [23] and a PRR of 0.7 as in [115]. From Eq.(3.5), the  $r_{min}$  requirements for FCW ( $N = 1$ ,  $T = 1$  s) and LCW ( $N = 2$ ,  $T = 1$  s) application are 4 Hz and 7 Hz respectively.

#### 3.6.2. Awareness range

All vehicles within the awareness range of a particular vehicle should have application reliability greater than or equal to  $T_{AR_{min}}$ . This can be ensured by maintaining a message-rate  $r_{min}$  and the desired packet reception ratio  $p$  for all vehicles within its awareness range (see Eq.(3.5)). However,  $p$  changes with the distance between sender and receiver, shadowing, and scenarios such as urban and rural affecting  $T_{AR}$ . Therefore, the communication parameters, in particular, the transmit power, the carrier sensing threshold, and the data-rate which largely determine the communication range, i.e., the maximum range over which a packet can be transmitted successfully, should be selected such that the PRR experienced by all vehicles within the awareness range is greater than or equal to  $p$ .

From the analysis, we observe that the message-rate influences the reliability of the application. For a given message-rate, transmit power, data-rate, and carrier sensing threshold communication parameters mainly influence the awareness range of the application.

### 3.7. Conclusion

In this chapter, we investigated the requirements of safety applications. We have discussed ways to measure the application reliability, which reflects the effect of unreliable wireless communication on the reliability of the application. The application requirements have been mapped to communication parameter requirements, in particular, the minimum message-rate, and PRR to ensure reliable safety applications. We have shown that increasing the message-rate can increase the application reliability. The analysis of this chapter will be utilized in the forthcoming chapters to design an efficient congestion control algorithm that can guarantee the reliable operation of safety applications.

We presented a preliminary model to analyze the effect of the PRR and message-rate on application reliability. Further analysis of the application reliability considering the mobility of vehicles, channel characteristics and scenarios should be part of a future study.

# Decentralized congestion control for vehicular communications

## 4.1. Introduction

Safety applications rely on beacon and event-driven messages. Beacon messages are transmitted periodically whereas event-driven messages are transmitted when a critical event occurs, which enables various applications such as EEBL and PCS. Messages are broadcast on a 10 *MHz* CCH using the CSMA/CA MAC as discussed in Section 2.2. CSMA/CA uses channel sensing to help avoid message collisions. However, channel sensing cannot prevent message collisions, and they become too high, as the channel load increases above a certain threshold, leading to congestion of the channel. This leads to a severe degradation of the PRR affecting application performance.

CCH should accommodate beacon and event-driven messages. Event-driven messages have higher priority than beacon messages. Due to the unpredictable nature of the events in the vehicular environment, we need to reserve a part of the channel for safety-critical event-driven messages (around 10% [36]).

The study in [116] estimates that with default communication parameters, i.e., 10 *Hz* message-rate, 300 *bytes* beacon size, 6 *Mbps* data-rate and 25 *dBm* transmit power (500 *m* communication range) the channel can at the maximum range support around 200 vehicles. However, there are cases where the number of vehicles is greater than 200 vehicles, e.g., an 8 lane highway scenario with inter-vehicle distance of 20 *m* has approximately 400 vehicles. In such cases, without specific measures congestion will occur and communication will not be possible anymore. Thus, to avoid congestion we need congestion control algorithms.

Congestion control algorithms are proposed to avoid congestion and reserve a part of the channel capacity for event-driven messages. Congestion control algorithms aim to adjust communication parameters of the vehicles that contribute to the channel load, such as the transmit power, message-rate, data-rate, and carrier sensing threshold. However, the choice of these communication parameters may affect the reliable functioning of the applications as discussed in the previous

chapter. Thus, congestion control algorithms should avoid congestion and guarantee the desired application performance.

Congestion control algorithms can be operated in a centralized or decentralized manner. The centralized approach has a single coordinator such as a RSU, which is responsible for regulating the channel load. The coordinator delivers the communication parameters to the other vehicles in its range. Another approach is decentralized congestion control where each vehicle sharing the channel has to adjust its communication parameters individually to avoid congestion. DSRC and ITS-G5 are designed to function without any centralized infrastructure. So Decentralized Congestion Control (DCC) strategies are implemented by ETSI [117] and SAE [58] standardization bodies. However, a decentralized mechanism introduces new challenges such as fairness.

Fairness in this context refers to equal channel use time for all vehicles sharing the channel. Channel use time of a vehicle is defined as the time occupied by the vehicle for beacon message transmissions. Unfair channel use time may lead to degradation of the application performance [94].

The chapter is organized as follows. Section 4.2 discusses the effects of DCC algorithms on the channel load and application performance. In Section 4.3, we discuss the design goals of DCC. Section 4.4 discusses metrics to assess DCC performance. Section 4.5 performs an extensive review of DCC algorithms. Section 4.6 draws the conclusions.

## 4.2. Effect of DCC tuning parameters

DCC algorithms adapt message-rate, data-rate, transmit power, and carrier sensing threshold to avoid congestion. In this section, we analyze the effect of DCC tuning parameters on the channel load and application performance. Note that there are various contention window based DCC algorithms [39,40,118–120]. Tuning the contention window decreases the message collisions and improves the PRR performance at the cost of increased delay but does not affect the channel load. Hence, this aspect is not considered in our study.

### 4.2.1. Channel load

Figure 4.1 compares the channel load of message-rate and data-rate DCC with the case where no congestion control is applied. We denote this as “no-DCC” case. The no-DCC case shows the channel load without any DCC algorithms as seen in Figure 4.1a. Message-rate DCC reduces the channel load by decreasing the number of beacon messages in the channel as seen in Figure 4.1b. Data-rate DCC

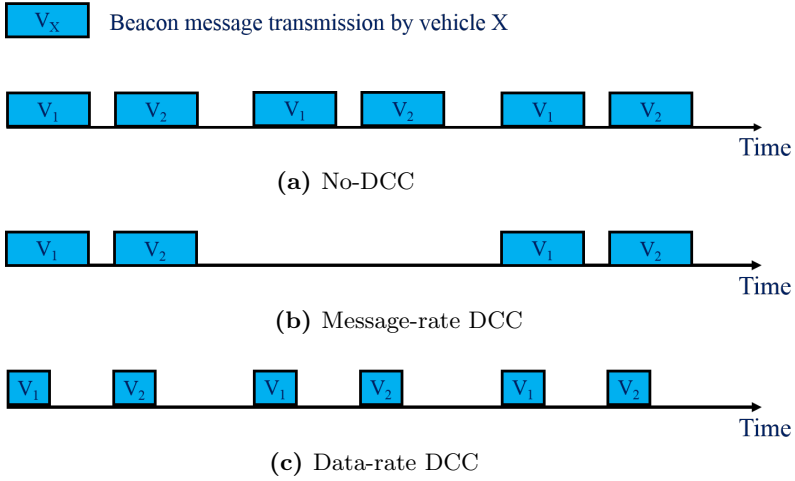


**Figure 4.1** – Channel load comparison for message-rate, data-rate and no-DCC case

reduces the channel load by transmitting messages at higher data-rates than the no-DCC case thus decreasing the transmission time of the beacon messages in the channel as shown in Figure 4.1c.

Transmit power, and carrier sensing threshold DCC tune the transmission range and sensing range of the vehicle respectively to change the number of vehicles sharing the channel, thus, the channel load. The sensing range is defined as the range around a vehicle within which the vehicle senses the channel busy if another vehicle transmits the message. Transmission range is defined as the range around a vehicle within which other vehicles sense the channel busy during its message transmission. However, carrier sensing threshold and transmit power DCC algorithms do not always affect the channel load as it depends on the specific spatial distribution of the neighbor vehicles [121].

To illustrate it let us consider two different scenarios, scenario-1 and scenario-2 as shown in Figure 4.2. Scenario-1 and scenario-2 represent a highway and intersection respectively. The sensing range for carrier sensing threshold DCC or transmission range for transmit power DCC,  $Ra$ , of the centered vehicle is shown by an arrow. In both scenarios, the center vehicle tries to reduce the channel load by decreasing its sensing range or transmission range from  $Ra_1$  to  $Ra_2$ . Reduction of  $Ra$  in scenario-1 reduces the channel load as the number of vehicles in  $Ra_2$  are less than in  $Ra_1$ . However, decreasing the  $Ra$  in scenario-2 did not affect the channel load as the number of vehicles in  $Ra_1$  and  $Ra_2$  remain the same (Figure 4.2b).



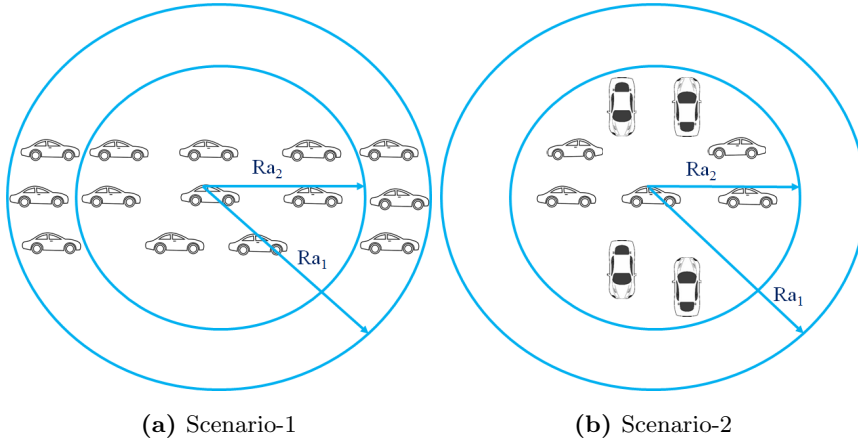


**Figure 4.2** – Tuning of the sensing range or transmission range

Data-rate DCC algorithms transmit beacon messages at shorter transmission time and thus can accommodate more beacon messages for a defined channel load than message-rate, transmit power, and carrier sensing threshold DCC algorithms.

#### 4.2.2. Application performance

Tuning the communication parameters may affect the application reliability and awareness range of the application.

Message-rate based DCC algorithms may decrease the message-rate below the minimum required message-rate to avoid congestion affecting the application reliability.

Transmit power and carrier sensing threshold DCC algorithms limit the transmission and sensing range respectively which may conflict with the awareness range requirements of the application.

Similarly data-rate DCC algorithms limit the communication range [115] which may affect the awareness range requirements of the application.

DCC algorithms should choose the appropriate communication parameters such that they avoid congestion and simultaneously satisfy the minimum application reliability and awareness range requirements of the application.

### 4.3. Design goals of DCC algorithms

Considering the above discussions, we formulate the following design goals for the DCC algorithms.

- Channel load: Maintain the channel load below the threshold to avoid congestion.
- Application performance: DCC algorithms should guarantee the reliable functioning of the application. Applications have requirements on minimum message-rate and awareness range. DCC algorithms should satisfy these application requirements.
- Fairness: Vehicles sharing the channel should have the same channel use time.

In a nutshell, DCC algorithms should avoid congestion in a fair manner and ensure reliable application performance. These design goals should be fulfilled for all application requirements and for different traffic scenarios, such as urban, highway and rural. Furthermore, DCC algorithms should be scalable to high vehicular densities to satisfy the design goals at large vehicular densities. It is important to note that the design goals are not independent, i.e., tuning communication parameters to avoid congestion may degrade application performance.

#### 4.4. Metrics to assess DCC performance

Keeping in view the DCC design goals, in this section we discuss metrics to assess the channel load, application and fairness performances of DCC algorithms. The application performance is quantified using application reliability and awareness range. These metrics are used to analyze and compare the performance of DCC algorithms in this thesis. The metrics measurement and analysis are performed over a defined area known as the observing zone.

##### **Channel load**

Similar to SAE and ETSI standardization bodies, we use Channel Busy Percentage (CBP), which is the percentage of time the channel is sensed busy over a time interval [36, 58]. We measure the average CBP experienced by the vehicles in the observing zone. The average CBP represents the average channel load over the observing zone. These measurements are performed discretely every  $\theta$  s. DCC algorithms should maintain the average CBP experienced in the observing zone below the channel load threshold ( $CBP_T$ ).

##### **Application reliability**

The application reliability is measured using the T-window application reliability  $T_{AR}$  discussed in Section 3.4.2.  $T_{AR}$  is defined as the probability of satisfying the information update requirements ( $N, T$ ) of the application.

A link is defined as a sender-receiver pair.  $T_{AR}$  classifies a link at time instant  $t$  to be reliable or T-window success ( $T_{su}$ ) if it receives at least  $N$  messages in  $[t-T, t]$ . Otherwise, the link at time instant  $t$  is said to be unreliable or T-window failure ( $T_{fu}$ ). Figure 4.3 shows a  $T_{su}$  and  $T_{fu}$  at time instant  $t$  of a link for an application with information update requirements  $N = 1$  and  $T = 1$  s. Checks

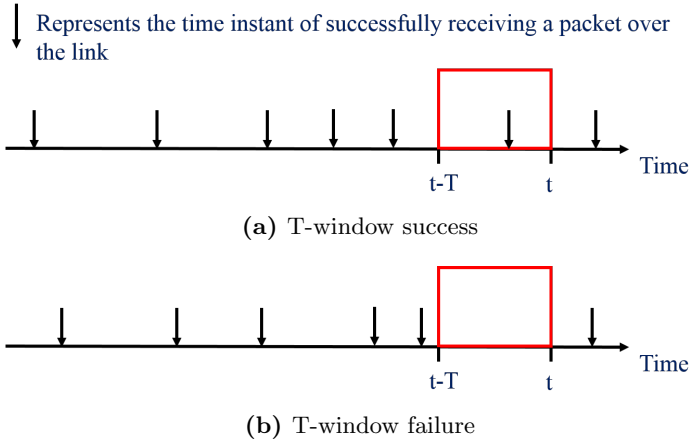


**Figure 4.3** – T-window success and T-window failure representation at time instant  $t$  for  $N = 1$  and  $T = 1$  s application requirements

are made to ascertain whether a link is reliable or not periodically every  $t_o$  s (e.g.,  $t_o$  could be of the order of 200 ms [111]).  $T_{AR}$  of a link is measured as the ratio of the total reliable time instants to the total number of checks performed over a time interval and is expressed as

$$T_{AR} = \frac{l_s}{l_s + l_f} \quad (4.1)$$

where  $l_s$  is the number of  $T_{su}$  observed over a time interval and  $l_f$  is the number of  $T_{fu}$  observed over a time interval.

The application reliability is assessed over the observing zone. The observing zone is one kilometer long and has multiple links. We first calculate  $T_{AR}$  of all links in the observing zone using Eq.(4.1). The links are not stationary and the distance between the sender and receiver changes over time. Therefore, we sort the links in bins based on the distance between the sender-receiver pair, among rings with a width of 25 m around a vehicle. We compute, the average of  $T_{AR}$  for each bin: 0-25, 25-50 m and so on as in [111]. The measured average  $T_{AR}$  over distance is used to assess the application reliability [111].

### Awareness range

Awareness range of an application for a vehicle is defined as the range within which all vehicles that may constitute a potential hazard for the vehicle are present. In our study, the awareness range supported by an application is assessed by measuring the maximum distance up to which the reliability of the application is above the required minimum  $T_{AR_{min}}$ .  $T_{AR}$  assessment over distance is used to find the awareness range performance of the application.

### Fairness

Fairness, for DCC algorithms, means that all vehicles sharing the channel have the same channel use time. This is based on the assumption that all vehicles sharing the channel have the same application requirements. The channel use time  $C_k$  of vehicle  $k$  is given by the equation below:

$$C_k = \sum_{j=1}^S T_{k,D_j} \quad (4.2)$$

where  $T_{k,D_j}$  is the transmission time of the  $j^{\text{th}}$  message transmitted by the vehicle  $k$  at the data-rate  $D_j$ .  $S$  is the number of messages transmitted by the vehicle  $k$  over a time interval.

The fairness evaluations are performed over the observing zone. Due to mobility, vehicles move in and out of the observing zone. Thus, the amount of time each vehicle spends in the observing zone is different.  $C_k$  depends on the time the vehicle stays in the observing zone.

We propose fraction of time spent on beacon transmission  $x$ , a normalized metric over time which is independent of the time a vehicle stays in the observing zone to measure the channel use time.  $x$  is defined as the fraction of time spent by a vehicle for beacon message transmission in the observing zone.  $x_k$  of the vehicle  $k$  is calculated as shown below:

$$x_k = \frac{C_k}{a_k} \quad (4.3)$$

where  $a_k$  is the time spent by the vehicle  $k$  in the observing zone. Fair allocation should ensure that all vehicles have the same  $x$ .

To quantify fairness, we use Jain's fairness index [122] over  $x$  as in [123]. The Jain's fairness index  $J$  of  $M$  vehicles passing through the observing zone during a time interval is given by

$$J = \frac{\left( \sum_{i=1}^M x_i \right)^2}{M \times \sum_{i=1}^M x_i^2} \quad (4.4)$$

Jain's fairness index can vary from  $\frac{1}{M}$  (worst case) to 1 (best case). The best case is when all vehicles spend the same fractional time for beacon message transmissions.

#### 4.5. Overview of proposed DCC algorithms

Several DCC algorithms have been proposed in the literature [27–43, 124–126]. DCC algorithms can tune either a single parameter such as message-rate or multiple parameters such as both message-rate and transmit power.

DCC algorithms from standardization bodies focus on message-rate or/and transmit power DCC algorithms. However, there are DCC algorithms which adapt the data-rate and the carrier sensing threshold in the literature. In this section, we provide an overview of the various DCC algorithms proposed by both academics and standardization bodies.

##### 4.5.1. DCC proposed by academics

The majority of congestion control algorithms adjust the message-rate or/and the transmit power, while a few are based on adapting the data-rate [35, 36] or the carrier sensing threshold [37, 38].

**Message-rate algorithms** adapt the message-rate of the vehicles, i.e., the number of beacon messages transmitted by a vehicle in a second.

A simpler approach to adapt message-rate is to increase or decrease the message-rate in discrete steps based on the comparison between the measured channel load and the channel load threshold. This approach is known as binary message-rate control. In [27], the authors have proposed the Additive Increase Multiplicative Decrease (AIMD) binary message-rate control algorithm. AIMD increases the message-rate by  $Y$  Hz when the channel load is less than the threshold and decreases the message-rate aggressively by  $Z \times Y$  Hz when the channel load is higher than the threshold ( $Z > 1$ ). AIMD may lead to unfair channel use time [127]. To tackle this, [128] has proposed the Periodically Updated Load Sensitive Adaptive Rate control (PULSAR). Local CBP measurements performed by each vehicle individually may not represent the real channel load around, considering the shadowing. Hence, PULSAR uses global channel load information obtained from the channel load information exchange among neighbor vehicles to guarantee fairness for AIMD. However, application requirements are not considered by PULSAR.

In [28], the authors have proposed the Linear Message Rate Integrated Control (LIMERIC). LIMERIC controls the channel load to converge to the desired threshold by adapting the message-rate proportionally to the difference between the threshold and the measured channel load. The authors have further demonstrated the fair allocation of message-rate by LIMERIC [129]. However, application requirements are not considered by LIMERIC.

A game theory based Non-cooperative Beacon Rate and Awareness Control (NORAC), is proposed in [30]. NORAC assigns beacon message-rate to every vehicle proportionally to the minimum message-rate requirement of the application and the measured channel load while ensuring fairness between vehicles with the same application requirements. However, there is no guarantee that the channel load will be maintained below the channel load threshold.

**Transmit power algorithms** limit the transmission range over which a beacon message is broadcast.

In [130, 131], the authors propose transmit power adaptation in discrete steps based on the lookup table and measured channel load. However, the algorithms may experience fairness issues [116].

The Stateful Utilization-based Power Adaptation (SUPRA) [33] algorithm adapts the transmit power based on the difference between the channel load threshold and the measured channel load. The authors prove through theory and simulation that it achieves a fair allocation of transmit power. However, application requirements are not considered.

[31, 32, 41] model the congestion control as an optimization problem, which limits the maximum channel load while maximizing transmit power and assuring fairness. However, the algorithms transmit additional information in their beacon messages, such as the position information of the two-hop neighbor vehicles and the histogram of vehicular density experienced by the vehicle, creating additional channel load.

[34] proposes an adaptation of transmit power based on the PRR experienced by the vehicle. The PRR is computed using the sequence numbers of the received messages. If the average PRR for all sender vehicles is above a certain threshold, the algorithm decides to decrease the transmit power. They increase the transmit power if the PRR is below a threshold. However, no guarantee is provided that the channel load will be maintained below the channel load threshold.

**Combined message-rate and transmit power algorithms** control both message-rate and transmit power simultaneously.

In [43], the authors propose message-rate and transmit power adaptation independently. The message-rate adaptation is based on the estimated tracking error resulting from the difference between the actual position of the vehicle and the position of the vehicle estimated by its neighbor vehicles. The transmission power is adapted based on the channel load similarly to SUPRA. [124] adapts the message-rate based on the PRR and tunes the transmit power based on the channel load and the vehicular density. In [126], the authors model congestion as an optimization problem and formulate two subproblems, one on message-rate control with fixed transmit powers and the other on transmit power control with fixed message-rates and develop a distributed algorithm to solve these two subproblems. These algorithms however, do not consider fairness and application requirements.

The algorithms proposed in [42, 113, 125], perform transmit-power and message-rate adaptation based on the application requirements. These algorithms adapt the message-rate based on the measured channel load, the minimum message-rate requirement of the application and the channel load threshold. In [42] and [125], a simple lookup table based on the communication range is used to assess the required transmit power. In [113], the authors propose to estimate the required transmit power based on the received power and the transmit power information transmitted in the beacon messages the vehicle receives. The exchange of transmit power information creates additional channel load. Each of these algorithms avoids congestion and considers the minimum message-rate and communication range requirements of the application; however, fairness is not assured.

**Carrier sensing threshold algorithms** control the channel load by limiting the sensing range of the vehicle.

The study in [37], indicates that as the carrier sensing threshold increases, the message delay and the channel load are reduced. However, the PRR at a larger distance (greater than 100  $m$ ) is degraded. They further propose a Carrier sensing Threshold Adaptation (CTA) algorithm [38], which adapts the carrier sensing threshold based on the amount of waiting time in the medium access layer. In [132], the authors propose carrier sensing threshold adaptation based on the vehicular density. These algorithms however, do not guarantee a channel load below the channel load threshold.

**Data-rate control algorithms** tune the transmission data-rate of the beacon messages to control the channel load.

In [133], the authors have demonstrated through simulations and experiments that the use of high data-rates have the potential to reduce the channel load without affecting application performance. In [35], the authors propose to increase or decrease the data-rate based on the channel load measurements. However, fairness and application requirements are not considered.

#### 4.5.2. DCC in standardization

Since the standardization of DCC is vital for interoperability and performance, both ETSI (ITS-G5) and SAE (DSRC) are active at specifying DCC algorithms.

##### ITS-G5

In [59], ETSI has proposed CAM message generation based on the vehicular dynamics such as position, speed, and direction of heading. This is also known as Triggering DCC (T-DCC) which adapts the message-rate [36]. A CAM message will be generated when the absolute difference between the current heading and the heading contained in the last CAM becomes greater than  $4^\circ$ , when the distance between the current position and the position in the preceding CAM message exceeds  $4\text{ m}$  or when the absolute difference between the current speed and the last speed exceeds  $0.5\text{ m/s}$ . Whether CAM message is to be transmitted or not will be evaluated every  $100\text{ ms}$  [59]. However, such vehicular dynamics based message-rate algorithms may experience simultaneous beacon generation, e.g., when platoon vehicles adapt velocity at the same time. This leads to increased beacon message collisions as shown in [114].

ETSI [36] has defined a framework for DCC, which can accommodate a variety of parameters to control channel load such as transmit power, message rate, data-rate, and carrier sensing threshold. Among them, ETSI has proposed a simple Reactive DCC (R-DCC) [134], which adapts the message-rate of the vehicles using the lookup table and measured CBP. Furthermore, in [123] ETSI compares the performance of R-DCC, T-DCC, and LIMERIC and it concludes that the application and fairness performance of LIMERIC is better than others.

##### DSRC

SAE has specified a combined message-rate and transmit power based DCC algorithm (SAE-DCC) [58] for DSRC. The message-rate is adjusted based on the vehicular density. The vehicular density is estimated based on the received beacon messages from vehicles within a  $100\text{ m}$  range. The transmit power is adapted based on the measured CBP similarly to SUPRA [33]. Furthermore, additional beacon



messages are generated based on the tracking error similar to [43] as discussed above. A detailed description of SAE-DCC is presented in Appendix B.

#### 4.6. Conclusion

In this chapter, we formulated the design goals of the DCC algorithms and discussed the metrics used to assess these design goals in the rest of the thesis. We summarized the literature review of DCC algorithms by both academics and standardization bodies. From the study, we observed that most DCC algorithms do not consider the effect on application performance and fairness. In this thesis, we intend to design DCC algorithms that avoid congestion in a fair manner and guarantee the reliable functioning of the application. Among the four discussed DCC parameters, data-rate based DCC algorithms are promising as they can increase the number of beacon messages supported by the channel. However, the impact of data-rate adaptation on the application performance is not yet clear. We analyze this further in the forthcoming chapter.

## Data-rate adaptation for congestion control

### 5.1. Introduction

The majority of congestion control algorithms decrease message-rate or transmit power as channel load increases, an alternative approach is to increase the channel capacity by increasing the data-rate. However, increasing data-rate may reduce the awareness range of the application [115]. The analytical study in [121] shows that a data-rate DCC can support larger awareness range than a transmit power DCC. In this chapter, we investigate how a data-rate based congestion control algorithm performs in comparison to other message-rate and transmit power congestion control algorithms.

In this chapter, we propose a Packet-count Data Rate DCC algorithm PDR-DCC, and analyze its performance. Specifically, our contributions are as follows:

- To the best of our knowledge, we are the first to propose a fair data-rate based congestion control algorithm that enforces homogeneous data-rate selection amongst all vehicles.
- We also propose a new technique to measure the channel load using packet count. The packet-count based channel load measurement ensures fair allocation of data-rate.
- We evaluate and compare the proposed algorithm with message-rate and transmit power based DCC algorithms using a simulation environment. The results show that the proposed data-rate DCC algorithm mitigates congestion and provides better application performance compared to message-rate and transmit power DCC, specifically at high vehicular densities and high minimum message-rate application requirements.

The chapter is organized as follows. Section 5.2 discusses the effect of different data-rates on channel capacity and application performance. We explain the PDR-DCC algorithm, and discuss its implementation aspects in Section 5.3. Section 5.4 evaluates and compares the performance of PDR-DCC with other

message-rate, transmit power, and data-rate based congestion control algorithms. We make concluding remarks in Section 5.5.

## 5.2. Effects of data-rate on channel capacity and application performance

For simplicity and to achieve sound performance in normal traffic density, 6 *Mbps* was selected as the default data-rate in both ITS-G5 [22] and DSRC [63]. However, ITS-G5 and DSRC permit 8 different data-rates 3, 4.5, 6, 9, 12, 18, 24, and 27 *Mbps* [22].

### 5.2.1. Channel capacity

Data-rates affect the transmission time of the beacon messages. Apart from payload the beacon message also contains other headers from transport, network, MAC and PHY layers. It should be noted that the PHY layer headers preamble and signal field are always transmitted at fixed 40  $\mu s$  [22] duration irrespective of the data-rate selected. The transmission time of  $L$  bytes  $T_{D,L}$  is given by

$$T_{D,L} = 40\mu s + \frac{8 \times L}{D} \quad (5.1)$$

where  $D$  is the data-rate. Figure 5.1 plots the transmission time (estimated using Eq.(5.1)) for different packet sizes and all the data-rates specified by IEEE 802.11p. Figure 5.1 shows that for a fixed packet size as the data-rate increases transmission time decreases.

The transmission time is a key factor to determine the channel capacity. We measure channel capacity in terms of the maximum number of beacon packets per second that can be supported by the channel. The maximum number of beacon packets ( $P_{max_{D,L}}$ ) that can be transmitted without any beacon packet collisions over one second within the sensing range is given by:

$$P_{max_{D,L}} = \frac{1}{AIFS + T_{D,L}} \quad (5.2)$$

where AIFS is the minimum waiting time between consecutive beacons. Because the beacons are transmitted using the AC\_VI access category, the AIFS in Eq.(5.2) is set to 71  $\mu s$  as specified in the standards [22].

Figure 5.2 shows the maximum number of beacon packets supported by different data-rates and packet sizes. From Figure 5.2, it is evident that for a fixed packet size, data-rates higher than 6 *Mbps* support a higher number of beacon packets than 6 *Mbps*. It can be observed that 27 *Mbps* can support around 1.7 to 4 times more beacon packets than 6 *Mbps*. Note that the maximum number of

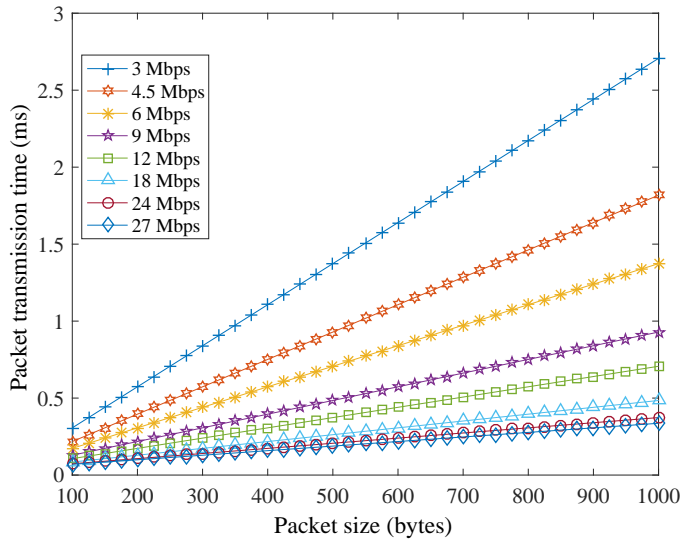


**Figure 5.1** – Packet transmission time as a function of packet size for different data-rates

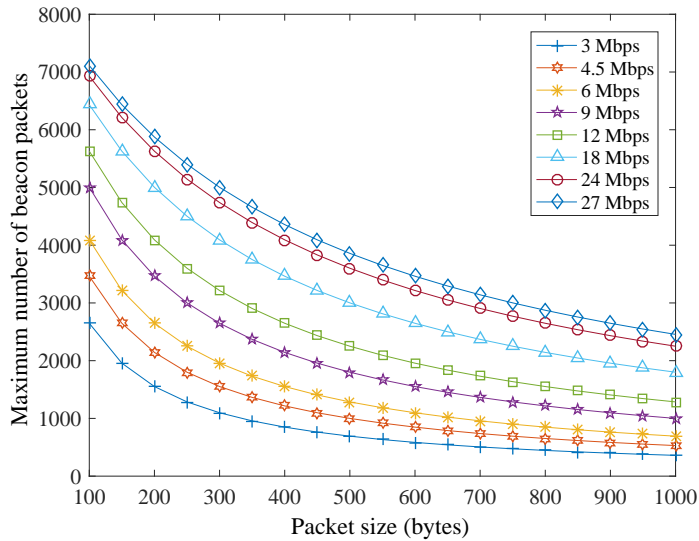


**Figure 5.2** – Maximum number of beacon packets per second in the channel for different data-rates and packet sizes

beacon packets is computed in an ideal scenario without interference and beacon

packet collisions. If more than the maximum number of beacons are transmitted, beacon collisions must happen in the channel.

### 5.2.2. Application performance

Increasing data-rate requires higher Signal-to-Interference-plus-Noise-Ratio (SINR) to correctly decode a received message, as shown in Table 5.1. Hence, for a fixed transmit power the communication range decreases as the data-rate increases, which may affect the awareness range of the application.

**Table 5.1** – IEEE 802.11p data-rates [135]

Data-rate	Modulation	Coding rate	SINR [135]
3 <i>Mbps</i>	BPSK	1/2	5
4.5 <i>Mbps</i>	BPSK	3/4	6
6 <i>Mbps</i>	QPSK	1/2	8
9 <i>Mbps</i>	QPSK	3/4	11
12 <i>Mbps</i>	16-QAM	1/2	15
18 <i>Mbps</i>	16-QAM	3/4	20
24 <i>Mbps</i>	64-QAM	2/3	25
27 <i>Mbps</i>	64-QAM	3/4	30

The study conducted in [115] demonstrates that data-rates with high SINR requirements are sensitive to multipath fading effects. Hence, 24 and 27 *Mbps* are more susceptible to multipath fading than other data-rates and experience drastic variation in PRR [115] even in the near region of 50 *m*. Thus, from all the data-rates that are defined by the standard, in our study we consider only 3, 4.5, 6, 9, 12, and 18 *Mbps* data-rates [115].

### 5.3. Packet count based data-rate DCC

In this section, we explain packet count based data-rate DCC (PDR-DCC) and present implementation details.

#### 5.3.1. PDR-DCC algorithm

PDR-DCC is an adaptive decentralized data-rate congestion control algorithm. When the vehicular density increases, PDR-DCC increases the data-rate. However, increasing data-rate may affect the awareness range of the application.

Thus, PDR-DCC selects the least possible data-rate to avoid congestion and maximize the awareness range of the application.

PDR-DCC adapts the data-rate based on the packet count  $P_C$ , i.e., the total number of packets sensed by the physical layer on the channel over a period of  $\theta$  s. Each vehicle selects a minimum data-rate  $D$ , which satisfies Eq.(5.3) every  $\theta$  s.

$$(P_C \times T_D) \leq (CBP_T \times \theta) \quad (5.3)$$

where  $T_D$  is the packet transmission time for the data-rate  $D$  in seconds,  $CBP_T$  is the channel busy percentage threshold,  $P_C \times T_D$  is the time for transmitting  $P_C$  packets on the channel, and  $CBP_T \times \theta$  is the available transmission time on the channel with a channel load  $CBP_T$ . Thus, satisfying Eq.(5.3) guarantees that the channel load is below the  $CBP_T$ . Furthermore, the selection of the minimum data-rate  $D$  that satisfies Eq.(5.3) maximizes the awareness range.

### 5.3.2. Packet count

In this section, we motivate the advantages of using packet count. We also discuss how the packet count is estimated.

#### Why packet count?

The channel load is generally measured using CBP. For a defined CBP the number of beacon packets supported by the channel is fixed for message-rate or transmit power based congestion control algorithms. However, data-rate congestion algorithms can vary the channel capacity, i.e., the number of packets supported by the channel for a defined CBP. For instance, a CBP of 50% can be due to 775 packets transmitted at 6 *Mbps* or 1324 packets transmitted at 12 *Mbps*. In such cases, the number of packets in the channel provides information of the channel capacity and thus the data-rate necessary to avoid congestion, which is not possible with CBP. Therefore, we propose a packet count based channel load metric which estimates the number of packets on the channel.

#### Packet count estimation

The  $P_C$  is calculated by every vehicle, based on the transmitted, decoded, and sensed packets from the physical layer.

$P_C$  is computed every  $\theta$  s as follows:

$$P_C = P_T + P_R + P_B \quad (5.4)$$

where  $P_T$  and  $P_R$  are the number of packets transmitted and decoded by a vehicle over a period  $\theta$  respectively.  $P_B$  is the number of sensed packets estimated when the physical layer of a vehicle senses that the channel is busy but it is not transmitting or decoding a packet over a period  $\theta$ .

$P_T$  and  $P_R$  are obtained from the physical layer.  $P_B$  is obtained from linear estimation over time,  $T_B$ , as follows:

$$P_B = \frac{((P_T + P_R) \times T_B)}{T_T + T_R} \quad (5.5)$$

where  $T_T$  and  $T_R$  are the time during which the channel is sensed busy due to transmission and decoding of packets respectively over a period  $\theta$ .  $T_B$  is the time during which the channel is busy while not decoding or transmitting over a period  $\theta$ .

$T_T$  and  $T_R$  are obtained from the physical layer.  $T_R$  can also be calculated based on the IEEE 802.11p packets PHY layer headers such as preamble and signal field [22]. The signal field consists of the data-rate and the packet length, which determines the transmission time. This information is used to obtain  $T_R$ .  $T_B$  is calculated based on CBP as

$$T_B = (CBP \times \theta) - (T_T + T_R) \quad (5.6)$$

The  $P_C$  measurement is performed by each vehicle individually. Note that the  $P_C$  estimation presented here is based on the assumption that all packets in the channel are of the same size. However, the idea can be extended to heterogeneous packet sizes.

### 5.3.3. Evaluation of DCC design goals

We address the design goals of the DCC algorithm discussed in Section 4.3 in our proposed PDR-DCC as follows:

- Congestion control: PDR-DCC adapts data-rate to avoid congestion.
- Fairness: PDR-DCC uses packet count based data-rate adaptation to assure fairness.
- Application performance: To satisfy the minimum message-rate and awareness range requirements of the application.
  - Minimum message-rate: PDR-DCC assures that the message-rate is always above the minimum message-rate as it uses a maximum message-rate permitted in the standards (10 Hz).
  - Awareness range: PDR-DCC maximizes the awareness range by selecting the minimum possible data-rate to avoid congestion.

### 5.4. Performance evaluation

In this section, we perform simulations to assess up to which degree the proposed PDR-DCC algorithm meets the design goals. Furthermore, we compare the application performance of PDR-DCC with other message-rate, transmit power and data-rate congestion control algorithms for different applications and vehicular densities.

For message-rate based algorithms, we choose LIMERIC because it is a widely accepted message-rate DCC algorithm, recommended by ETSI report [123]. SUPRA is selected as the representative of the transmit power DCC algorithms because it is implemented by SAE [58]. DR-DCC is selected to represent the data-rate DCC algorithm as it is similar to the data-rate based DCC algorithms proposed in the ETSI standard [36]. All three algorithms function based on the CBP information. Appendix B provides a detailed description of LIMERIC, SUPRA, and DR-DCC.

#### 5.4.1. Simulation setup

The simulations are performed using the network simulator ns-3 [46] combined with the vehicle traffic simulator SUMO [47] as discussed in Appendix C. We consider a realistic highway scenario: a road section of approximately 3 km with 4 lanes in each direction (Figure 5.3). The width of each lane is 3.25 m [136]. When a vehicle reaches the end of the road, it takes a U-turn and enters in the opposite direction. This is done to have control over the vehicular densities we simulate. The length of the vehicles is fixed to 4 m [137]. The velocity of the vehicles ranges from 0 to 40 m/s [138] whereas their acceleration ranges from -2 to 3 m/s<sup>2</sup> [27]. SUMO initializes the position and the velocity of the vehicle randomly. To eliminate the effects of random positioning and velocity of vehicles SUMO simulates the mobility of vehicles for 60 s before providing the mobility of the vehicles to ns-3.

We consider three vehicular densities:

- Density-1: 25 vehicles per lane/km
- Density-2: 50 vehicles per lane/km
- Density-3: 62 vehicles per lane/km

Density-1, density-2, and density-3 represent free flow, medium velocity and slow velocity scenarios corresponding to an average velocity of 27, 17 and 10 m/s respectively. For each density, we simulate four different DCC algorithms LIMERIC, SUPRA, DR-DCC, and PDR-DCC.



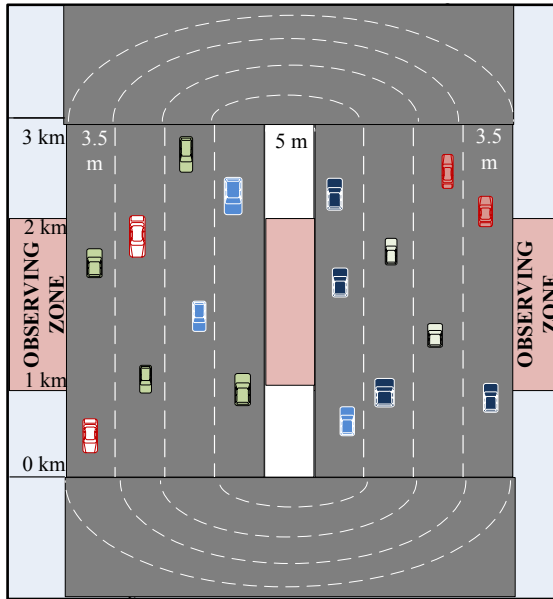


Figure 5.3 – Simulation scenario

We discuss various simulation parameter settings. They are listed in Table 5.2.

**Simulation area:** The simulation is performed over an area of  $3000m \times 35m$ . To eliminate the boundary effects of the network, we collect data on the vehicles in an observing zone of  $1km$  in the middle of the  $3km$  long highway section, as shown in Figure 5.3.

**Simulation time:** Due to mobility, vehicles move in and out of the observing zone. Thus, the vehicles and the links (sender-receiver pairs) on which the data is collected change over time. Over a simulation time of  $60s$ , we collect data on 600 to 800 vehicles and 900,000 to 1,500,000 links passing through the observing zone. The specific number of vehicles and links depends on the vehicular density and the DCC algorithm. Furthermore, for statistical confidence, each combination of density and algorithm is simulated with three independent runs.

**Initialization of ns-3:** All vehicles irrespective of the vehicular density or the DCC algorithm are initialized by transmitting beacon packets with the default communication parameters, i.e.,  $10Hz$  message-rate,  $25dBm$  transmit power and  $6Mbps$  data-rate.

**Channel model:** The channel model and parameters are shown in Table 5.2. The parameters for the channel models are obtained from the highway scenario

**Table 5.2** – Simulation parameters

Traffic density	Density-1, density-2, and density-3		
Channel model	(Large scale fading) Dual slope model	Path loss exponent 1 (until 80 m)	1.9
		Path loss exponent 2 (after 80 m)	3.8
	(Small scale fading) Nakagami $m$ model	Distance bin in meters	$m - value$
		0-50	3
		51-150	1.5
Above 150	1		
Carrier sensing threshold	-85 dBm		
Simulation time	60 s		
Simulation area	3000 m $\times$ 35 m		
Channel load threshold ( $CBP_T$ )	70%		
DCC adaptation period ( $\theta$ )	0.2 s		
Beacon size	300 bytes		
Message-rate	LIMERIC	1 to 10 Hz	
	SUPRA	10 Hz	
	DR-DCC	10 Hz	
	PDR-DCC	10 Hz	
Data-rate	LIMERIC	6 Mbps	
	SUPRA	6 Mbps	
	DR-DCC	3, 4.5, 6, 9, 12 and 18 Mbps	
	PDR-DCC	3, 4.5, 6, 9, 12 and 18 Mbps	
Transmit power	LIMERIC	25 dBm	
	SUPRA	25 to 10 dBm	
	DR-DCC	25 dBm	
	PDR-DCC	25 dBm	

channel specifications mentioned in the ETSI standard [139]. This channel model has been validated by field trials results [140].

**Channel load threshold ( $CBP_T$ ):** The channel load has a threshold  $CBP_T$ . When the channel load is increased beyond this threshold, the number of packet collisions increases and the channel load saturates. A channel load of more than 80% leads to saturation [117], however to leave headroom for safety-critical event-driven DENMs, the beacon packets should not load the channel more than 70% [117]. Thus, in our study, we consider a  $CBP_T$  of 70% for all algorithms.

**DCC adaptation period ( $\theta$ ):** DCC algorithms adapt based on the channel load measurements over a period  $\theta$  s. Since,  $\theta$  influences the adaptation time of the DCC algorithm its length should be minimized. However, due to fading and shadowing, channel load measurements fluctuate, In these cases a larger value of  $\theta$  provides more accurate channel load measurements. A reasonable value of  $\theta$  is between 0.2 s and 0.4 s as discussed in [128]. Hence, in our study, we have selected  $\theta$  of 0.2 s for all algorithms.

**Carrier sensing threshold and beacon size:** The carrier sensing threshold of -85 dBm is selected as in the standard [22]. A reasonable beacon size for beacon packets is around 200-400 bytes [117] [133]. Hence, we have selected a beacon size of 300 bytes.

**Message-rate:** The standard permits message-rate ranging from 1 to 10 Hz [22]. LIMERIC tunes the message-rate from 1 to 10 Hz. However, PDR-DCC, DR-DCC, and SUPRA have a default message-rate of 10 Hz.

**Transmit power:** The standard limits the maximum transmit power to 33 dBm [22]. Commercial hardware can introduce further limitations. In fact, several commercial IEEE 802.11p-based devices limit the maximum transmit power to 25 dBm [48, 141, 142]. Hence, the default transmit power of LIMERIC, PDR-DCC and DR-DCC is set to 25 dBm. However, SUPRA reduces the transmit power from 25 to 10 dBm to avoid congestion.

**Data-rate:** IEEE 802.11p permits 8 different data-rate 3, 4.5, 6, 9, 12, 18, 24 and 27 Mbps. Among them, 6 Mbps is considered as the default data-rate. Thus, the data-rate of LIMERIC, SUPRA is set to 6 Mbps. DR-DCC and PDR-DCC select among 3, 4.5, 6, 9, 12 and 18 Mbps data-rates (as discussed in section 5.2).

The evaluation is performed in terms of channel load, fairness and application performance to address the following questions:

- Are PDR-DCC, LIMERIC, SUPRA, and DR-DCC able to avoid congestion at high densities?
- Is the allocation of data-rate by PDR-DCC fair?
- How are the application reliability and the awareness range of PDR-DCC, LIMERIC, SUPRA, and DR-DCC compared to each other?

### 5.4.2. Channel load observations

The congestion control algorithms is expected to keep the channel load below a desired threshold  $CBP_T$  irrespective of the vehicular density. The average CBP  $CBP_{avg}$ , of vehicles in the observing zone is measured every  $\theta$  s.

Figures 5.4, 5.5 and 5.6 show the CBP measured for different DCC algorithms in the observing zone for density-1, density-2 and density-3 respectively. The blue line connecting all discrete measurements shows the average CBP. The  $CBP_T$  is indicated by a horizontal black line.

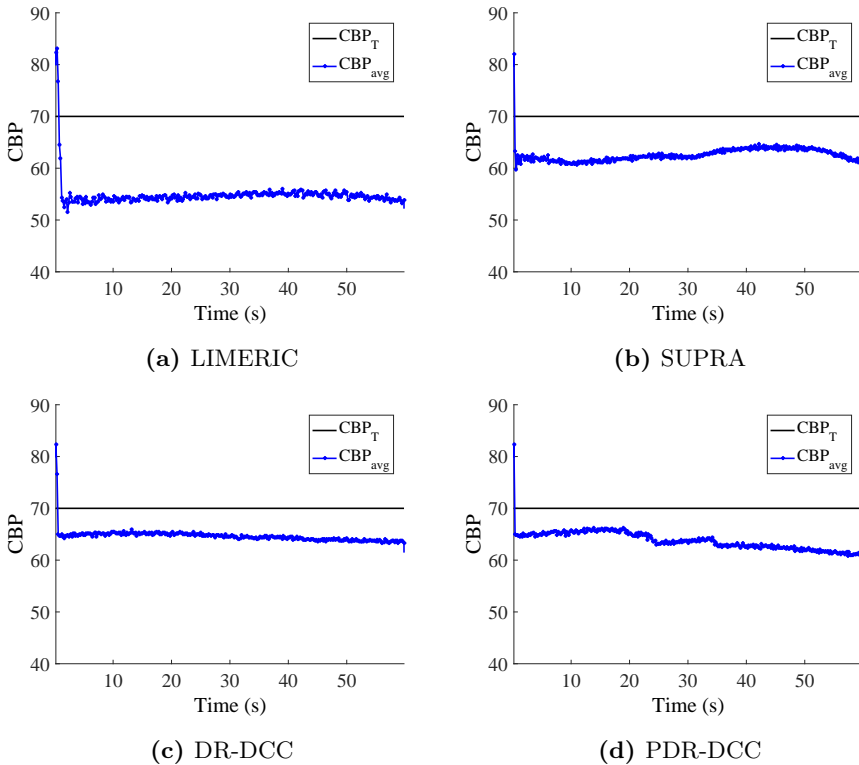


**Figure 5.4** – CBP vs. time for different algorithms for density-1

Irrespective of the density and algorithm, the simulation starts with all vehicles initialized with the default communication parameters, i.e., message-rate (10 Hz), data-rate (6 Mbps) and transmit power (25 dBm). Thus, at high vehicular densities, the default communication parameters result in an average CBP above  $CBP_T$  as seen at the start of the simulation (0.2 s) of the Figures 5.4, 5.5 and 5.6. The DCC algorithms adapt, depending on the algorithm, the message-rate,

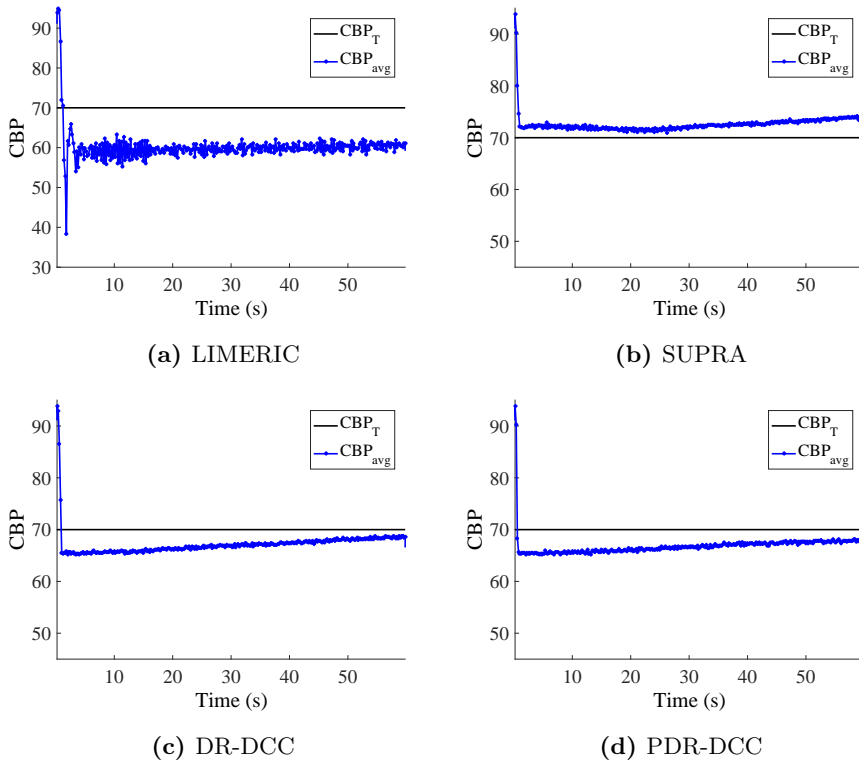


**Figure 5.5** – CBP vs. time for different algorithms for density-2

data-rate, and transmit power to force the CBP below  $CBP_T$ . This leads to a transient period (0 to 1 s) where the CBP is above  $CBP_T$ .

For density-1 (Figure 5.4) after the transient period, all four algorithms maintain the  $CBP_{avg}$  below  $CBP_T$ . For density-2 (Figure 5.5), LIMERIC, DR-DCC and PDR-DCC maintain the  $CBP_{avg}$  below  $CBP_T$ . However, SUPRA (Figure 5.5b) can no longer maintain the  $CBP_{avg}$  below  $CBP_T$  at density-2 as SUPRA selects its minimum transmit power 10 dBm and can no longer reduce transmit power to avoid congestion.

In Figure 5.6, we observe that the  $CBP_{avg}$  of all four algorithms is above  $CBP_T$ . For density-3, LIMERIC, SUPRA, DR-DCC, and PDR-DCC can no longer avoid congestion. In the case of PDR-DCC and DR-DCC this is because they have already selected the maximum data-rate of 18 Mbps. LIMERIC experiences unstable oscillations of  $CBP_{avg}$  above and below  $CBP_T$  (Figure 5.6a).

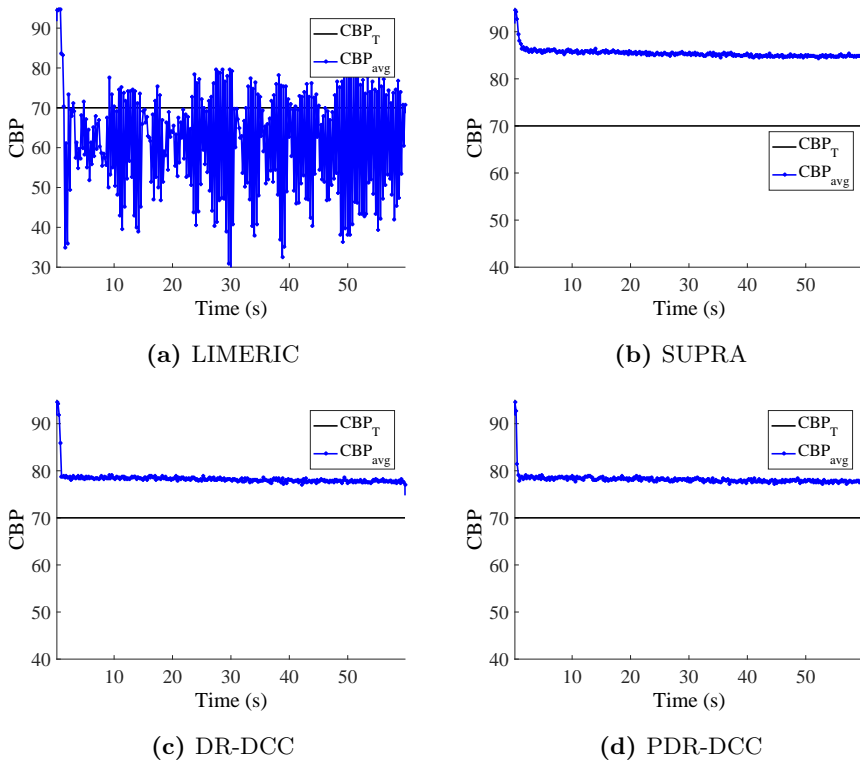


**Figure 5.6** – CBP vs. time for different algorithms for density-3

### 5.4.3. Fairness observations

All vehicles sharing the channel should have the same channel use time to assure fairness. It is shown that LIMERIC [28] and SUPRA [33] assure fairness. We quantify fairness using Jain's fairness index as discussed in Section 4.2.

Figure 5.7 shows the Jain's fairness index of LIMERIC, SUPRA, DR-DCC, and PDR-DCC at density-1 and density-2 simulations. The fairness performance of density-3 is not considered as none of the algorithms can avoid congestion.

From Figure 5.7a and 5.7b, we observe that for both density-1 and density-2 the Jain's fairness index of PDR-DCC is higher than 0.99. Furthermore, the fairness performance of PDR-DCC is comparable (difference less than 1%) to LIMERIC and SUPRA that assure fairness.

For density-1 (Figure 5.7a), we observe that the Jain's fairness index of DR-DCC is 10% less than the PDR-DCC. However, at density-2 the Jain's fairness index of DR-DCC is the same as PDR-DCC. To get more insights, we measured the percentage of packets transmitted at different data-rates in the observing zone

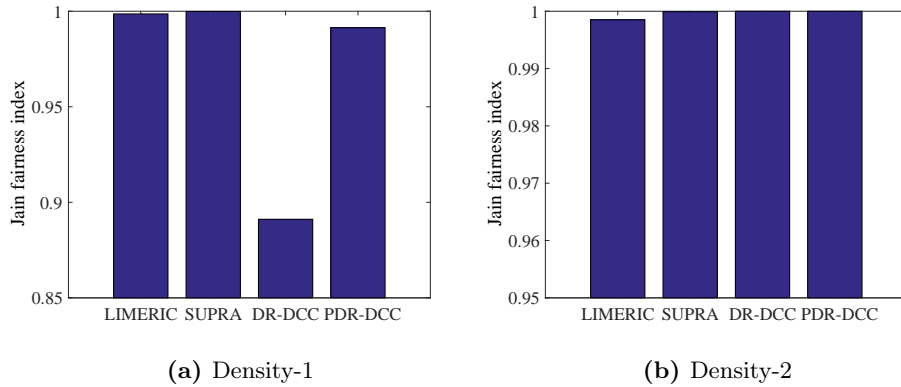


**Figure 5.7** – Jain's fairness index for different algorithms for density-1 and density-2

over the simulation period. The percentage of packets transmitted by the data-rate of PDR-DCC and DR-DCC at density-1 and density-2 are shown in Figure 5.8. Note that LIMERIC and SUPRA use a fixed data-rate of 6 *Mbps* hence, this is not shown in Figure 5.8.

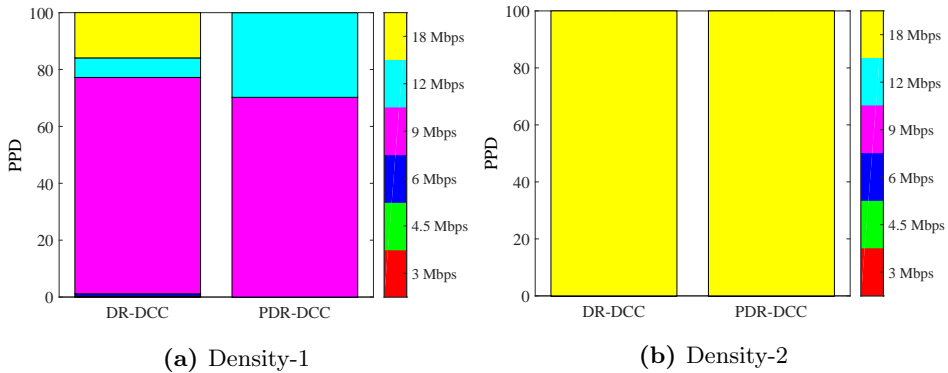


**Figure 5.8** – Percentage of packets transmitted by the data-rate (PPD) for different algorithms and densities

In Figure 5.8a, we observe that PDR-DCC vehicles select 9 and 12 *Mbps* whereas DR-DCC vehicles select 4.5, 6, 9, 12, and 18 *Mbps*. The selection of 4.5, 6, 9, 12, and 18 *Mbps* data-rates leads to unfair channel use time allocation (see Section 4.4) resulting in degradation of the fairness in Figure 5.7a. However, for density-2 in Figure 5.8b, PDR-DCC and DR-DCC select the maximum data-rate, 18 *Mbps*. Thus, they have the same fairness performance (Figure 5.7b).

#### 5.4.4. Application performance observations

In this section, we analyze the application reliability and awareness range of different DCC algorithms for density-1 and density-2. Because for density-3 none of the algorithms is able to keep the channel load below the threshold we do not consider this case further.

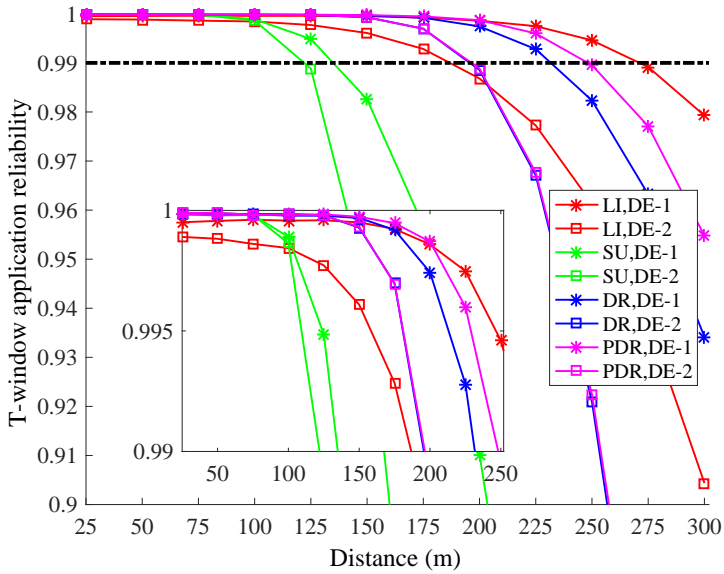
##### Application reliability

The application reliability is measured using the T-window application reliability  $T_{AR}$  discussed in Section 4.4. In our study, we evaluate the performance of the FCW and LCW applications introduced in Section 3.5. FCW requires one packet every second ( $N = 1, T = 1 s$ ) and LCW requires two packets every second ( $N = 2, T = 1 s$ ).

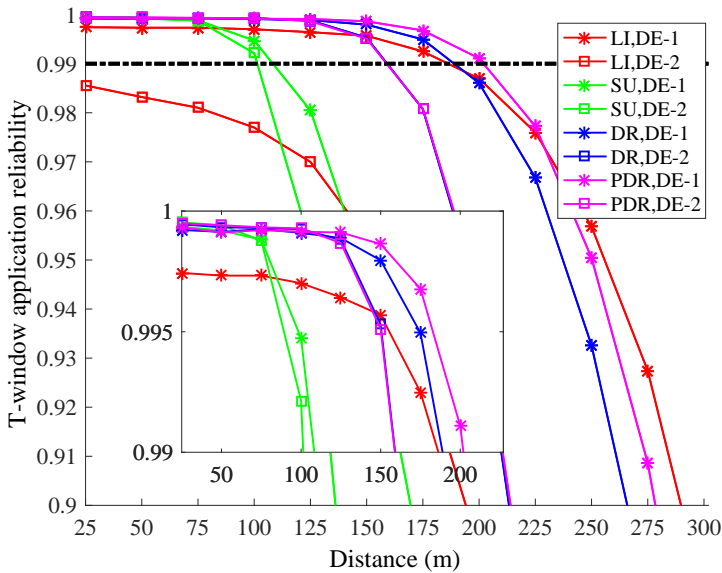
Figure 5.9 shows the  $T_{AR}$  of LIMERIC, SUPRA, DR-DCC, and PDR-DCC for different densities and application requirements. We observe that irrespective of the vehicular density and the application requirements, PDR-DCC has better application reliability than LIMERIC at near range (less than 250  $m$ ) as PDR-DCC maintains a message-rate of 10  $Hz$ . On the contrary, the application reliability of LIMERIC is better than PDR-DCC at a faraway range (greater than 250  $m$ ) as LIMERIC maintains 6  $Mbps$  that has better PRR than PDR-DCC at larger distance, although its message-rate is lower than PDR-DCC.

At low densities (density-1), PDR-DCC has better application reliability for FCW (Figure 5.9a) and LCW (Figure 5.9b) than DR-DCC as PDR-DCC improves fairness with packet count by using only 9 and 12  $Mbps$  whereas DR-DCC uses 4.5, 6, 12 and 18  $Mbps$  leading to unfairness and degradation of the application reliability.





(a) Forward collision warning



(b) Lane change warning

LI= LIMERIC, SU= SUPRA, DR= DR-DCC and PDR= PDR-DCC, DE-y= Density, where y represents different densities

**Figure 5.9** – Application reliability for different densities and applications as function of the distance

### Awareness range

Awareness range is the maximum possible range up to which an application can be supported reliably. We assess the awareness range as the maximum possible range up to which the  $T_{AR}$  is greater than 0.99 [23]. This 0.99 application reliability is indicated by a horizontal line in Figure 5.9.

Table 5.3 shows the awareness range for various application requirements and densities. The instances with the largest awareness range among all cases are highlighted. We observe that the awareness range of LIMERIC is better than PDR-DCC for FCW at density-1. However, as the density increases, PDR-DCC has better performance than LIMERIC. Furthermore, the awareness range of PDR-DCC for LCW is better than LIMERIC at both densities (density-1 and density-2). This hints that a combined strategy for data-rate and message-rate control may improve awareness range and application reliability further.

For density-2, LIMERIC can no longer support the LCW application even in the close range of 20  $m$ , whereas PDR-DCC supports the LCW application till a range of 160  $m$ .

Irrespective of density and application, the awareness ranges of PDR-DCC and DR-DCC are better than SUPRA by at least 50  $m$ . The finding is similar to the analytical study in [87], which shows that the awareness range of transmit power DCC is less than data-rate DCC algorithms.

The beacon packets may support many applications simultaneously. Among these applications, the one with the most stringent requirements has to be satisfied with the maximum possible awareness range, and for varying densities. We observe that only SUPRA, PDR-DCC and DR-DCC can support the most stringent LCW application reliably at high density (density-2).

**Table 5.3** – Awareness range of the FCW and LCW applications for different DCC algorithms and densities

Application	Vehicular Density	Awareness range ( $m$ )			
		LI	SU	DR	PDR
Forward collision warning ( $N = 1, T = 1 s$ )	Density-1	<b>270</b>	130	230	250
	Density-2	180	120	<b>195</b>	<b>195</b>
Lane change warning ( $N = 2, T = 1 s$ )	Density-1	180	105	185	<b>200</b>
	Density-2	0	100	<b>160</b>	<b>160</b>

LI= LIMERIC, SU= SUPRA, DR= DR-DCC and PDR= PDR-DCC

### 5.5. Conclusion

Data-rate DCC algorithms are promising as they increase the channel capacity as channel load increases, and in this way they are able to accommodate more beacon messages. In this chapter, we have proposed a packet count based decentralized data-rate congestion control algorithm PDR-DCC, which enforces a homogeneous data-rate selection amongst all vehicles to ensure fairness. The performance of PDR-DCC was evaluated and compared to other message-rate (LIMERIC), transmit power (SUPRA) and data-rate (DR-DCC) congestion control algorithms for different vehicle densities and application requirements.

The results have shown that PDR-DCC can increase the channel capacity in terms of number of beacon messages supported by the channel. Furthermore, the results have shown that PDR-DCC assures fairness and supports more stringent application requirements with better application reliability and awareness range than LIMERIC (message-rate) and SUPRA (transmit power) DCC algorithms. In addition, the results suggest that a combined data-rate and message-rate congestion control strategy may improve the application performance even further. We dwell more on this in the next chapter.

## Combined message-rate and data-rate decentralized congestion control

### 6.1. Introduction

In the previous chapter, we observed that DCC algorithms that adjust only one parameter are not able to hold the CBP below the target channel load threshold at large vehicular densities. Furthermore, we observed that a combined message-rate and data-rate tuning can provide better application reliability and awareness range than tuning a single-parameter. In this chapter, we propose a combined message-rate and data-rate congestion control algorithm, MD-DCC, that tries to overcome the degradation of application reliability and awareness range that single-parameter tuning DCC algorithms experience at large vehicular densities.

The key contributions of the chapter are as follows:

- To the best of our knowledge, we are the first to propose a combined message-rate and data-rate based congestion control algorithm MD-DCC, that enforces fairness.
- Adaptation of message-rate and data-rate simultaneously enables MD-DCC to support around 2.7 and 10 times more vehicles than message-rate and data-rate based congestion control algorithms respectively.
- We discuss the approach to select the MD-DCC parameters based on the application reliability requirements.
- MD-DCC provides improved application reliability and larger awareness range compared to three other DCC algorithms, which are based on different principles. This is found through our performance evaluation of MD-DCC for several application requirements at different vehicle densities.

The rest of the chapter is structured as follows. The design and functioning of MD-DCC are explained in Section 6.2. The adaptation of various parameters of MD-DCC based on the safety application requirements is discussed in Section 6.3. Section 6.4 presents an analysis of how MD-DCC can support larger vehicular

densities than the message-rate and the data-rate DCC algorithms. In Section 6.5, we present simulations of a highway scenario for different application requirements and densities to analyze and compare the channel load, fairness and application performance of MD-DCC with other DCC algorithms. Finally, Section 6.6 summarizes our results and conclusions.

## 6.2. Combined message-rate and data-rate DCC

### 6.2.1. MD-DCC algorithm

We design MD-DCC considering the minimum message-rate ( $r_{min}$ ) and awareness range application requirements. MD-DCC adapts the message-rate and data-rate to ensure channel load is below the threshold and maintains a message-rate greater than or equal to the application required  $r_{min}$ . The data-rate adaptation is performed based on the vehicular density and channel load threshold to ensure that the channel has sufficient capacity to maintain a message-rate greater than or equal to  $r_{min}$ . However, since a higher data-rate requires a better SINR, increasing the data-rate also causes the awareness range to be reduced. Therefore, MD-DCC increases the data-rate by no more than is needed, so that the awareness range, for a defined transmit power, is kept as high as possible. The data-rate selection is discrete thus the selected data-rate may support message-rate greater than  $r_{min}$ . To optimize the usage of the channel for a defined data-rate we perform message-rate adaptation. The message-rate selected by the vehicle is always greater than or equal to  $r_{min}$  and less than 10 Hz (maximum supported in the standard [22]).

The flowchart in Figure 6.1 shows how MD-DCC is implemented. MD-DCC vehicles are initialized with default communication parameters, i.e., 6 Mbps data-rate and 10 Hz message-rate, as discussed in Section 5.4.1. The message-rate and the data-rate are adapted every  $\theta$  and  $\gamma$  seconds respectively. The message-rate should be adapted at a faster rate than data-rate, i.e.,  $\gamma > \theta$ , with  $\gamma$  being multiple of  $\theta$ . Further explanation is provided in Section 6.3.

#### Message-rate adaptation

The message-rate adaptation in MD-DCC is an extension of LIMERIC [28]. MD-DCC adapts the message-rate based on the difference between the measured  $CBP_k(t)$  and the channel threshold  $CBP_T$ . It iteratively adapts the message-rate such that the difference between  $CBP_k(t)$  and  $CBP_T$  is reduced. The message-rate  $R_k(t)$  of vehicle  $k$  is adjusted periodically every  $\theta$  s as follows:

$$R_k(t) = (1 - \alpha) \times R_k(t - \theta) + \beta \times (CBP_T - CBP_k(t - \theta)) \quad (6.1)$$

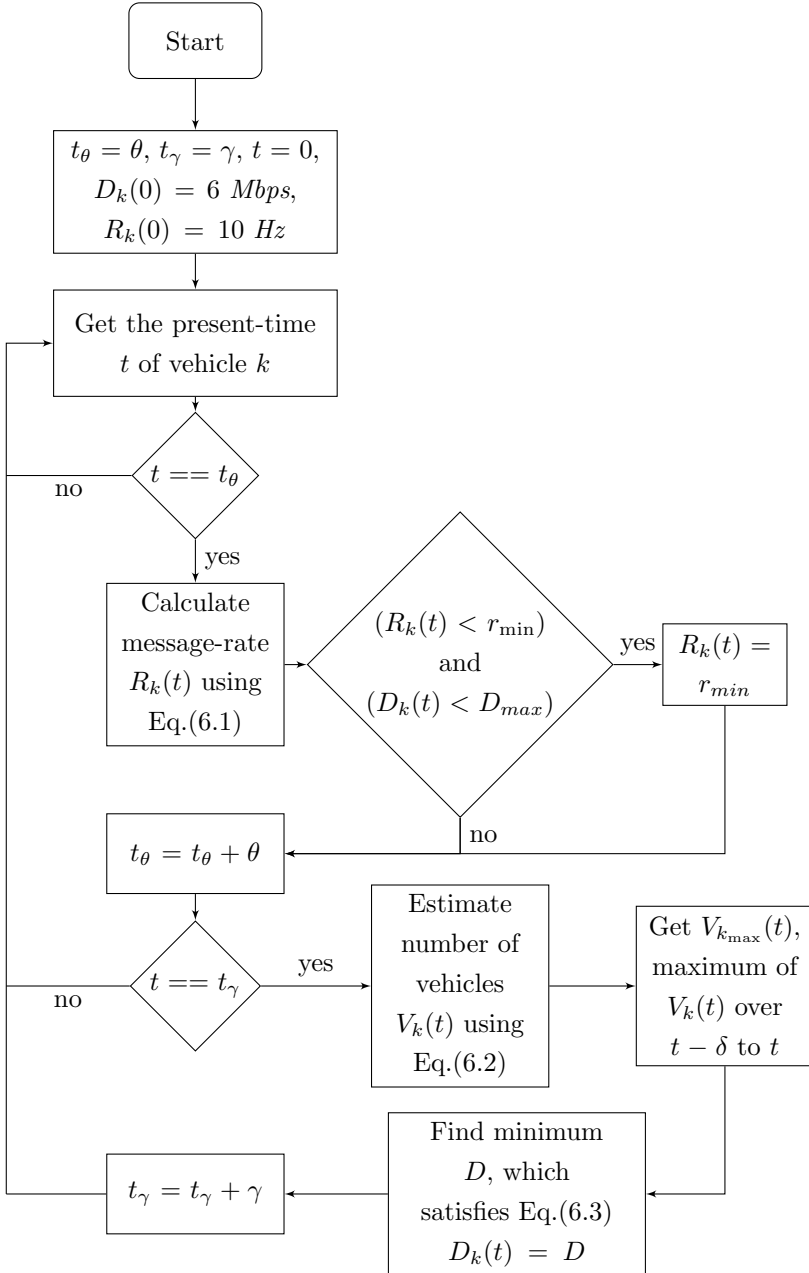


**Figure 6.1** – Flowchart of the MD-DCC algorithm

where  $CBP_k(t)$  is the global channel load estimation of vehicle  $k$ , which is computed by averaging the CBP measurements of the vehicle and its neighbor

vehicles within its communication range. The selection of  $\alpha$  and  $\beta$  on MD-DCC is discussed in Appendix A.

### Data-rate adaptation

The data-rate of each vehicle is selected based on an estimate of the maximum number of vehicles within its communication range and the minimum message-rate  $r_{min}$ .

Each vehicle  $k$  estimates  $V_k(t)$ , the number of vehicles within its communication range at time  $t$ , as follows:

$$V_k(t) = \frac{P_k(t)}{R_{k_{min}}(t)} \quad (6.2)$$

where  $P_k(t)$  is the packet count estimated by vehicle  $k$  over a period  $\gamma$  as defined in Section 5.3.2.  $R_{k_{min}}(t)$  is the minimum message-rate  $R_k(t)$  selected by  $k$  over a period  $\gamma$ . A sliding window over a period  $\delta$  is used to obtain  $V_{k_{max}}(t)$ , the maximum  $V_k(t)$  over the interval  $(t - \delta, t)$ . Each vehicle  $k$  selects the lowest data-rate which satisfies the following equation:

$$\frac{V_{k_{max}}(t) \times r_{min} \times T_D}{\gamma} \leq CBP_T \quad (6.3)$$

where  $T_D$  is the beacon transmission time for data-rate  $D$ .

Based on  $V_{k_{max}}(t)$  and  $r_{min}$  the data-rate  $D_k(t)$  is selected to set the channel capacity sufficient for maintaining the message-rate not lower than  $r_{min}$  while maximizing the awareness range. However, when the vehicle density increases to the point where MD-DCC would have to select a data-rate greater than maximum data-rate  $D_{max}$ , the message-rate still has to be decreased below  $r_{min}$  to avoid congestion.

#### 6.2.2. Modification for stability

The values of  $\alpha$  and  $\beta$  influence the stability of MD-DCC, i.e., the steady-state convergence of CBP below  $CBP_T$ . The number of vehicles sharing the channel is unknown and keeps on changing as a result of the mobility of vehicles. Hence, for one predefined pair of  $\alpha$  and  $\beta$  values, it is not possible to assure the stability of MD-DCC for all vehicular densities and  $r_{min}$  application requirements. Stability analysis of MD-DCC is discussed in detail in Appendix A. To avoid unstable situations the gain saturation approach proposed in [129] is used in MD-DCC,

which modifies the message-rate control of MD-DCC as follows:

$$R_k(t) = (1 - \alpha) \times R_k(t - \theta) + \text{sign}(CBP_T - CBP_k(t - \theta)) \times \min[X, |\beta \times (CBP_T - CBP_k(t - \theta))|] \quad (6.4)$$

In unstable situations the magnitude of  $|\beta \times (CBP_T - CBP_k(t - \theta))|$ , which influences the message-rate selection may become very large leading to a large increase of CBP as there is no upper limit for the value  $\beta \times (CBP_T - CBP_k(t - \theta))$  in Eq.(6.1). Thus, the gain saturation approach proposes to limit the value to  $X$  Hz, with the sign of the error term  $(CBP_T - CBP(t - \theta))$  specifying whether to increase or decrease the message-rate. By limiting it to  $X$  Hz, we avoid a large increase of CBP. However, in unstable situations this gain saturation cannot avoid oscillations of the CBP. In-depth analysis of the gain saturation approach can be found in [28, 129].

### 6.2.3. Evaluation of DCC design goals

The MD-DCC design achieves the DCC design goals discussed in Section 4.3 as follows:

- Congestion control: MD-DCC adapts message-rate and data-rate to maintain the channel load below the threshold.
- Fairness: The message-rate allocation of MD-DCC is performed using a scheme similar to LIMERIC and the data-rate allocation of MD-DCC is based on the estimated vehicular density to assure fairness.
- Application performance: To satisfy the application requirements in terms of minimum message-rate and awareness range.
  - Minimum message-rate: MD-DCC maintains a message-rate greater than or equal to  $r_{min}$ .
  - Awareness range: Similar to PDR-DCC, MD-DCC selects the least possible data-rate to avoid congestion and maximize the awareness range.

### 6.3. MD-DCC parameter selection

Let us discuss how the value of  $\gamma$ ,  $\delta$ ,  $\alpha$ ,  $\beta$ , and  $X$  should be determined. We will also examine the relationship between the value of  $r_{min}$  and  $\beta$ . The MD-DCC parameters  $\theta$ ,  $D_{max}$  and  $CBP_T$  are selected to be 0.2 s, 18 Mbps and 70% respectively as discussed in Section 5.4.1.

**Data-rate adjustment period  $\gamma$ :** The data-rate adaptation is performed based on the vehicular density estimation. The vehicular density estimation in



our study is dependent on the message-rate selected by MD-DCC as discussed in the previous section. Because vehicular density changes over time, we use the worst-case vehicular density estimation, i.e., the maximum vehicular density estimation over a period. The worst-case vehicular density is obtained based on the multiple message-rate estimations. Thus, the message-rate adaptation in MD-DCC should be done at a faster rate than the data-rate adaptation ( $\gamma > \theta$ ). The value of  $\gamma$  is selected to be 1 s for a  $\theta$  of 0.2 s, so that LIMERIC has at least five message-rate measurements to obtain the worst-case vehicle density estimation.

**Sliding window period  $\delta$ :** The worst-case vehicular density estimation performed every  $\gamma$  seconds fluctuates due to the mobility of vehicles. Hence, the maximum number of vehicles over a period of  $\delta$  s is used to assess the required data-rate, thus avoiding unnecessary increase or decrease of the data-rate.  $\delta$  should be greater than  $\gamma$  to get multiple estimations of the vehicular density. The value of  $\delta$  is selected to be 5 s for a  $\gamma$  of 1 s, so that we have at least five vehicular density estimations to assess the variation in vehicular density as suggested by SAE-DCC [58].

**$\alpha$ :**  $\alpha$  takes values between 0 and 1. It determines the speed of convergence and the degree of variations in CBP. A higher value of  $\alpha$  leads to faster convergence of CBP below  $CBP_T$ ; on the contrary, a small  $\alpha$  leads to lower variations in CBP. In our study  $\alpha$  is selected to be 0.1 as proposed by LIMERIC [28] and ETSI report [123].

**$\beta$ :** The most critical parameter of the MD-DCC algorithm is  $\beta$  as it controls the stability as well as the allocation of the message-rate and data-rate. A detailed analysis of  $\beta$ , its role in stability, and its relation with  $r_{min}$  are mathematically defined and derived in Appendix A.  $\beta$  is computed as follows:

$$\beta = \frac{(1 - \alpha) \times r_{min}}{CBP_T} \quad (6.5)$$

**$X$ :**  $X$  takes values from 0 to 10 Hz. A smaller value of  $X$  increases the convergence time of CBP below  $CBP_T$ . However, a higher value of  $X$  leads to large oscillation of CBP [28, 129]. In our study  $X$  is selected to be 1 Hz as in [28, 129].

#### 6.4. Analytical performance evaluation

In this section, we perform a mathematical analysis to assess the adaptation of MD-DCC based on the application requirements. We compare the maximum number of vehicles supported by MD-DCC with the message-rate based DCC LIMERIC and the data-rate based PDR-DCC.

To simplify the analysis, we assume an ideal scenario where all vehicles are within the sensing range of each other and experience the same CBP. We assume an ideal MAC where the beacon messages are transmitted without any collisions. Further simulations using realistic MAC and vehicular distribution are presented in the next section.

The CBP experienced by the vehicles is as follows:

$$CBP(t) = \left( \frac{\sum_{j=1}^L (R_j(t) \times \theta) \times T_{D_j}}{\theta} \right) \quad (6.6)$$

where  $R_j(t)$  is the message-rate of the  $j^{\text{th}}$  vehicle at time  $t$ .  $T_{D_j}$  is the transmission time of the  $j^{\text{th}}$  vehicle with data-rate  $D$ .  $R_j(t) \times \theta$  is the number of packets transmitted by the  $j^{\text{th}}$  vehicle in  $\theta$  s. Thus, the summation of  $R_j(t) \times \theta \times T_{D_j}$  is the amount of time taken for packet transmission by all  $L$  vehicles sharing the channel over a period  $\theta$ .

The  $T_D$  for different data-rates for a packet size of 300 bytes is calculated using Eq.(5.1). The message-rate of LIMERIC is adjusted as in Eq.(B.1). The data-rate of PDR-DCC is adjusted as in Eq.(5.3). The message-rate and data-rate of MD-DCC are adapted as discussed in Section 6.2. The proposed analytical model will be validated using practical experiment in Section 8.3.2.

For all the three algorithms, we select  $CBP_T = 70\%$  [143] and  $\theta = 0.2$  s. The message-rate of MD-DCC varies from 1 Hz to 10 Hz as in the standard, and the data-rates are 3, 4.5, 6, 9, 12 and 18 Mbps. The data-rate of LIMERIC is fixed to 6 Mbps; for PDR-DCC the message-rate is fixed to 10 Hz. We analyze the steady-state message-rate, data-rate and CBP of the algorithms over varying vehicular density (number of vehicles sharing the channel). For each vehicular density, the algorithms are initialized to 6 Mbps data-rate and 10 Hz message-rate. For each density, we run the algorithm for 600 s (3000 iterations) to obtain the steady-state message-rate, data-rate and CBP performance of the algorithms. The message-rate, CBP, and data-rate of all vehicles are the same as they have the same DCC algorithm and experience the same CBP under the ideal conditions discussed above.

### Congestion point

In this section, we compare the congestion point of MD-DCC, LIMERIC, and PDR-DCC. The congestion point is defined as the maximum supported vehicular density above which the algorithm can no longer keep the CBP below the threshold  $CBP_T$ . The  $\beta$  value of MD-DCC is chosen for a  $r_{\min}$  of 2 Hz [112].

Figures 6.2a, 6.2b and 6.2c depict the steady-state message-rate, data-rate and CBP performance of the three algorithms as function of the vehicular density. The congestion point of the DCC algorithms are pointed by an arrow in Figure

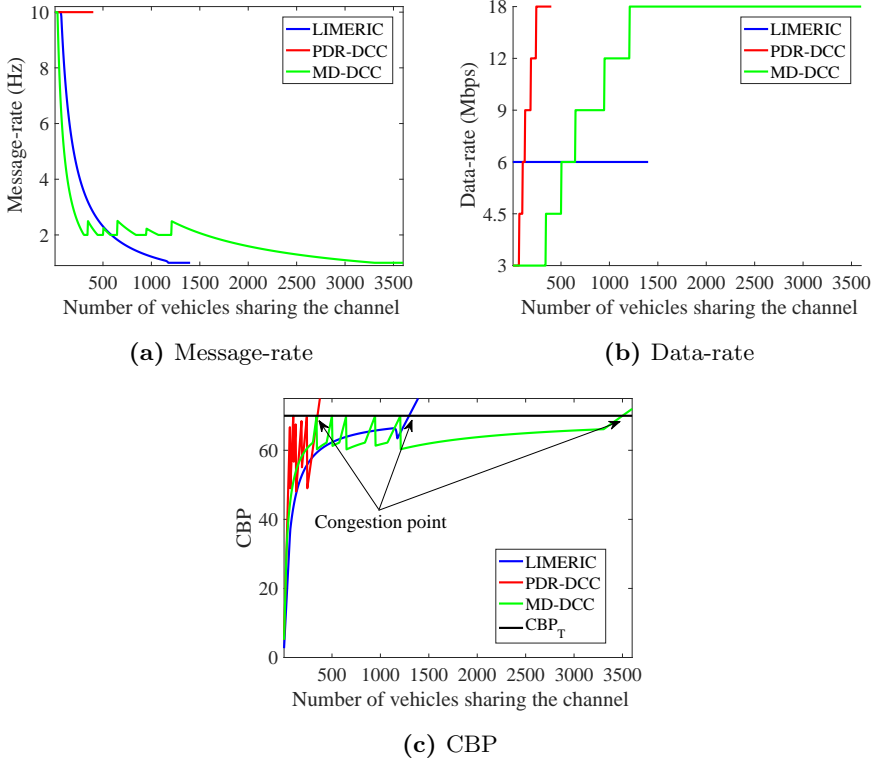


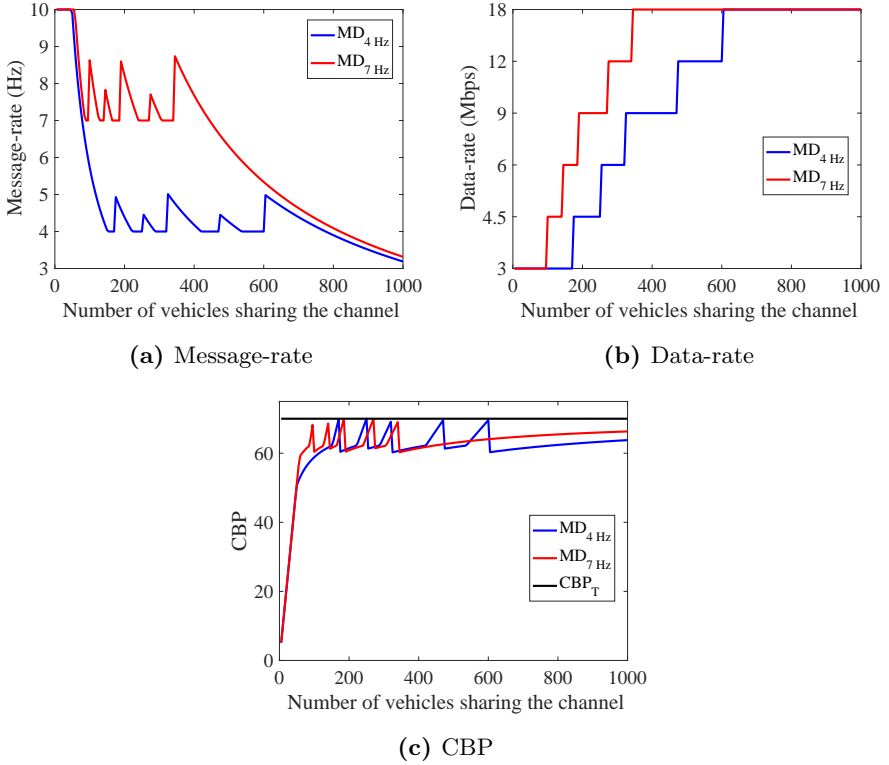
**Figure 6.2** – LIMERIC, PDR-DCC and MD-DCC performance as a function of number of vehicles sharing the channel

6.2c. The congestion point of PDR-DCC, LIMERIC, and MD-DCC are around 350, 1300, and 3500 vehicles respectively. It is evident that MD-DCC can avoid channel congestion even at very high vehicular density. MD-DCC can support around 10 times and 2.7 times higher vehicular densities than PDR-DCC and LIMERIC respectively. At the congestion point LIMERIC selects the minimum message-rate of 1 Hz (Figure 6.2a), PDR-DCC selects the maximum data-rate of 18 Mbps (Figure 6.2b) and MD-DCC selects the minimum message-rate of 1 Hz (Figure 6.2a) and the maximum data-rate of 18 Mbps (Figure 6.2b).

### Adaptation of MD-DCC for different application requirements

As discussed in Section 6.2, the values of  $r_{min}$  and  $\beta$  depend on the application requirements. In our study, we focus on the FCW and LCW applications. FCW and LCW require a minimum message-rate ( $r_{min}$ ) of 4 Hz and 7 Hz respectively as discussed in Section 3.6.  $\beta$  is calculated using Eq.(6.5) for a  $CBP_T$  of 70 and  $\alpha$  of 0.1. Thus, the values of  $\beta$  for FCW and LCW application are 0.0051 and 0.009 respectively.

Figures 6.3a, 6.3b and 6.3c show the steady-state message-rate, data-rate and CBP respectively as a function of the traffic density of MD-DCC for the FCW and LCW applications.  $MD_{4\text{ Hz}}$  and  $MD_{7\text{ Hz}}$  represent the MD-DCC implementation for the FCW and LCW applications respectively.



$MD_x =$  MD-DCC, where x represents  $r_{min}$  requirements of the application

**Figure 6.3** – MD-DCC adaptation for different  $r_{min}$  requirements and number of vehicles sharing the channel

In Figure 6.3a, the message-rates of  $MD_{4\text{ Hz}}$  and  $MD_{7\text{ Hz}}$  are greater than or equal to 4 Hz and 7 Hz respectively as long as the data-rate is less than

$D_{max}$ . MD-DCC is designed to maintain a message-rate greater than or equal to  $r_{min}$ . However, the message-rate of  $MD_{4\text{ Hz}}$  and  $MD_{7\text{ Hz}}$  decreases below  $r_{min}$  at 650 and 450 vehicles respectively because the data-rate of  $MD_{4\text{ Hz}}$  and  $MD_{7\text{ Hz}}$  have already reached  $D_{max}$  of 18 *Mbps* as seen in Figure 6.3b. Hence, to avoid congestion MD-DCC reduces message-rate below  $r_{min}$ .

In Figure 6.3b, the data-rate of  $MD_{7\text{ Hz}}$  is always greater than or equal to  $MD_{4\text{ Hz}}$  as  $MD_{7\text{ Hz}}$  has higher  $r_{min}$  requirements than  $MD_{4\text{ Hz}}$ .

In Figure 6.3c, the CBP of  $MD_{4\text{ Hz}}$  and  $MD_{7\text{ Hz}}$  is maintained below  $CBP_T$  by increasing data-rate as density increases (Figure 6.3b).

## 6.5. Simulation performance evaluation

In this section, we perform simulations to assess up to which degree MD-DCC satisfies the DCC design goals discussed in Section 4.3. Furthermore, we compare the application performance of MD-DCC with other DCC algorithms.

Message-rate based LIMERIC, data-rate based PDR-DCC and the combined message-rate and transmit power based SAE-DCC are chosen for comparison. LIMERIC is chosen as it is one of the most prominent and widely accepted message-rate based DCC algorithm. PDR-DCC is chosen as it has better application reliability performance than LIMERIC at high densities. SAE-DCC is selected as it is proposed by the SAE standardization body [58]. Appendix B provides a detailed explanation of LIMERIC and SAE-DCC. PDR-DCC has been explained in Chapter 5.

### 6.5.1. Simulation setup

The simulations are performed using a combined network simulator (ns-3) [46] and vehicle traffic simulator (SUMO) [47] as discussed in Appendix C. We consider a road section with of approximately 3 *km* with 5 lanes in each direction similar to the Dutch A2 highway from Amsterdam to Utrecht [144] as shown in Figure 6.4. The width of each lane is 3.35 *m* [136]. The velocity of the vehicles ranges from 0 to 120 *km/h* [138, 144] whereas their acceleration ranges from -2 to 3 *m/s<sup>2</sup>* [27]. The length of the vehicles is fixed to 4 *m* [137]. When a vehicle reaches the end of the road; it enters in the opposite direction. This is done to have control over the vehicular densities we simulate. The initial position and the velocity of each vehicle are selected randomly. SUMO simulates the mobility for 60 *s* before providing them to ns-3 to eliminate the effect of random positioning and velocity of vehicles.

We consider three vehicular densities:

- Density-4: 40 vehicles per lane/km
- Density-5: 50 vehicles per lane/km
- Density-6: 60 vehicles per lane/km

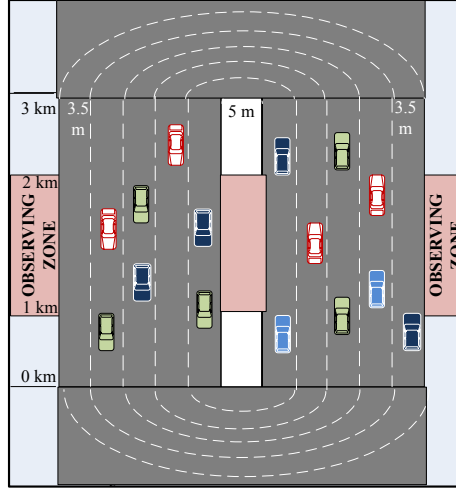


**Figure 6.4** – Simulation scenario

Density-4, density-5 and density-6 represent medium velocity, slow velocity and traffic congested scenarios corresponding to an average velocity of 80, 35 and 20  $km/hr$  respectively. For each density, we simulate four different DCC algorithms. The channel model, beacon size, simulation time, channel load threshold, and carrier sensing threshold simulation parameters are the same as in Table 5.2 and have been discussed in Section 5.4.1. Message-rate, data-rate, and transmit power of LIMERIC, MD-DCC, PDR-DCC, and SAE-DCC are shown in Table 6.1. The choice of parameters for LIMERIC and SAE-DCC algorithm are discussed in Appendix B. The parameters of PDR-DCC algorithm are discussed in Chapter 5. MD-DCC parameters are as discussed in Section 6.3. Note that all four algorithms have the same channel load threshold ( $CBP_T = 70\%$ ).

We will limit ourselves to the two critical applications selected in the previous section: FCW and LCW. The evaluations will be done for the three traffic densities selected before.

**Table 6.1** – Message-rate, data-rate and transmit power of DCC algorithms

LIMERIC	Message-rate	1 to 10 <i>Hz</i>
	Data-rate	6 <i>Mbps</i>
	Transmit power	25 <i>dBm</i>
PDR-DCC	Message-rate	10 <i>Hz</i>
	Data-rate	3, 4.5, 6, 9, 12 and 18 <i>Mbps</i>
	Transmit power	25 <i>dBm</i>
MD-DCC	Message-rate	1 to 10 <i>Hz</i>
	Data-rate	3, 4.5, 6, 9, 12 and 18 <i>Mbps</i>
	Transmit power	25 <i>dBm</i>
SAE-DCC	Message-rate	1 to 10 <i>Hz</i>
	Data-rate	6 <i>Mbps</i>
	Transmit power	10 to 25 <i>dBm</i>

### 6.5.2. Channel load observations

The average CBP of the vehicles in the observing zone over the simulation period is used to assess the channel load as discussed in Section 4.4. Each of these measurements is performed discretely every  $\theta$  *s*.

Figures 6.5, 6.6 and 6.7 show the CBP experienced by the different algorithms in the observing zone for density-4, density-5 and density-6 respectively. The average CBP,  $CBP_{avg}$ , is represented by the blue line connecting all discrete measurements. A horizontal black line represents the  $CBP_T$ .

Irrespective of density and algorithm, the simulation starts with all vehicles initialized with the default communication parameters, which leads to congestion and average CBP above  $CBP_T$  as seen at 0.2 *s* in Figures 6.5, 6.6 and 6.7. The DCC algorithms adapt the communication parameters and try to reduce the CBP below  $CBP_T$  as seen in the transient period (0 to 1 *s*).

For density-4 (Figure 6.5), after the transition period, the average CBP of all four algorithms is below  $CBP_T$ . However, as the density increases, for density-5 (Figure 6.6) and density-6 (Figure 6.7), the average CBP of LIMERIC and PDR-DCC is above  $CBP_T$ . LIMERIC leads to oscillations of the average CBP around  $CBP_T$  due to unstable situation as discussed in Section 6.2.2. PDR-DCC can no longer reduce the average CBP below  $CBP_T$  as it has already reached the maximum data-rate of 18 *Mbps*.

We observe that for density-5 (Figure 6.6) and density-6 (Figure 6.7), the average CBP of SAE-DCC and MD-DCC with different  $r_{min}$  is below  $CBP_T$

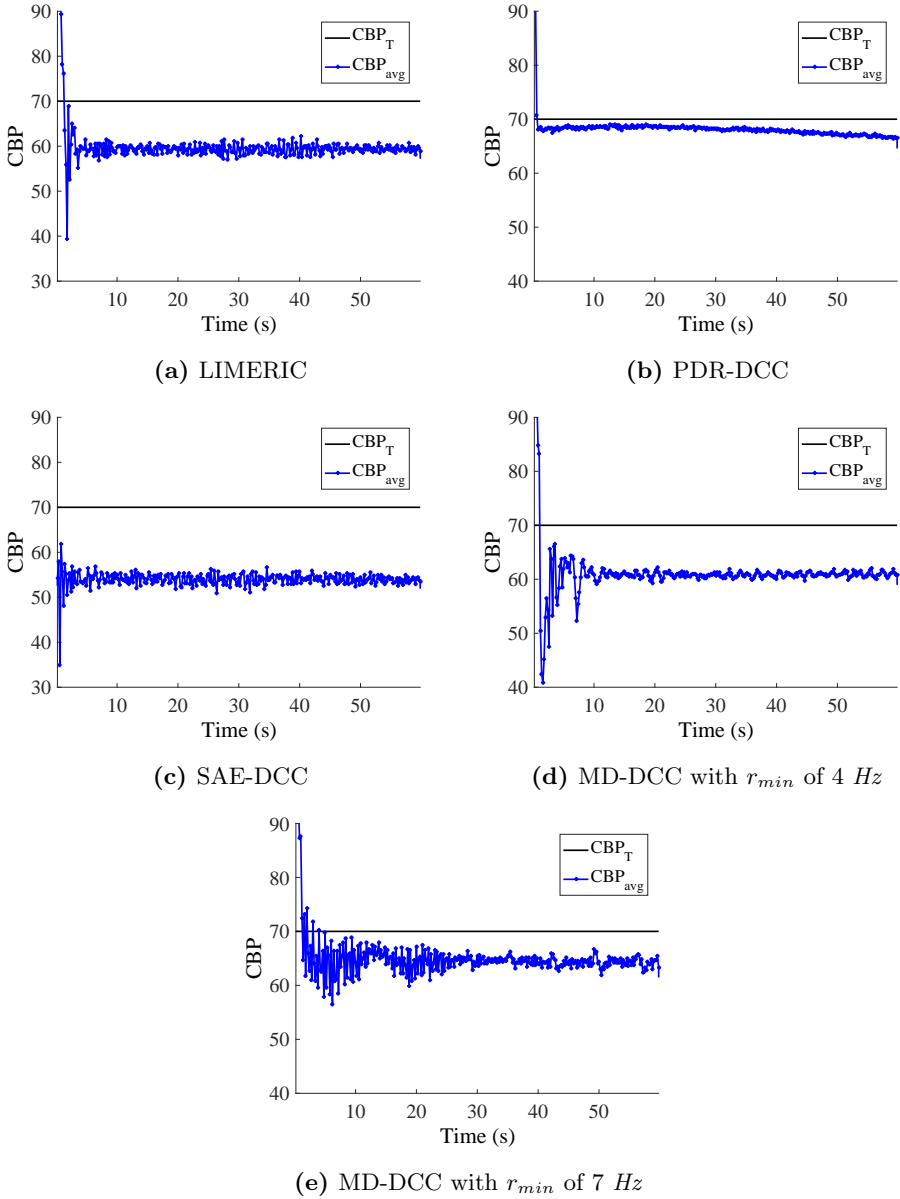


**Figure 6.5** – CBP vs. time for different DCC algorithms for density-4

after the transition period. SAE-DCC and MD-DCC tune two communication parameters to reduce the channel load. Thus, they are able to avoid congestion at larger vehicular densities than LIMERIC and PDR-DCC which tune only one communication parameter.



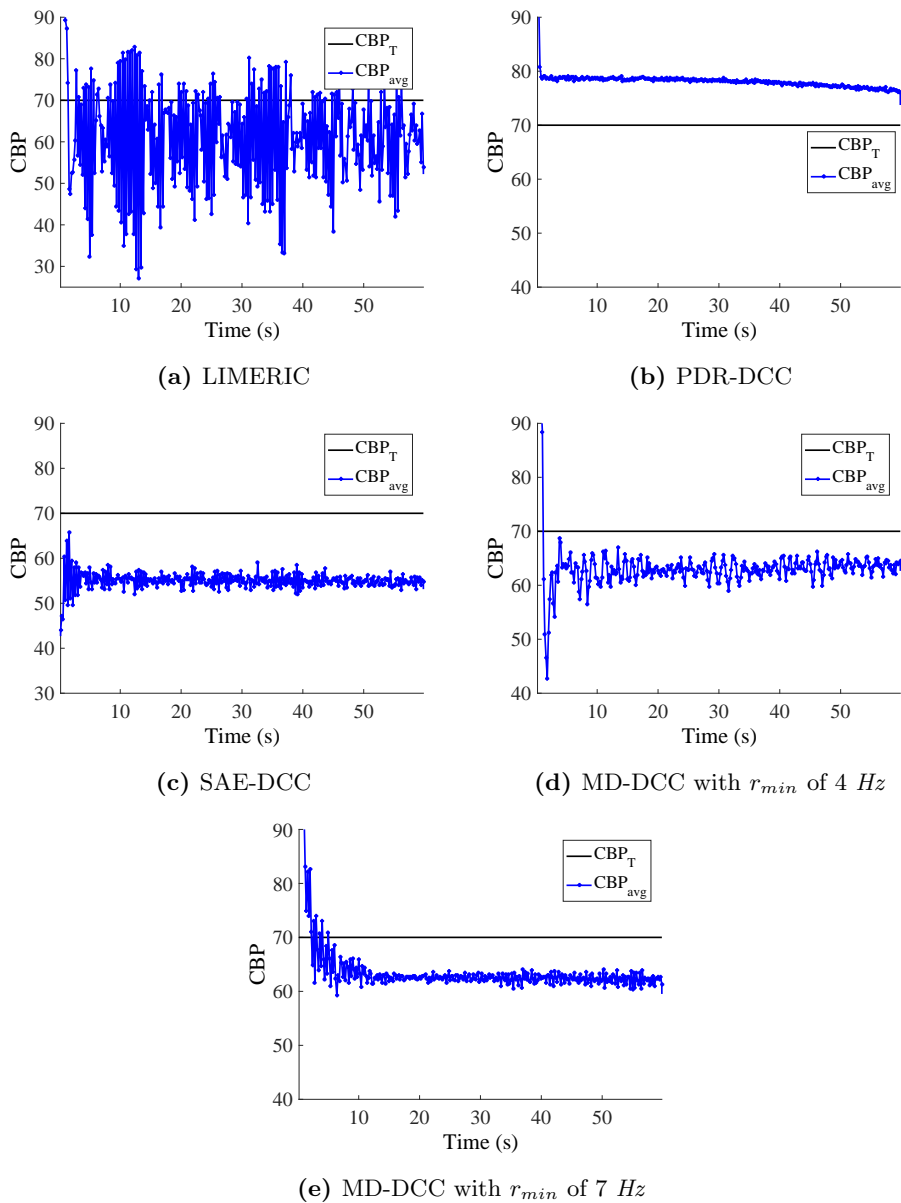


**Figure 6.6** – CBP vs. time for different DCC algorithms for density-5

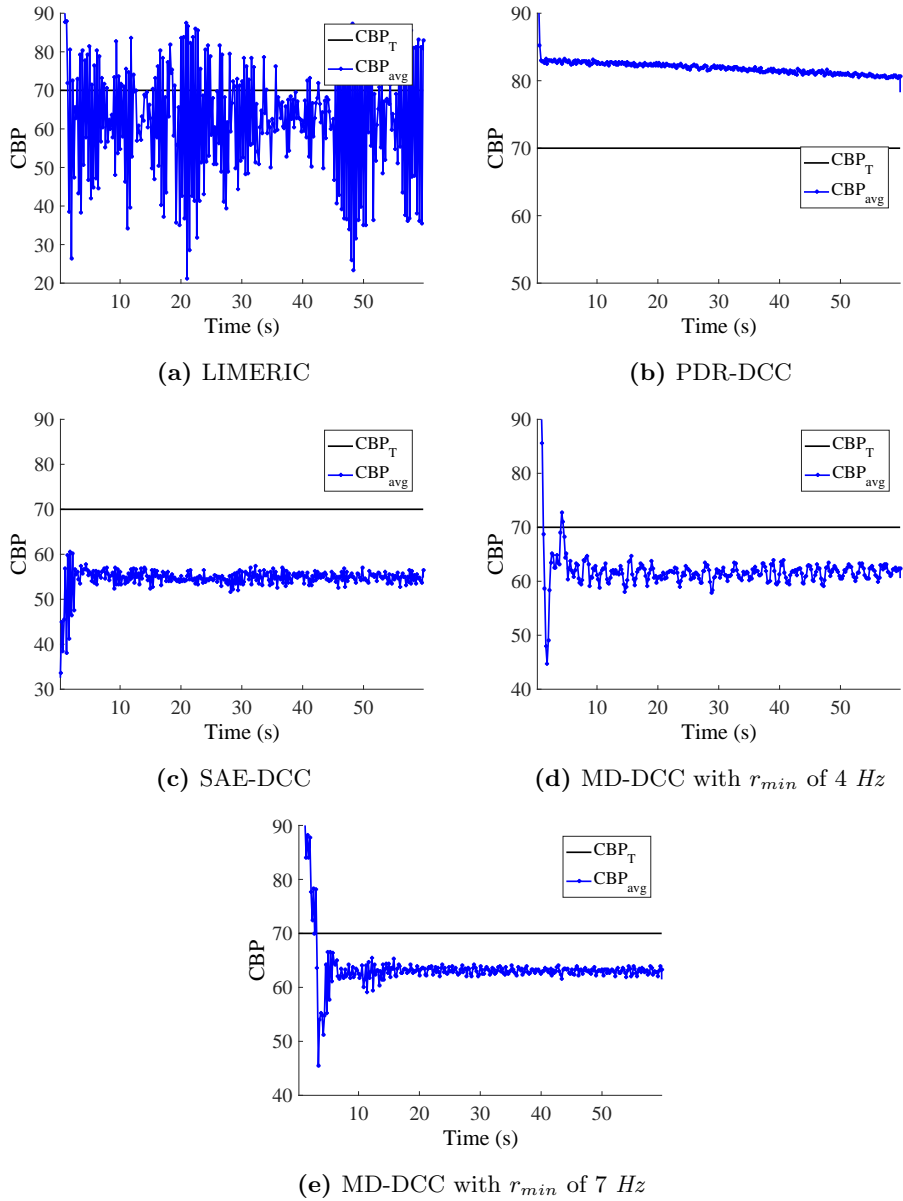
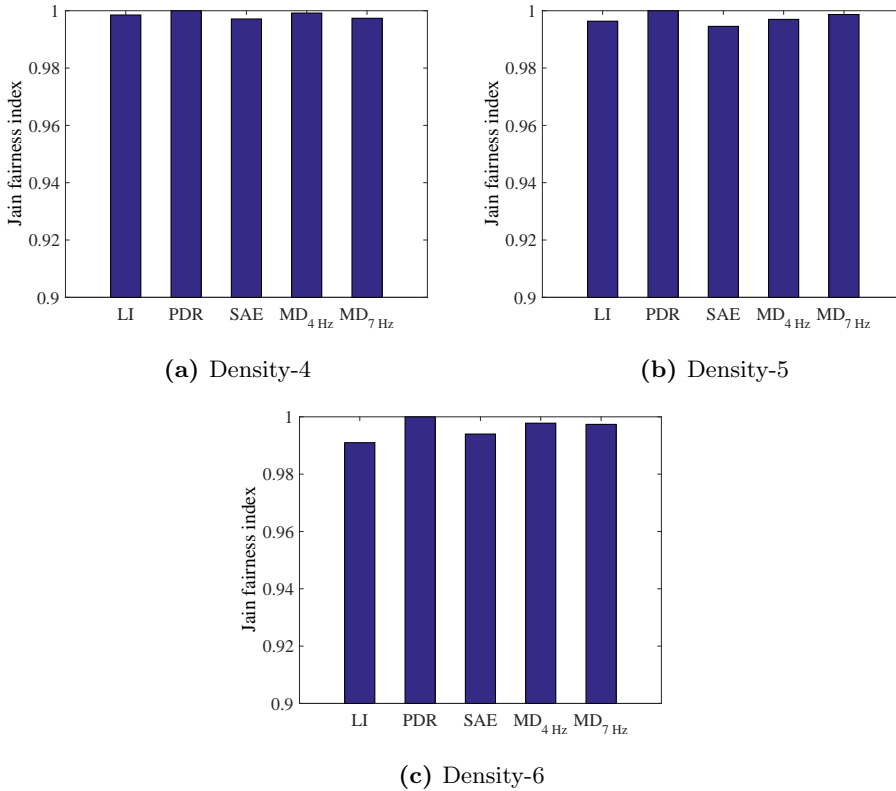


**Figure 6.7** – CBP vs. time for different DCC algorithms for density-6

### 6.5.3. Fairness observations

Fairness is assessed using Jain's fairness index as discussed in Section 4.4. Figure 6.8 shows the Jain's fairness index of LIMERIC, PDR-DCC, SAE-DCC, and MD-DCC with different  $r_{min}$  requirements for different vehicular densities. For all three densities, the Jain's fairness index of  $MD_{4\text{ Hz}}$  and  $MD_{7\text{ Hz}}$  is higher than 0.99 indicating fair allocation of channel use time by MD-DCC. The Jain's fairness index of MD-DCC is comparable to those of LIMERIC and PDR-DCC, which control only a single communication parameter (difference less than 1%) and better than SAE-DCC which controls two communication parameters.



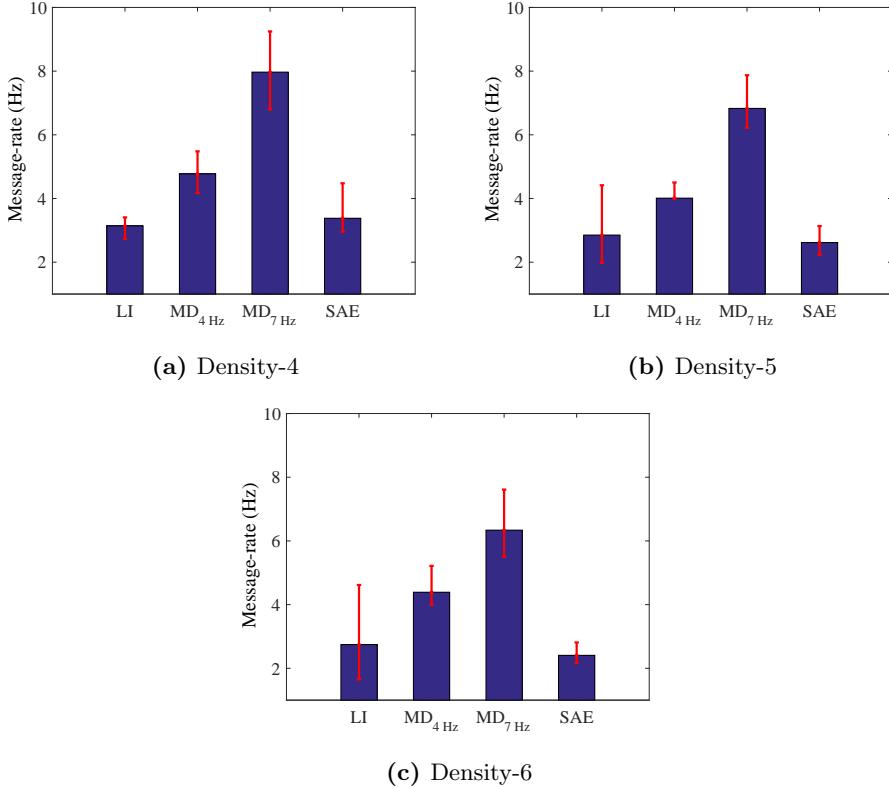
$LI$  = LIMERIC,  $PD$  = PDR-DCC,  $SAE$  = SAE-DCC and  $MD_x$  = MD-DCC, where  $x$  represents  $r_{min}$

**Figure 6.8** – Jain's fairness index for different DCC algorithms and densities

### Message-rate

To assess if MD-DCC maintains the message-rate above  $r_{min}$ , we measure the average, minimum and maximum message-rate selected by the vehicles in the observing zone over the simulation period. The message-rates are evaluated after the transition period over the observing zone. We compare the message-rate of LIMERIC, SAE-DCC and MD-DCC with different  $r_{min}$  requirements. PDR-DCC vehicles use a fixed message-rate of 10 *Hz* hence it is not considered for the comparison.

Figure 6.9 shows the message-rates of LIMERIC, SAE-DCC, and MD-DCC for different densities. The blue bar shows the average message-rate, the red bars above and below the average message-rate show the maximum and minimum message-rate respectively.



$LI$  = LIMERIC,  $SAE$  = SAE-DCC and  $MD_x$  = MD-DCC, where  $x$  represents  $r_{min}$

**Figure 6.9** – Message-rate for different DCC algorithms and densities

In Figure 6.9, we observe that  $MD_{4 \text{ Hz}}$  maintains a message-rate greater than or equal to the application requirements of 4 Hz for all three density. However, for density-5 and density-6,  $MD_{7 \text{ Hz}}$  can no longer maintain the average message-rate above the application requirements of 7 Hz because the MD-DCC vehicles have selected the maximum data-rate  $D_{max}$  of 18 Mbps (Figure 6.10). Thus, to avoid congestion MD-DCC vehicles decrease the message-rate below 7 Hz. From the above observations, it is evident that MD-DCC vehicles maintain a message-rate greater than or equal to  $r_{min}$  as long as the data-rate selected is less than  $D_{max}$ .

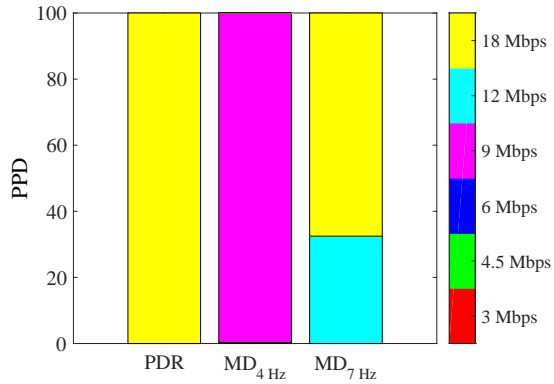
The average message-rate (Figure 6.9) of  $MD_{4 \text{ Hz}}$  and  $MD_{7 \text{ Hz}}$  is greater than LIMERIC and SAE-DCC at all three densities as MD-DCC increases the channel capacity by tuning the data-rate. The difference in the maximum and the minimum message-rate for  $MD_{4 \text{ Hz}}$  and  $MD_{7 \text{ Hz}}$  at density-5 is 0.8 Hz and 1.2 Hz respectively, which depicts a fair allocation of the message-rate by MD-DCC.

### Data-rate

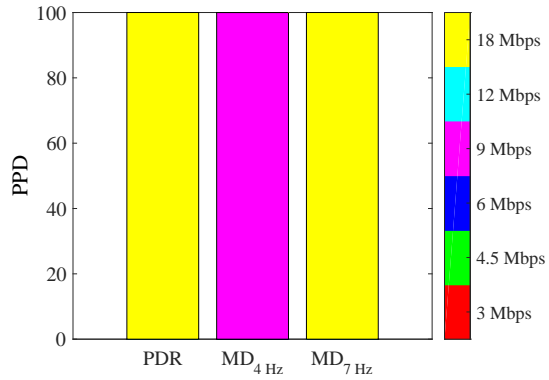
To assess if MD-DCC selects the least possible data-rate to avoid congestion, we measure the percentage of packets transmitted by the data-rate in the observing zone. The percentages of packets transmitted by the data-rate of PDR-DCC and MD-DCC with different  $r_{min}$  requirements for different densities are shown in Figure 6.10. LIMERIC and SAE-DCC use a fixed data-rate of 6 Mbps hence they are not shown in Figure 6.10.

In Figure 6.10, we observe that for all three densities PDR-DCC selects the maximum data-rate 18 Mbps. At high densities, i.e., density-5 and density-6, PDR-DCC can no longer maintain the channel load below threshold as seen in Figure 6.7 as it has already selected the maximum data-rate (18 Mbps).

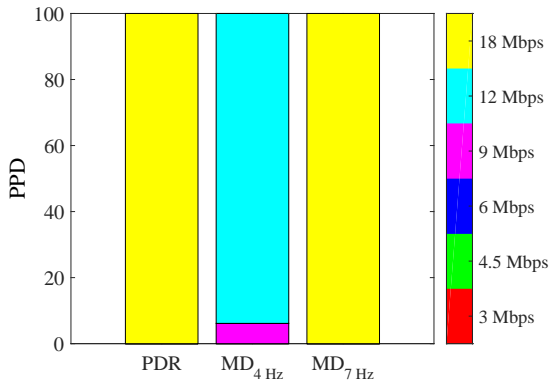
In Figure 6.10, we observe that  $MD_{4 \text{ Hz}}$  and  $MD_{7 \text{ Hz}}$  increase data-rate as the density increases as higher density requires higher channel capacity to avoid congestion. Furthermore, the data-rates selected by  $MD_{7 \text{ Hz}}$  are greater than  $MD_{4 \text{ Hz}}$  (Figure 6.10) at all three densities as  $MD_{7 \text{ Hz}}$  has a  $r_{min}$  larger than  $MD_{4 \text{ Hz}}$ . These observations show that MD-DCC selects the least possible data-rate to avoid congestion.



(a) Density-4



(b) Density-5



(c) Density-6

$PD = \text{PDR-DCC}$  and  $MD_x = \text{MD-DCC}$ , where  $x$  represents  $r_{min}$

**Figure 6.10** – Percentage of packets transmitted by the data-rate (PPD) for different DCC algorithms and densities

#### 6.5.4. Application performance observations

In this section, we evaluate the application reliability and awareness range performance of the FCW and LCW applications.

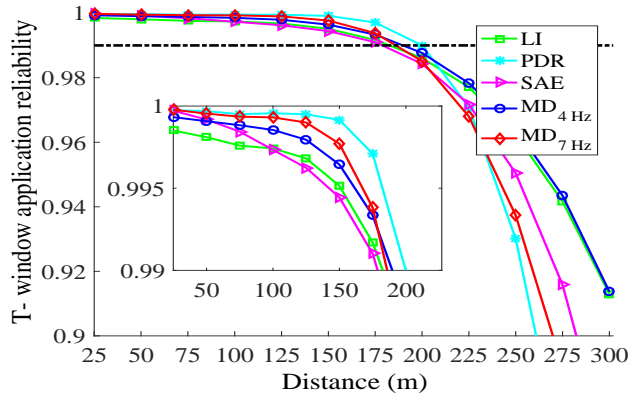
##### Application reliability

T-window application reliability ( $T_{AR}$ ) described in Section 4.4 is used to assess the application reliability. For density-4, we compare the application reliability of LIMERIC, PDR-DCC, SAE-DCC, and MD-DCC. For density-5 and density-6, we compare the application reliability performance of SAE-DCC, and MD-DCC. LIMERIC and PDR-DCC are not considered at density-5 and density-6 as they cannot hold the CBP below threshold.

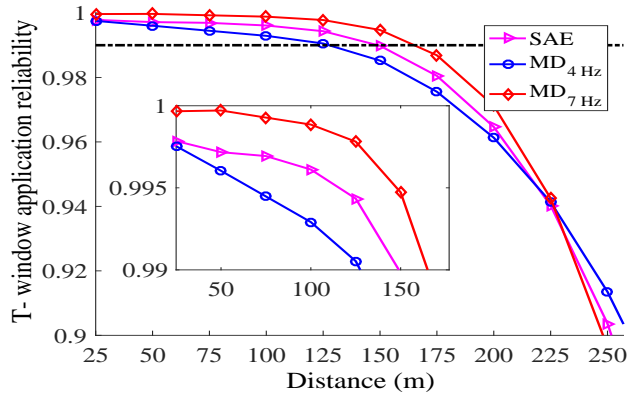
$MD_{4 \text{ Hz}}$  and  $MD_{7 \text{ Hz}}$  are adapted for FCW and LCW respectively. However, the beacon messages may need to support many applications simultaneously. We assess if MD-DCC satisfies these requirements by evaluating the application reliability performance of  $MD_{4 \text{ Hz}}$  and  $MD_{7 \text{ Hz}}$  for LCW and FCW application respectively.

Figure 6.11 and Figure 6.12 show the  $T_{AR}$  of FCW and LCW respectively for different DCC algorithms and densities. For density-4, PDR-DCC has better application reliability for FCW and LCW than other DCC algorithms till a range of 200  $m$  as it uses a fixed 10  $Hz$  message-rate.

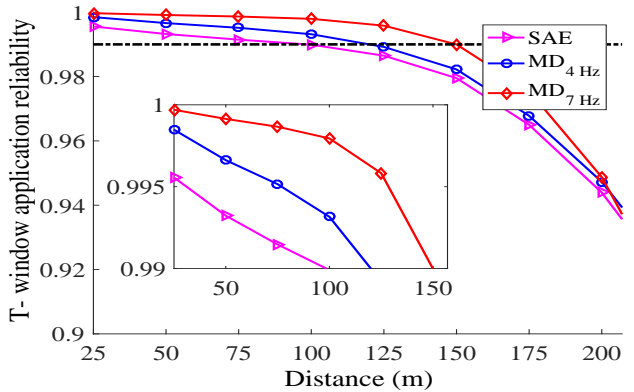
For density-5 and density-6,  $MD_{7 \text{ Hz}}$  has better application reliability for FCW and LCW than  $MD_{4 \text{ Hz}}$  and SAE-DCC till a range of 200  $m$  as  $MD_{7 \text{ Hz}}$  has higher message-rate (Figure 6.9) than  $MD_{4 \text{ Hz}}$  and SAE-DCC. However, for a range greater than 200  $m$ ,  $MD_{4 \text{ Hz}}$  has better application reliability for FCW and LCW than  $MD_{7 \text{ Hz}}$  as  $MD_{4 \text{ Hz}}$  has lower data-rate than  $MD_{7 \text{ Hz}}$ . SAE-DCC has better application reliability than  $MD_{4 \text{ Hz}}$  for a range greater than 200  $m$ , as SAE-DCC has lower data-rate than  $MD_{4 \text{ Hz}}$ .



(a) Density-4



(b) Density-5

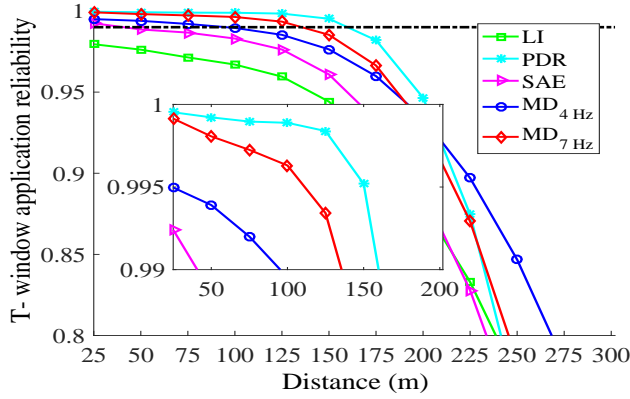


(c) Density-6

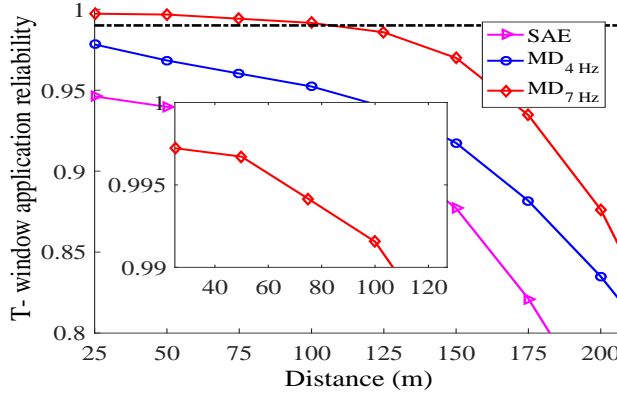
$LI$ = LIMERIC,  $PD$ = PDR-DCC,  $SAE$ = SAE-DCC and  $MD_x$ = MD-DCC, where  $x$  represents  $r_{min}$

**Figure 6.11** – Forward collision warning (FCW) application reliability for different DCC algorithms and densities as function of the distance

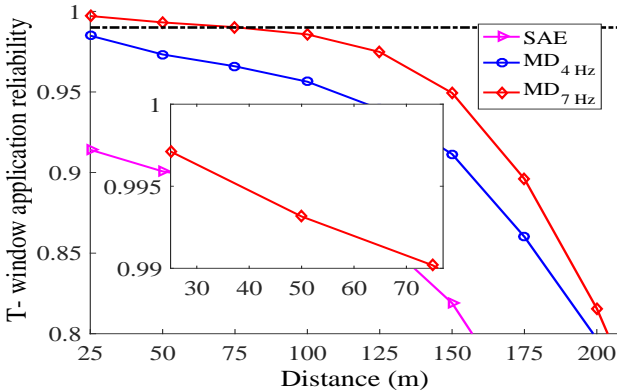




(a) Density-4



(b) Density-5



(c) Density-6

$LI =$  LIMERIC,  $PD =$  PDR-DCC,  $SAE =$  SAE-DCC and  $MD_x =$  MD-DCC, where  $x$  represents  $r_{min}$

**Figure 6.12** – Lane change warning (LCW) application reliability for different DCC algorithms and densities as function of the distance

### Awareness range

The awareness range is the maximum possible range up to which an application can be supported with a given reliability. In general, an application is considered to be reliable if the  $T_{AR}$  is greater than 0.99 as discussed in Section 4.4. This 0.99 application reliability is indicated by a horizontal line in Figure 6.11 and Figure 6.12.

Table 6.2 shows the awareness range of LIMERIC, PDR-DCC, SAE-DCC and MD-DCC for FCW and LCW application at density-5. Table 6.3 shows the awareness range of SAE-DCC and MD-DCC of FCW and LCW application for density-5 and density-6. Similar to application reliability, the awareness ranges of LIMERIC and PDR-DCC for density-5 and density-6 are not considered as they cannot hold the CBP below threshold.

For density-4, PDR-DCC has the best awareness range for the FCW and LCW application as it has the highest message-rate. FCW and LCW awareness range of  $MD_{7 \text{ Hz}}$  for density-4 is similar to PDR-DCC with a difference of less than 20  $m$  (Table 6.2).

**Table 6.2** – Awareness range of different applications and DCC algorithms for density-4

Application	Awareness range ( $m$ )				
	$MD_{4 \text{ Hz}}$	$MD_{7 \text{ Hz}}$	SAE-DCC	PDR-DCC	LIMERIC
Forward collision warning	185	180	175	195	175
Lane change warning	90	145	40	155	0

**Table 6.3** – Awareness range of different applications and DCC algorithms for density-5 and density-6

Application	Traffic Density	Awareness range ( $m$ )		
		$MD_{4 \text{ Hz}}$	$MD_{7 \text{ Hz}}$	SAE-DCC
Forward collision warning	Density-5	130	160	150
	Density-6	120	150	100
Lane change warning	Density-5	0	105	0
	Density-6	0	80	0

For density-4, LIMERIC can no longer support the LCW application even in the very near range ( $<25 m$ ) as it has a message-rate lower than 7  $\text{Hz}$   $r_{min}$ .

For density-5 and density-6,  $MD_{4\text{ Hz}}$  can no longer support the LCW application even in a very near range ( $<25\text{ m}$ ) as  $MD_{4\text{ Hz}}$  is designed for  $4\text{ Hz}$   $r_{min}$  requirements, whereas LCW has  $7\text{ Hz}$   $r_{min}$  requirement. For density-5 and density-6,  $MD_{7\text{ Hz}}$  has better FCW and LCW awareness range than  $MD_{4\text{ Hz}}$  as it has higher message-rate than others. We observe that the design of MD-DCC based on the most stringent  $r_{min}$  application requirement supports multiple applications simultaneously (Figures 6.12 and 6.11).

For density-5 and density-6, SAE-DCC can no longer support the LCW application even in the very near range ( $<25\text{ m}$ ) as it has limited channel capacity.

For FCW application at density-4,  $MD_{4\text{ Hz}}$  has better awareness range than  $MD_{7\text{ Hz}}$ . However, for FCW application at density-5 and density-6,  $MD_{7\text{ Hz}}$  has better awareness range than  $MD_{4\text{ Hz}}$ . This indicates that increasing message-rate does not always increase the awareness range of the application.

## 6.6. Conclusion

In this chapter, we proposed a combined message-rate and data-rate based congestion control algorithm MD-DCC, which keeps the message-rate above  $r_{min}$  to support application reliably. Furthermore, it maximizes the awareness range by selecting the least possible data-rate to avoid congestion.

Several aspects on the selection of various parameters of MD-DCC and their relation with the application requirements have been discussed. We have shown that MD-DCC assures fairness and has better application reliability and awareness range than other DCC algorithms through our simulation studies of a highway scenario with different vehicle densities and  $r_{min}$  application requirements. Furthermore, we have shown that MD-DCC supports large vehicular densities, specifically 2.7 and 10 times higher vehicular densities than LIMERIC (message-rate) and PDR-DCC (data-rate) algorithms respectively.

The message-rate adaptation of MD-DCC is performed using LIMERIC; however, other message-rate algorithms capable of fair message-rate allocation such as NORAC can also be utilized for MD-DCC implementation. Research is needed to see how transmit power adaptation could be combined with message-rate and data-rate strategies to guarantee the required awareness range.

## Coexistence of MD-DCC with LIMERIC

### 7.1. Introduction

Future demanding applications such as automated driving (e.g., platooning) and infrastructure supported applications (e.g., green light optimization speed advisory) will increase the channel load of vehicular communication. Furthermore, the introduction of other vulnerable road users such as pedestrians and cyclists [49] will also dramatically increase the number of vehicular communication modules. Therefore, over time, there is a need for improved congestion control algorithms, which can support the substantially higher channel loads. It is however mandatory that these new algorithms should coexist with the already deployed algorithms [49]. We should bear in mind that the coexistence of different DCC algorithms can affect the channel load, fairness and application performance as shown in [44, 45].

In the previous chapter, we proposed a combined message-rate and data-rate based congestion control algorithm (MD-DCC) which can support large vehicular densities. In this chapter, we investigate the coexistence of MD-DCC with other DCC algorithms. In Section 4.5, we have discussed several DCC algorithms that have been proposed [27–40]. We study the coexistence of MD-DCC with LIMERIC which is recommended by ETSI [123].

The specific questions we address in this chapter are:

- How does the coexistence of MD-DCC and LIMERIC affect the channel load?
- Does the introduction of MD-DCC degrade the application performance of vehicles using LIMERIC?
- How do the application reliability and awareness range of LIMERIC and MD-DCC compared to each other?
- How does the coexistence of MD-DCC and LIMERIC affect the fairness?
- Does MD-DCC retain its support to high vehicular densities in the presence of LIMERIC?

This chapter is organized as follows. Section 7.2 discusses the basic simulation setup and analyzes the simulation results to evaluate the coexistence of MD-DCC

and LIMERIC for different DCC algorithm mixes and densities. We make concluding remarks in section 7.3.

## 7.2. Coexistence performance evaluation

We perform simulations to address the questions posed in the introduction. We investigate the effects that coexistence has on channel load, fairness, and application reliability of the FCW application. We consider different mixes of vehicles using LIMERIC and MD-DCC vehicles from 0% (all vehicles run LIMERIC) to 100% (all vehicles run MD-DCC) at different vehicle densities.

### 7.2.1. Simulation setup

The simulations are performed using ns-3 [145] combined with SUMO [146] as discussed in Appendix C. The simulation setup is the same as described in Section 6.5.1.

We consider five different coexistence cases:

- Case-1: All vehicles run LIMERIC ( $LI_{100}$ )
- Case-2: 80% of the vehicles run LIMERIC ( $LI_{80}$ ) and 20% run MD-DCC ( $MD_{20}$ )
- Case-3: 50% of the vehicles run LIMERIC ( $LI_{50}$ ) and 50% run MD-DCC ( $MD_{50}$ )
- Case-4: 20% of the vehicles run LIMERIC ( $LI_{20}$ ) and 80% run MD-DCC ( $MD_{80}$ )
- Case-5: All vehicles run MD-DCC ( $MD_{100}$ )

For each of these case, we consider three vehicular densities, which are the same as in Section 6.5.1:

- Density-4: 40 vehicles per lane/km
- Density-5: 50 vehicles per lane/km
- Density-6: 60 vehicles per lane/km

In the simulation, the channel model, beacon size, simulation time, channel load threshold, and carrier sensing threshold simulation parameters are provided in Table 5.2. Message-rate, data-rate and transmit power of LIMERIC and MD-DCC are shown in Table 7.1.

LIMERIC and MD-DCC algorithm parameters are discussed in Section 6.3 and Appendix B respectively. The simulation uses the algorithm parameters shown in Table 7.2. For MD-DCC the values of  $r_{min}$  and  $\beta$  should be based on the application requirements. In this study, we focus on the performance of the FCW

**Table 7.1** – Message-rate, data-rate and transmit power of LIMERIC and MD-DCC

LIMERIC	Message-rate	1 to 10 <i>Hz</i>
	Data-rate	6 <i>Mbps</i>
	Transmit power	25 <i>dBm</i>
MD-DCC	Message-rate	1 to 10 <i>Hz</i>
	Data-rate	3, 4.5, 6, 9, 12 and 18 <i>Mbps</i>
	Transmit power	25 <i>dBm</i>

application, which requires one packet every second ( $N = 1, T = 1$  s). The value of  $r_{min}$  and  $\beta$  for the FCW application were calculated in Section 6.3.

**Table 7.2** – Algorithm parameters of MD-DCC and LIMERIC

Algorithm	Parameter	Value
LIMERIC and MD-DCC (common parameters)	$\alpha$	0.1
	$\beta$	0.051
	$X$	1 <i>Hz</i>
MD-DCC (additional parameters)	$\delta$	1 <i>s</i>
	$\gamma$	5 <i>s</i>

### 7.2.2. Channel load observations

First, we examine whether the mix of the two DCC algorithms is still able to keep the channel load below the threshold  $CBP_T$ . The average CBP of the vehicles in the observing zone over the simulation period is used to assess the channel load. Each of these measurements is performed discretely every  $\theta$  s.

Figures 7.1, 7.2 and 7.3 show the CBP experienced by different coexistence cases for density-4, density-5 and density-6 respectively. The blue line connecting all discrete measurements shows the average CBP  $CBP_{avg}$ , and the horizontal black line shows the  $CBP_T$ .

The simulations are initialized with the default communication parameters, which leads to an average CBP above  $CBP_T$  during the transition period of 0 to 1 s as discussed in Section 5.4.2.

From Figures 7.1 and 7.2, for density-4 and density-5 we observe that case-2, case-3, case-4, and case-5 maintain the average CBP below  $CBP_T$  after the transition period. The average CBP may go above  $CBP_T$  as the vehicular density changes due to mobility, however, both algorithms, operating concurrently in

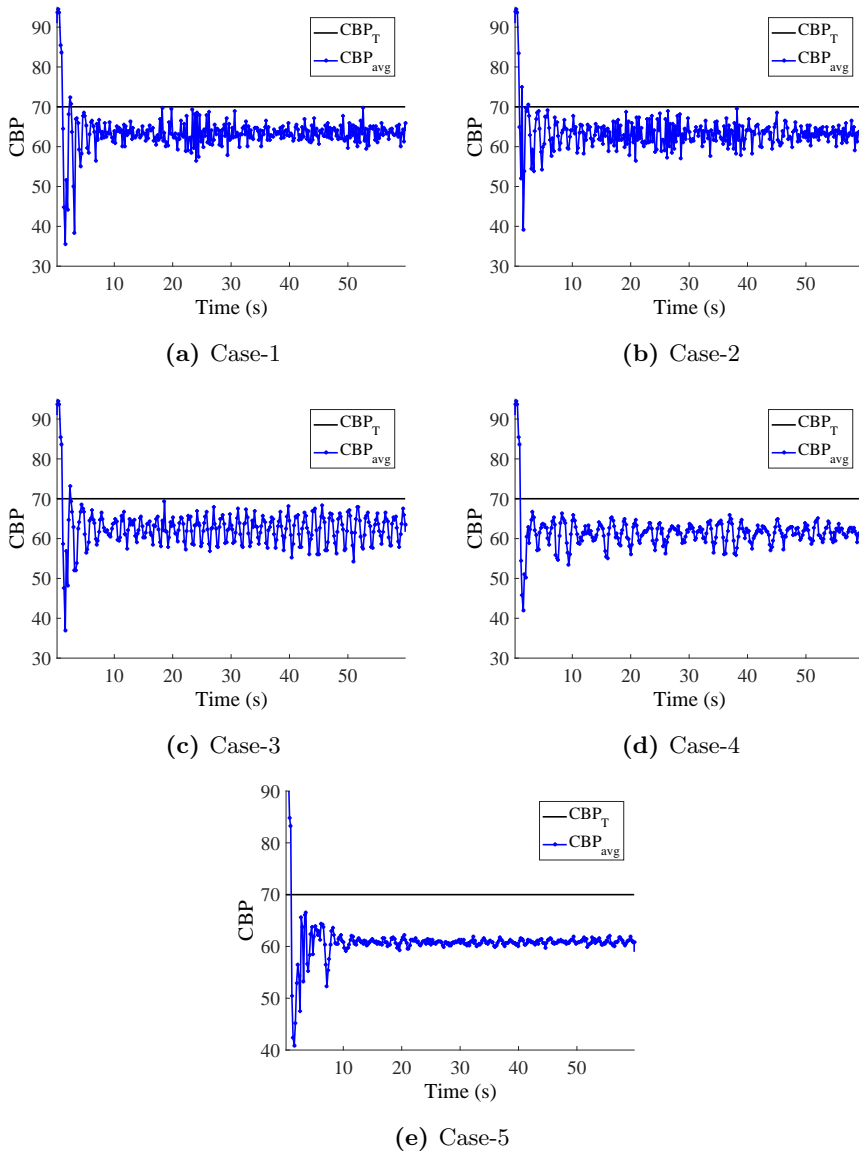


**Figure 7.1** – CBP vs. time for different coexistence cases for density-4

different vehicles, maintain the channel load below  $CBP_T$ , most of the time. For density-5, case-1 leads to oscillations of the CBP around  $CBP_T$  as seen in Figure 7.2. The CBP oscillations of LIMERIC vehicles are due to the unstable situation as discussed in Section 6.2.2.

For high densities (density-6, Figure 7.3), LIMERIC vehicles experience oscillations in the CBP around  $CBP_T$  (case-1, Figure 7.3) whereas MD-DCC

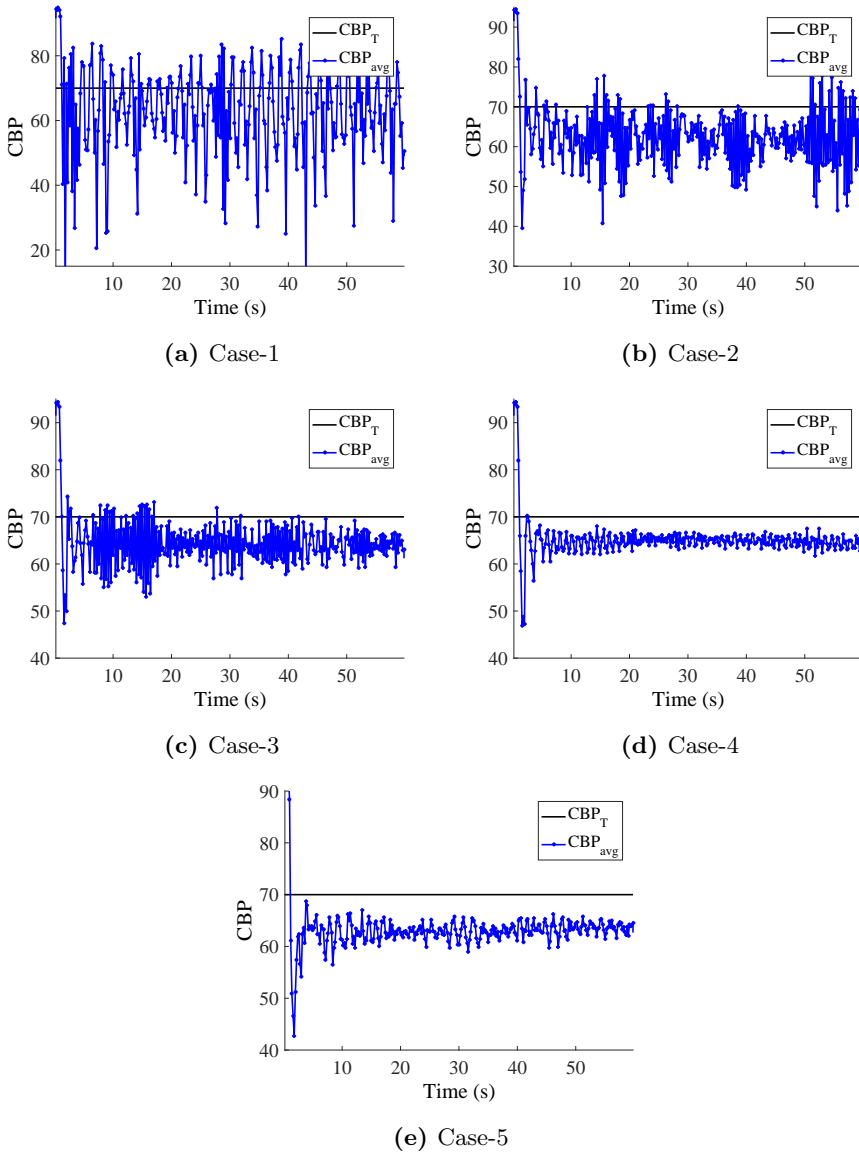


**Figure 7.2** – CBP vs. time for different coexistence cases for density-5

vehicles maintain the CBP below  $CBP_T$  (case-5, Figure 7.3). For density-6, the average CBP of case-2 (Figure 7.3) leads to oscillations similar to case-1 as LIMERIC vehicles are predominant in the mix. However, the average CBP of case-4 for density-6 is below  $CBP_T$  (Figure 7.3) as MD-DCC vehicles are now predominant in the mix. Furthermore, we observe that as MD-DCC vehicles increase in the mix the oscillation of CBP above  $CBP_T$  is reduced. The oscillations



of CBP above  $CBP_T$  indicate that vehicles very occasionally occupy part of the channel load reserved for safety-critical event-driven DENM messages, which may still affect the successful delivery of DENM messages and degrade the application performance.

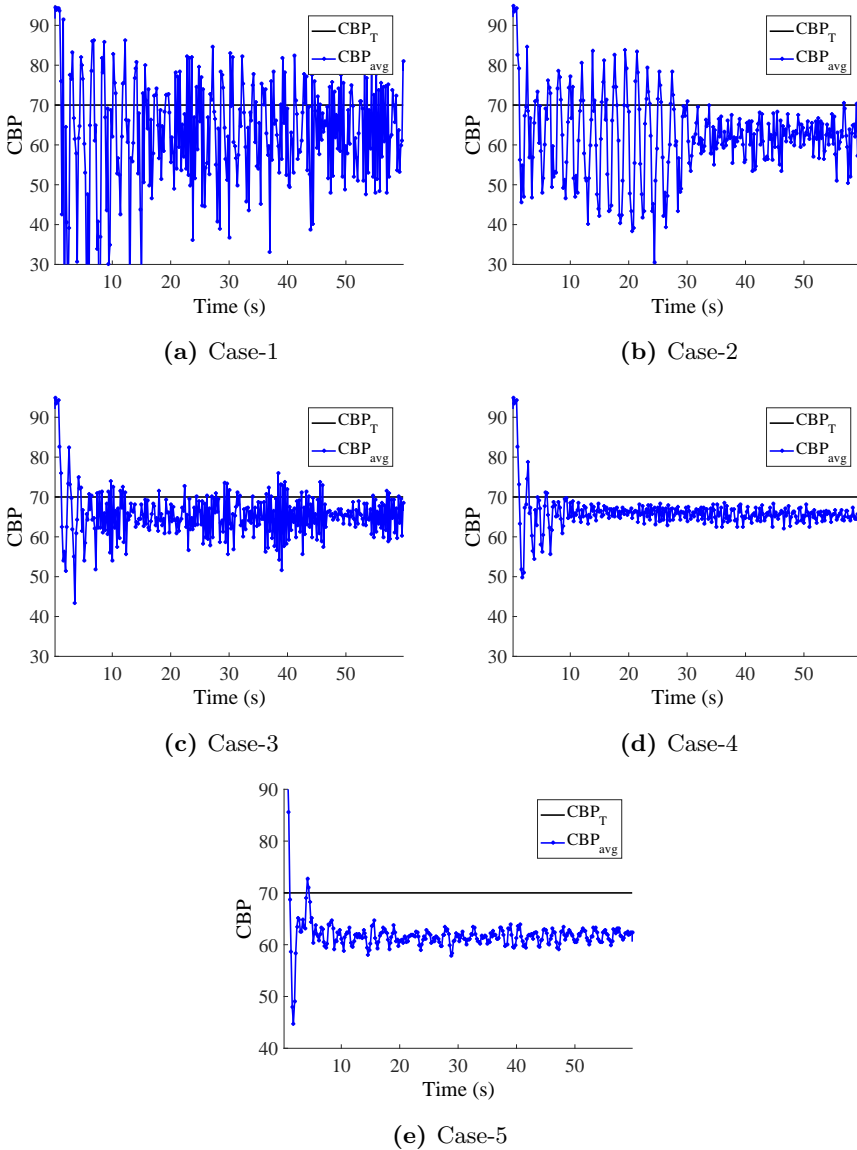
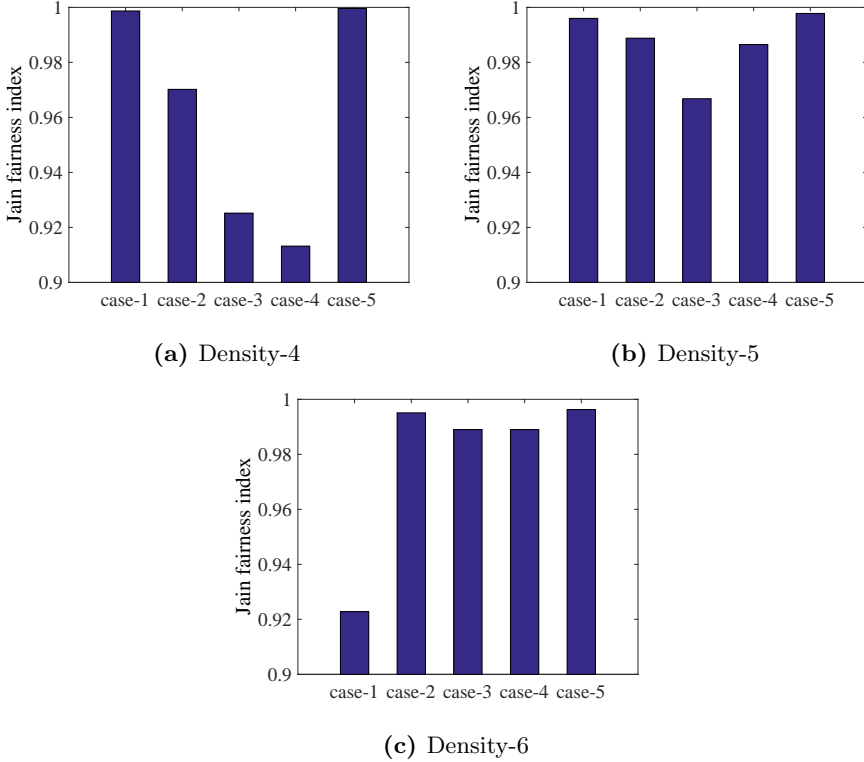


Figure 7.3 – CBP vs. time for different coexistence cases for density-6

### 7.2.3. Fairness observations

Jain's fairness index is used to quantify fairness as discussed in Section 4.4. Figure 7.4 shows the Jain's fairness index for different coexistent cases and densities.

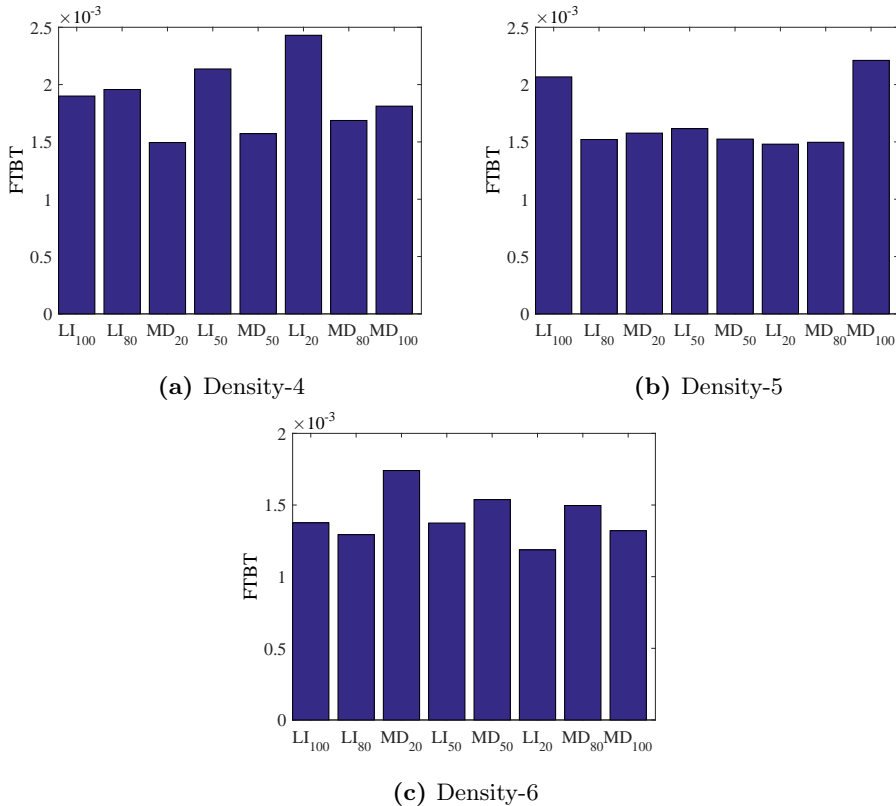


**Figure 7.4** – Jain's fairness index for different densities and coexistence cases

For density-4 and density-5 (Figures 7.4a and 7.4b), we observe that mixing MD-DCC and LIMERIC (case-2, case-3, and case-4) leads to degradation of Jain's fairness index compared to all vehicles using LIMERIC (case-1) or MD-DCC (case-5). Degradation of Jain's fairness index shows unequal distribution of channel use time. However, for density-6 (Figures 7.4c), we observe that apart from case-1 all other cases have similar Jain's fairness index.

To get a better insight, we analyze the average fraction of time spent on beacon transmission, the average message-rate and the percentage of packets transmitted by the data-rate by LIMERIC and MD-DCC vehicles in the observing zone over the simulation period as they influence the fairness performance of the vehicles as discussed in Section 4.4.

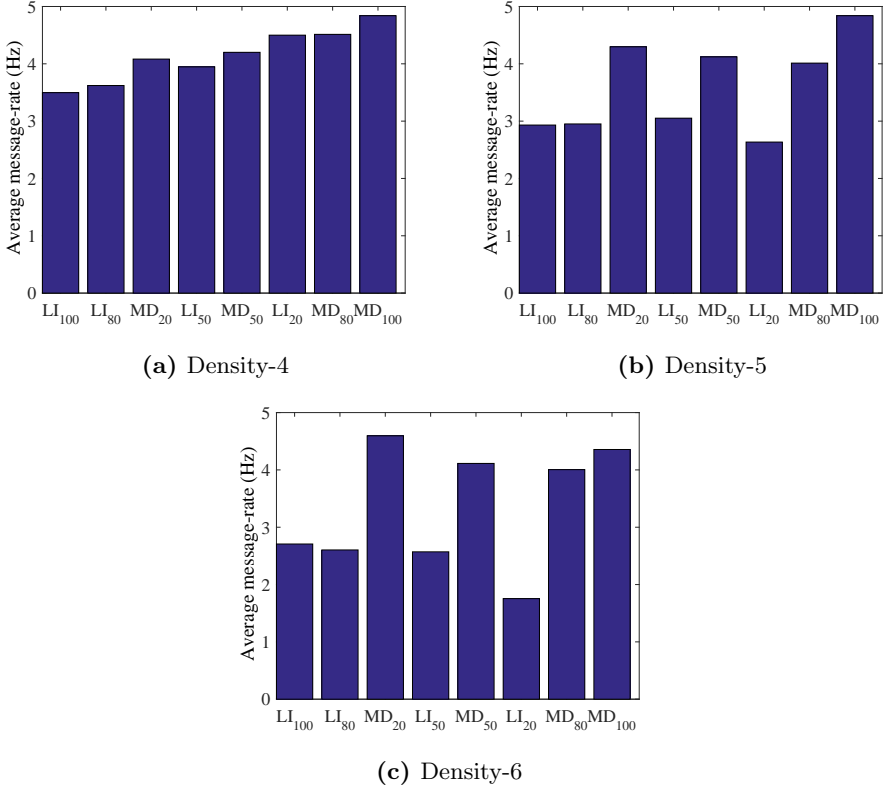
To assure fairness during coexistence, the channel use time for LIMERIC and MD-DCC should be the same. The channel use time is measured using the fraction of time spent on beacon transmission as discussed in Section 4.4. It is defined as the fraction of time spent by the vehicle for beacon message transmission in the observing zone. Figure 7.5 shows the average fraction of time spent on beacon transmission by both LIMERIC and MD-DCC. For coexistence cases, i.e. case-2, case-3 and case-4, at density-4 LIMERIC has better average fraction of time spent on beacon transmission than MD-DCC as seen in Figure 7.4a. On the contrary, for coexistence cases at density-6 MD-DCC has better average fraction of time spent on beacon transmission than for LIMERIC. This is because MD-DCC tunes both message-rate and data-rate to assure a message-rate greater than  $r_{min}$ , which is not the case for LIMERIC.



$LI_x$ = LIMERIC and  $MD_y$  = MD-DCC, where  $x$  and  $y$  are the percentage of LI and MD vehicles respectively

**Figure 7.5** – Average fraction of time spent on beacon transmission (FTBT) for different densities and coexistence cases

Figures 7.6 and 7.7 show the average message-rate and the percentage of packets transmitted by the data-rate respectively for various coexistence cases and densities. Because LIMERIC vehicles have a fixed data-rate of 6 *Mbps*, this is not shown in Figure 7.7.

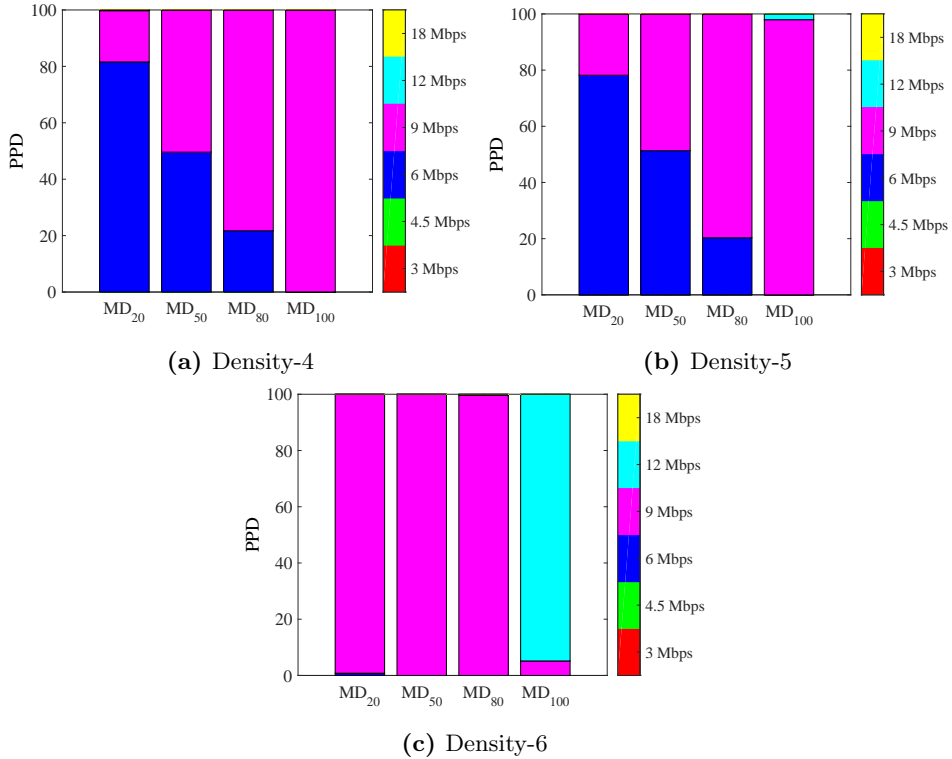


$LI_x$  = LIMERIC and  $MD_y$  = MD-DCC, where  $x$  and  $y$  are the percentage of LI and MD vehicles respectively

**Figure 7.6** – Average message-rate for different densities and coexistence cases

For density-4 (Figure 7.6a), we observe that the average message-rate of  $LI_{80}$  and  $MD_{20}$  in case-2,  $LI_{50}$  and  $MD_{50}$  in case-3 and  $LI_{20}$  and  $MD_{80}$  in case-4 are quite similar. However, for density-4 the MD-DCC vehicles may use 9 *Mbps* (Figure 7.7a) whereas LIMERIC uses 6 *Mbps* data-rate. This leads to difference of the average fraction of time spent on beacon transmission for LIMERIC and MD-DCC as seen in Figure 7.5a decreasing fairness.

For density-6 (Figure 7.6c), we observe that the average message-rate of MD-DCC vehicles is greater than for LIMERIC vehicles for case-2, case-3, and



$LI_x =$  LIMERIC and  $MD_y =$  MD-DCC, where  $x$  and  $y$  are the percentage of LI and MD vehicles respectively

**Figure 7.7** – Percentage of packets transmitted by the data-rate (PPD) for different densities and coexistence cases

case-4. However, for density-6, most of the MD-DCC vehicles use 9 *Mbps* (Figure 7.7c) whereas LIMERIC uses 6 *Mbps* data-rate. The higher message-rate of MD-DCC is compensated by its higher data-rate. Thus, difference of the average fraction of time spent on beacon transmission for LIMERIC and MD-DCC is smaller than for density-4 as seen in Figure 7.5c. This leads to better fairness for density-6 than for density-4.

To summarize, the coexistence of MD-DCC and LIMERIC may lead to unfair allocation of channel use time among the LIMERIC and MD-DCC vehicles as MD-DCC tunes both message-rate and data-rate whereas LIMERIC tunes only message-rate. The difference between channel use time between LIMERIC and MD-DCC vehicles depends on factors such as vehicular densities and mix percentage of LIMERIC and MD-DCC vehicles.

### 7.2.4. Application performance observations

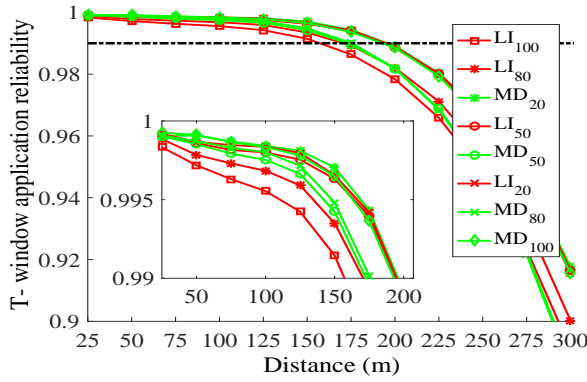
In this section, we investigate the effect of coexistence of LIMERIC and MD-DCC on application reliability and awareness range.

#### Application reliability

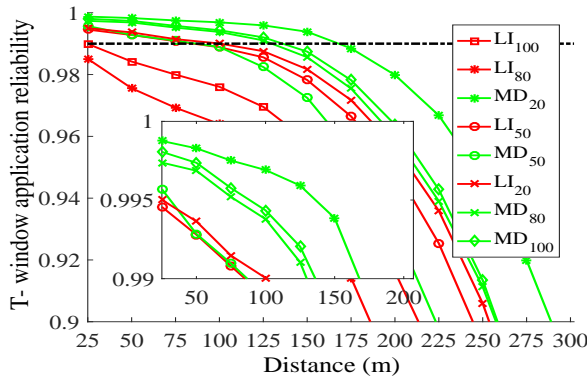
The application reliability is measured using the T-window application reliability  $T_{AR}$  discussed in Section 4.4.

Figure 7.8 shows the  $T_{AR}$  of the FCW application for different coexistence cases and densities. For density-4 and density-5 (Figures 7.8a and 7.8b), we observe that  $LI_{80}$ ,  $LI_{50}$ , and  $LI_{20}$  have better reliability performance than when all vehicles are using LIMERIC ( $LI_{100}$ ). Coexistence of MD-DCC and LIMERIC vehicles does not lead to any application reliability degradation for LIMERIC. On the contrary, mixing LIMERIC with MD-DCC leads to better reliability performance for LIMERIC vehicles as mixing increases the message-rate (Figure 7.6) of LIMERIC vehicles.

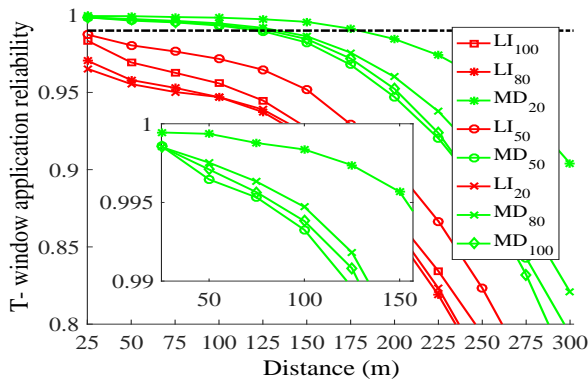
For high densities (density-6, Figure 7.8c), the application reliability of MD-DCC is better than LIMERIC vehicles because, unlike LIMERIC, MD-DCC guarantees that the message-rate does not go below  $r_{min}$ .  $MD_{20}$  for density-6 has higher message-rate than  $MD_{100}$ ,  $MD_{50}$ , and  $MD_{80}$  (Figure 7.6c) due to oscillations of the CBP above  $CBP_T$ . Hence,  $MD_{20}$  has better application reliability than  $MD_{100}$ ,  $MD_{50}$ , and  $MD_{80}$ . The results show that MD-DCC retains its support to high vehicular densities in the presence of LIMERIC.



(a) Density-4



(b) Density-5



(c) Density-6

$LI_x =$  LIMERIC and  $MD_y =$  MD-DCC, where  $x$  and  $y$  are the percentage of LI and MD vehicles respectively

**Figure 7.8** – T-window application reliability for different densities and coexistence cases

### Awareness range

Awareness range is the maximum possible range up to which an application can be supported reliably. We consider communication support to the application to be reliable if the  $T_{AR}$  is greater than 0.99 [23]. This is indicated by a horizontal line in Figure 7.8. Table 7.3 shows the awareness range of the FCW application for different coexistence cases and densities.

For all three densities, case-5 has larger awareness range than case-1. Mixing LIMERIC with MD-DCC (case-2 case-3 and case-4) leads to better awareness range for LIMERIC vehicles. For density-4 and density-5, LIMERIC and MD-DCC vehicles for coexistence case-2, case-3 and case-4 have similar awareness range, with an awareness range difference of less than 20  $m$ . For high density (density-6), MD-DCC has an awareness range of 130  $m$  whereas LIMERIC can no longer support application reliably even at a very close range ( $< 25m$ ). The results (Figure 7.8 and Table 7.3) show that MD-DCC retains its support to high vehicular densities in the presence of LIMERIC.

**Table 7.3** – Awareness range of FCW application for different coexistent cases and densities

Density	Awareness range in ( $m$ )							
	Case-1	Case-2		Case-3		Case-4		Case-5
	$LI_{100}$	$LI_{80}$	$MD_{20}$	$LI_{50}$	$MD_{50}$	$LI_{20}$	$MD_{80}$	$MD_{100}$
Density-4	195	230	205	210	210	210	220	200
Density-5	155	175	175	190	175	190	190	180
Density-6	0	0	170	0	130	0	135	130

### 7.3. Conclusion

In this chapter, we studied the coexistence of MD-DCC, a message-rate and data-rate congestion control algorithm proposed in the previous chapter, with the message-rate based LIMERIC algorithm proposed in the ETSI standard. The question of how well LIMERIC and MD-DCC coexist was answered by performing simulation studies in a highway scenario, with different mixes of LIMERIC and MD-DCC equipped vehicles and densities. We have shown that the coexistence of LIMERIC and MD-DCC avoids congestion and improves the application performance of LIMERIC vehicles. Furthermore, we have shown that MD-DCC supports application reliably at high vehicular densities even when it coexists with LIMERIC. In addition, we observed that fairness is not assured



when LIMERIC and MD-DCC coexist. Therefore, ways to assure fairness during coexistence of LIMERIC and MD-DCC should be further studied.

The study focuses on the coexistence of LIMERIC. We believe similar results could be obtained for other message-rate DCC algorithms. Future work should confirm this. Effect of coexistence of MD-DCC with other DCC algorithms such as transmit power DCC algorithms (SUPRA) and combined message-rate and transmit power DCC algorithms (SAE-DCC) on application performance needs to be studied.

## Experimental evaluation of MD-DCC

### 8.1. Introduction

In the previous chapters, it has been shown through simulations that the proposed MD-DCC outperforms other message-rate and data-rate DCC algorithms. The simulations were performed over a broad range of vehicular densities with a predefined path-loss and fading model.

In this chapter, we present an experimental evaluation of MD-DCC and validate our simulation results from the previous chapters. We use commercial off-the-shelf On-Board Units (OBUs) for V2X communication [48]. To evaluate MD-DCC for a large number of vehicles, we would need a large number of OBUs. In order to limit the cost of our experiments, we utilize an emulation platform where each OBU emulates multiple OBUs.

The goal of our experiments is to address the following questions:

- Do MD-DCC and PDR-DCC algorithms implemented on commercial OBUs adapt message-rate and data-rate as intended?
- How does the congestion point of MD-DCC compares with the results of the mathematical analysis presented in Chapter 6?
- Does MD-DCC assure fairness?
- How do abrupt traffic density changes affect MD-DCC?
- How do abrupt traffic density changes affect the coexistence of MD-DCC and LIMERIC?

The chapter is organized as follows. In Section 8.2, we describe the emulation platform and its limitations. Section 8.3 discusses the emulation set-up, the experiments we performed and what we learned from these. Finally, Section 8.4 summarizes the results and draws conclusions.

### 8.2. Emulation platform

We have built an emulation platform on commercially available MK5 OBUs from Cohda Wireless [48], as shown in Figure 8.1, on which MD-DCC is implemented and evaluated. From a V2X perspective, the MK5 can act as either an OBU or a Roadside Unit (RSU) and supports both DSRC and ITS-G5. The

emulation platform has been designed in cooperation with a master student as part of his thesis project [147]. In this section, the implementation of the DCC in MK5 and the limitations of the emulation platform are discussed.



**Figure 8.1** – The MK5 OBU used by emulation platform

We are interested in the behavior of the DCC algorithms for large vehicular densities. Since in reality each vehicle has its own OBU operating independently from other OBUs, we would, in principle, need a number of OBUs in the order of three thousand. Since this is infeasible due to cost reasons, we chose to emulate multiple virtual OBUs on one physical OBU. We call a physical OBU an Emulation Node (EN), i.e., a device that emulates the behavior of multiple OBUs. The number of physical MK5 devices we had available was four. Each EN generates and transmits several beacon messages as if generated by many OBUs (several hundreds). To be precise, for emulating  $Y$  OBUs the EN transmits at a message-rate of  $Y \times R$ , where  $R$  is the message-rate of a single OBU.

Of course, our emulation approach deviates from the behavior of OBUs in real traffic scenarios. In Section 8.2.2, we examine what this means, and consequently what the limitations are of the emulation platform and the impact on the behavior of OBUs.

### 8.2.1. DCC implementation in MK5

MK5 devices support ITS-G5 and have a DCC architecture specified by ETSI [36]. We adopt this architecture, shown in Figure 8.2, where the interaction between the DCC algorithm and the protocol layers in MK5 are shown. This is

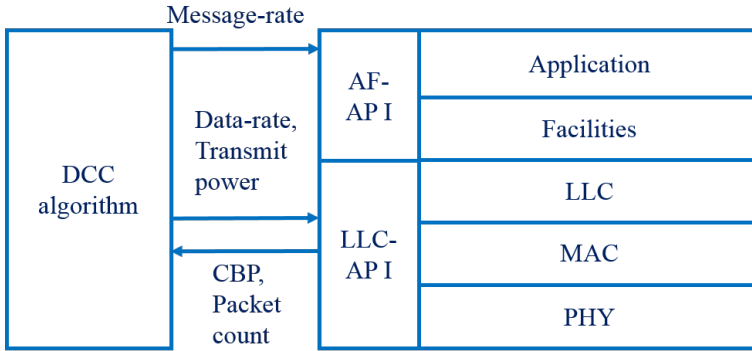


**Figure 8.2** – DCC architecture in MK5

similar to the ETSI architecture presented in Section 2.2.3. The PHY, MAC and LLC layers of IEEE 802.11p in MK5 are accessed via the Logical Link Control Application Programming Interface (LLC-API). The application and facilities layer of MK5 are accessed using the Application Facilities Layer Application Programming Interface (AF-API). The application layer runs a pseudo application to generate the beacon messages. The facilities layer controls the message-rate as determined by the DCC algorithm. The focus of the experiments is on the broadcast transmission of beacon messages and DCC algorithms in which the network and transport layers are not involved, hence, these are not considered in our implementation. Note that in our implementation, we leave out security and privacy of beacon messages. Implementing this would require a lot of processing by the MK5 devices, which would seriously restrict the number of OBUs that can be emulated by an EN, while leaving this out has no influence on the performance aspects of DCC we are interested in.

The DCC algorithms obtain the channel load information, CBP and packet count, sensed by the physical layer via the LLC-API and they adjust the message-rate, data-rate, and transmit power accordingly. The data-rate and transmit power are adjusted via the LLC-API, while the message-rate is adjusted via the AF-API.

In each EN, we implemented only one DCC instance to control all emulated OBUs because the CBP measurements are the same for all OBUs emulated by the same EN. Thus, all virtual OBUs emulated by the same EN, have identical communication parameters at all times. In reality, different OBUs may have different parameters. The implications of the differences between the emulator and the real system will be discussed in the next section.

### 8.2.2. Shortcomings of the present emulation platform

The MK5 devices are designed to function as a single OBU in one vehicle, transmitting at most 10 beacon messages per second. However, when used as an EN, each MK5 device should transmit 1000 beacon messages per second to emulate 100 OBUs. Using MK5 devices as EN has several shortcomings, which are discussed below.

#### Deviation between intended and actual beacon generating rate

For our experiments, an EN should generate beacon messages with a message-rate which is equal to  $Y$  (number of emulated OBUs) times the message-rate computed by the DCC algorithm. This is, because of processing delays in the MK5 device. For the high message-rates, i.e., of the order of 1000 *Hz*, the resulting inter-beacon generation time can be hundreds of microseconds more than intended by the DCC algorithm. To compensate this, we have implemented a controller on the ENs to correct the inter-beacon transmission delay. The controller adapts based on the difference between the EN message-rate and the desired DCC message-rate. More details on the operation and implementation of the controller can be found in [147]. The controller assures that the desired message-rate is maintained by the ENs.

#### Scenario limitations

In our study, we emulate a scenario where all vehicles are well within the sensing range of each other and utilize the same channel. The proposed scenario allows us to emulate large vehicular densities with a limited number of MK5 devices. However, the OBUs emulated by a particular EN, will behave as co-located OBUs as shown in Figure 8.3. This corresponds to an unrealistic traffic scenario where the vehicles are concentrated in a small number of geographical points, equal to the number of ENs. The emulated scenarios bear resemblance to scenarios such as traffic jams on the highway, where the separation between OBUs is minimal.

Further study and modifications of the emulation platform are necessary to emulate more realistic scenarios. The effect of co-located OBUs on the DCC performance is analyzed in next section.

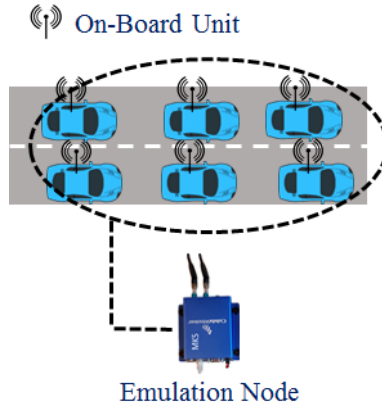


**Figure 8.3** – EN emulating multiple OBUs

### Physical limitations

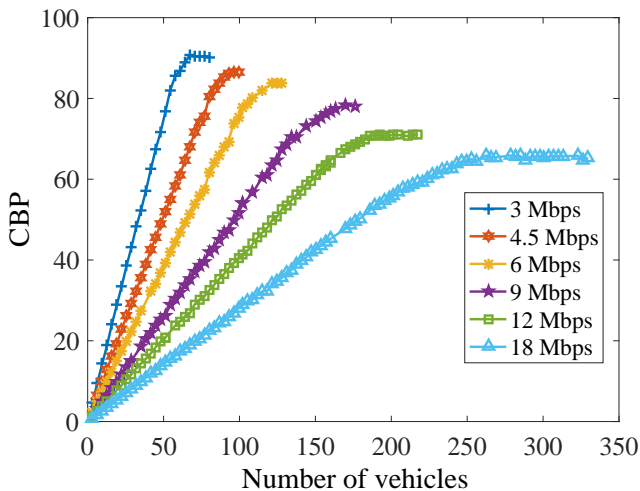
An EN emulates multiple OBUs, however, it has a single PHY and MAC protocol entity. In reality, the OBUs belonging to different vehicles generate their messages independently and use their own MAC entity to access the channel, competing with the other OBUs. Since, in case of contention, the MAC protocol uses random backoff, the order in which messages finally access the channel is also random. In our emulation experiments, however, messages generated by multiple OBUs, emulated by the same EN, queue up in the same MAC layer queue, and hence try to access the channel one after the other, in the order in which they were generated. The implications of this are:

- There is no contention between messages generated by the same EN emulating several OBUs. Thus, there are no collisions between the messages from OBUs emulated by the same EN. In reality collisions occur. On the other hand, messages generated by different ENs, still compete. In brief, the packet reception ratio (PRR) experienced by the emulated vehicles is better than in reality. Further study is necessary to quantify the effect of the emulation platform on PRR performance.
- Since the beacon messages emulated by the same EN access the channel sequentially, the channel access time is increased. This effect is discussed in detail in [147]. The study concludes that the increased channel access time limits the maximum channel load that can be created by the emulation platform. Furthermore, the study shows that augmenting

the beacon size increases the maximum channel load attainable by the emulation platform.

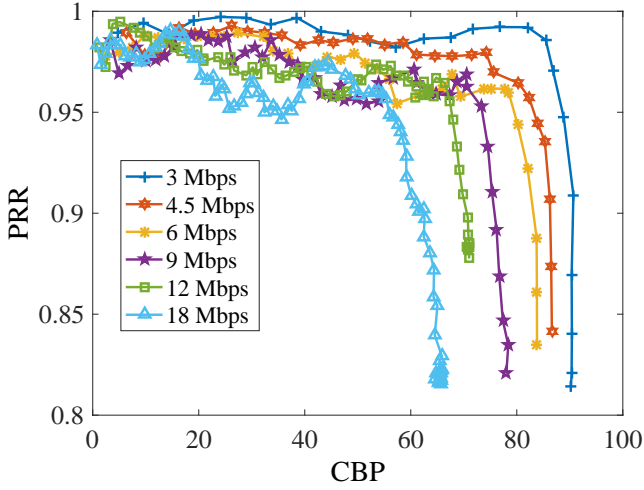
To analyze the effect of the limitations of the emulation platform, we first assess the channel load (CBP) and PRR experienced by the emulated vehicles for different data-rates and vehicular densities (number of vehicles sharing the channel). In order to emulate a large number of vehicles, we use four ENs that are placed well within the communication range of each other. The detailed set-up and parameters will be presented in Section 8.3.1. Each EN emulates a quarter of the total number of vehicles. In our preliminary experiments, the OBUs transmit at the default 10 *Hz* message-rate without any DCC. The maximum data-rate of the emulation platform is fixed at 18 *Mbps* as discussed in Section 5.2. For each vehicular density and data-rate, we run the experiment for 60 *s*. We average the CBP and PRR measurements of all four ENs.

Figure 8.4 shows the total number of vehicles and the CBP for each data-rate value. We observe that there is a limit on the CBP that can be generated by the



**Figure 8.4** – Channel busy percentage (CBP) for different vehicular densities and data-rates

platform for each data-rate. After a linear increase with the number of vehicles, the CPB levels off because of the physical limitations discussed above. The maximum CBP supported at 18 *Mbps* data-rate is around 65%. However, the more important limitation is the PRR value associated with a particular load. Figure 8.5 shows the PRR as a function of the CBP, for each data-rate. We observe that as the CBP increases beyond a data-rate dependent threshold, the PRR drastically degrades



**Figure 8.5** – Packet reception ratio (PRR) vs. channel busy percentage (CBP) for different data-rates

due to congestion of the channel and the resulting collisions of the beacon messages as observed in [117]. For instance, for 18 *Mbps* the PRR drops drastically once the CBP exceeds 60%. To support a PRR greater than 0.95 as in [23] irrespective of data-rate, we select a channel load threshold ( $CBP_T$ ) of 60% for our emulation study.

### 8.3. Experimental evaluations

In this section, we perform experiments to address the questions posed in the introduction. But first we describe in detail the emulation setup.

#### 8.3.1. Emulation setup

The basic emulation setup is shown in Figure 8.6. A computer is used to process and analyze data collected from the MK5 modules. A router is used to connect the MK5 devices to the computer using Ethernet. Due to space limitations we chose to place the four MK5 devices on the corners of a  $1\ m \times 1\ m$  table. The transmit power, carrier sensing threshold and peak antenna gain of the MK5 devices have been selected to ensure that all four devices are within the communication range of each other and share the 10 *MHz* CCH channel at 5.9 *GHz*. Thus, the distance between the MK5 devices does not affect the DCC performance study. The selection of  $CBP_T$  has been justified in Section 8.2.2. The



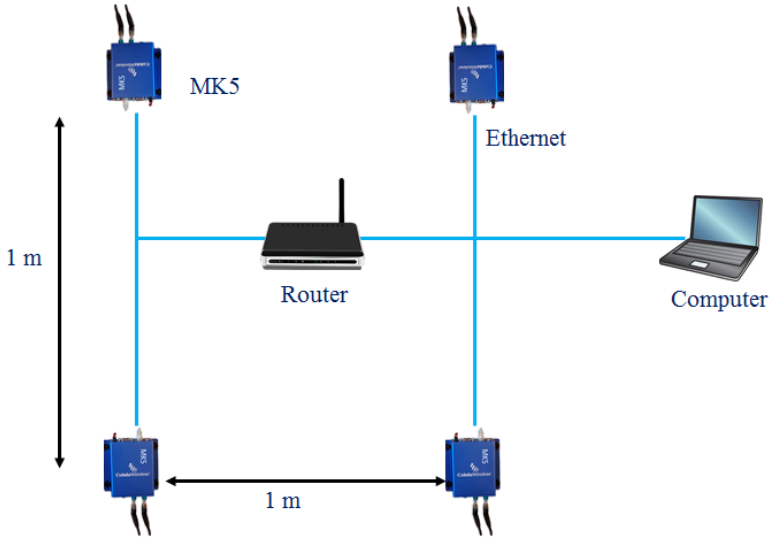


**Figure 8.6** – Lab test set-up with all four MK5 devices

beacon size is selected as in [147]. The message-rate and data-rate are selected as discussed in Section 5.4.1.

**Table 8.1** – Emulation parameters

Beacon size (Payload)	500 bytes
Channel load threshold ( $CBP_T$ )	60 %
Transmit power	0 dBm
Peak antenna gain	4.6 dBi
Carrier sensing threshold	-95 dBm
Message-rate	1 to 10 Hz
Data-rate	3, 4.5, 6, 9, 12, and 18 Mbps
Channel (CCH)	5.9 GHz

Each MK5 device can function either as an EN or as an Observing Node (ON). An ON is just another MK5 device that is used as a single OBU, as originally intended. So, an ON does not experience the limitations discussed in section 8.2.2 and therefore can provide DCC performance of a single OBU. The number of ENs and ONs depends on the vehicular density we intend to emulate.

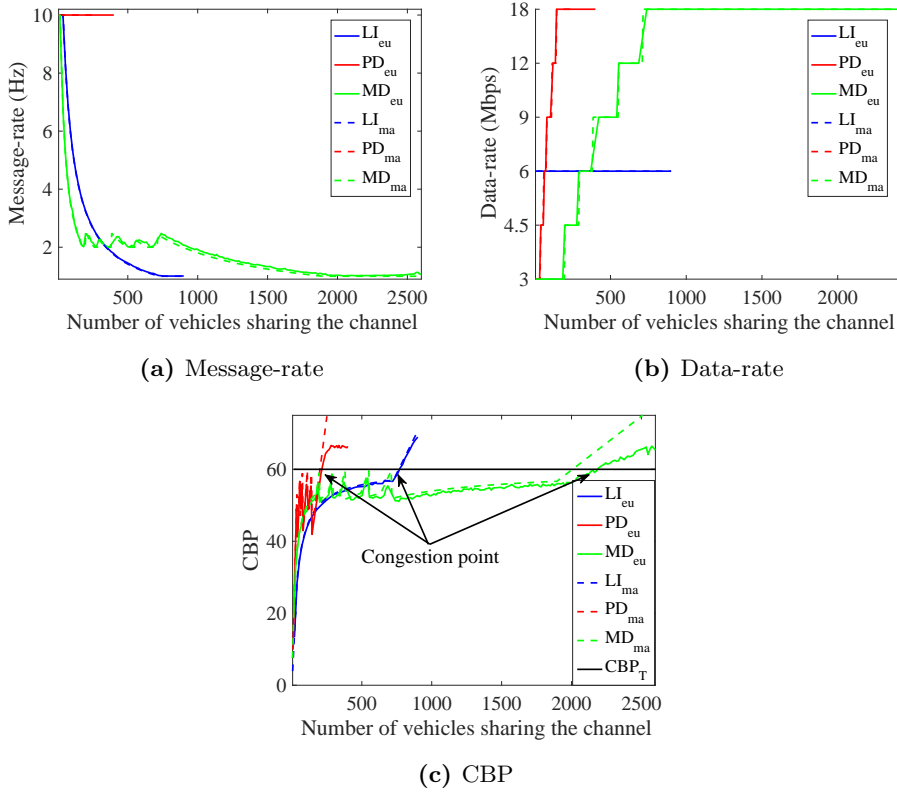
### 8.3.2. Congestion point

In this section, for the LIMERIC, PDR-DCC, and MD-DCC algorithms, we determine the congestion points and analyze their message-rate, CBP and data-rate adaptation. Furthermore, we compare the experimental results with the mathematical model presented in Section 6.4. The congestion points of LIMERIC, PDR-DCC, and MD-DCC have been computed using the mathematical model introduced in Section 6.4. Due to physical limitations of the emulation platform discussed in Section 8.2.2, we use a different  $CBP_T$  and beacon size for the emulation experiments than the ones we used in the study in Section 6.4. Thus, we need to reassess the congestion point using the mathematical model, to be able to do a comparison for the same  $CBP_T$  and beacon size as in the emulation experiments.

In order to generate sufficiently high channel load, the emulation platform uses all four MK5 devices as ENs. Each EN emulates a quarter of the number of vehicles. The implementation details and parameter selection of MD-DCC, LIMERIC, and PDR-DCC algorithms are discussed in Section 6.3, Appendix B, and Section 5.4.1 respectively. We observed that after 60 s of emulation the message-rate, data-rate and CBP of ENs are constant for a defined density and algorithm. Thus for each vehicular density, we run the algorithms for 60 s (300 iterations) to obtain the steady-state performance of the algorithms. Because LIMERIC, MD-DCC, and PDR-DCC are intended to be fair. Thus, in steady-state the message-rate and data-rate selected by all four ENs are the same.

Figure 8.7 shows the steady-state message-rate, data-rate, and CBP selected by the vehicles in both mathematical analysis and emulation experiments. From Figures 8.7a and 8.7b, we observe that the message-rate and data-rate selected by the vehicles from the mathematical model and the DCC algorithms in the emulation platform are very similar. This validates the implementation of MD-DCC, PDR-DCC, and LIMERIC DCC algorithms on the emulation platform.

Each of the congestion points of LIMERIC, PDR-DCC, and MD-DCC are indicated by an arrow in Figure 8.7c. The congestion point of the three DCC algorithms evaluated by the emulations and the mathematical model differ by less than 5% as shown in Table 8.2. A negligible difference is observed between the two results, as long as the channel load is below  $CBP_T$ . This is because in the emulation platform beacon collisions occur, while the mathematical model assumes an ideal MAC without any beacon collisions, which leads to an increasing difference with increasing message-rate and data-rate. The emulations results confirm as we



$LI_x$ = LIMERIC,  $PD_x$ =PDR-DCC, and  $MD_x$ = MD-DCC, where x represents emulations (*eu*) or mathematical (*ma*)

**Figure 8.7** – Message-rate, data-rate and CBP as a function of number of vehicles sharing the channel for LIMERIC, PDR-DCC and MD-DCC

**Table 8.2** – Congestion point of different DCC algorithms

Algorithm		Congestion point (number of vehicles)
LIMERIC	Emulation	770
	Mathematical model	770
PDR-DCC	Emulation	208
	Mathematical model	200
MD-DCC	Emulation	2150
	Mathematical model	2050

see from Table 8.2, that MD-DCC indeed supports higher vehicular densities than LIMERIC and PDR-DCC.

### 8.3.3. Fairness of MD-DCC

Fairness of the MD-DCC algorithm means that all vehicles sharing the channel should have the same message-rate and data-rate at steady-state.

In Section 6.5.1, through simulations we have shown that MD-DCC is fair. However, at the time, we did not consider whether and how fast MD-DCC converges to steady-state values. Therefore, in this section, we experimentally assess the fairness of MD-DCC and compare the results with simulations of the emulation platform.

The simulations are performed using ns-3 [46]. The simulation scenario is the one of the emulation experiments (Figure 8.6), i.e., with four ENs and the same parameters as shown in Table 8.1. The channel model is the one discussed in Section 5.4.1.

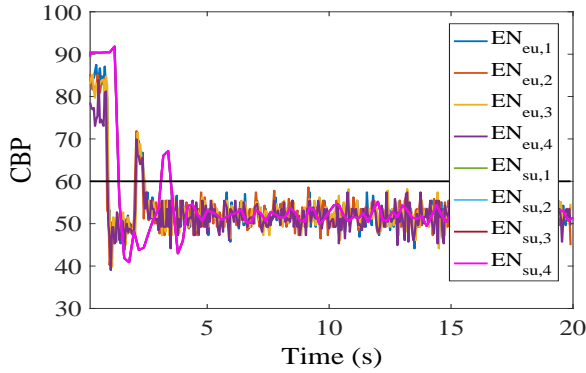
We create a medium traffic density scenario by emulating 240 vehicles, i.e., 240 OBUs with 4 ENs, where each EN is emulating 60 OBUs running MD-DCC. The initial message-rate and data-rate selected by the ENs are shown in Table 8.3. The initial data-rates are different so that we can check the convergence of MD-DCC.

**Table 8.3** – Initial message-rate and data-rate of the ENs

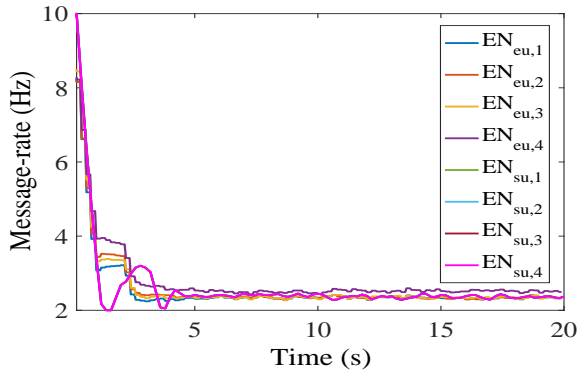
$EN_1$	Message-rate	10 Hz
	Data-rate	3 Mbps
$EN_2$	Message-rate	10 Hz
	Data-rate	6 Mbps
$EN_3$	Message-rate	10 Hz
	Data-rate	9 Mbps
$EN_4$	Message-rate	10 Hz
	Data-rate	18 Mbps

Figure 8.8 shows the CBP, message-rate, and data-rate selected by the vehicles for both emulation experiments and simulation. All virtual OBUs emulated by the same EN, have identical CBP, message-rate, and data-rate at all times. Hence the message-rate, data-rate and CBP measurements are obtained from an emulated OBU of the ENs every 200 ms over a period of 60 s.

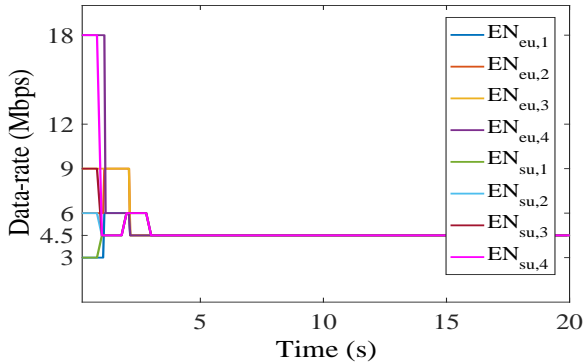
From Figure 8.8a, we observe that the initial message-rate and data-rate lead to a channel load above the threshold  $CBP_T$ . However, MD-DCC running on ENs of both emulation and simulation platform adapts the message-rate and data-rate



(a) CBP



(b) Message-rate



(c) Data-rate

$EN_{x,y}$  = Emulation Node, where  $x$  represents emulations ( $eu$ ) or simulations ( $su$ ) and  $y$  represents device number

**Figure 8.8** – MD-DCC adaptation with time

as seen in Figure 8.8b and Figure 8.8c respectively to reduce the channel load below the threshold  $CBP_T$ .

In Figures 8.8b and 8.8c, we observe that after 5  $s$  irrespective of their initial message-rate and data-rate, of ENs in both experiments and simulation select very similar message-rate (we found difference less than 2%) and the same data-rate (4.5  $Mbps$ ). This validates the implementation of MD-DCC algorithm on the simulation platform. Furthermore, it demonstrates that MD-DCC leads to a convergence of message-rate and data-rate for all ENs in steady-state to assure fairness.

#### 8.3.4. MD-DCC adaptation to abrupt changes in vehicle density

DCC algorithms should be able to always keep the CBP below the threshold  $CBP_T$ . In Chapter 6 we have verified that MD-DCC keeps the CBP below the threshold  $CBP_T$ , through simulations, for different traffic densities. However, we did not consider dynamically changing densities. In this section we address this by looking how MD-DCC responds to sudden traffic density changes in an emulation scenario.

The emulation set-up uses three ENs and one ON. All vehicles run the MD-DCC algorithm. The ENs are used to emulate the required density and the ON is used to study the adaptation of MD-DCC. The MD-DCC parameters are selected for an  $r_{min}$  of 4  $Hz$  as discussed in Section 6.3. The experiment started with all vehicles having the default message-rate of 10  $Hz$  and data-rate of 6  $Mbps$ .

Figure 8.9 shows different aspects of the adaptation of MD-DCC to abrupt density changes. Figure 8.9a shows the vehicular density changes. The scenario is designed to mimic the movement of a given vehicle, emulated by an ON, from a sparse environment (30 vehicles/ $km^2$ ) to a very dense environment (240 vehicles/ $km^2$ ) corresponding to an adjoining 4 lane congested highway (inter-vehicle distance of around 10  $m$ ) and back (Figure 8.10). This leads to a sudden surge and decline of vehicular density. Figures 8.9b, 8.9c and 8.9d show the CBP, message-rate, and data-rate selected by MD-DCC respectively. These measurements are obtained from the ON every 200  $ms$ .

Figure 8.9b, shows that the abrupt change in density leads to a sudden spike of the CBP at 10  $s$ . However, MD-DCC quickly adapts the message-rate and the data-rate to maintain CBP below  $CBP_T$  very soon after the density increases, as seen in Figures 8.9c and 8.9d. Furthermore, when the density abruptly decreases at time 42  $s$ , MD-DCC decreases the data-rate and increases the message-rate

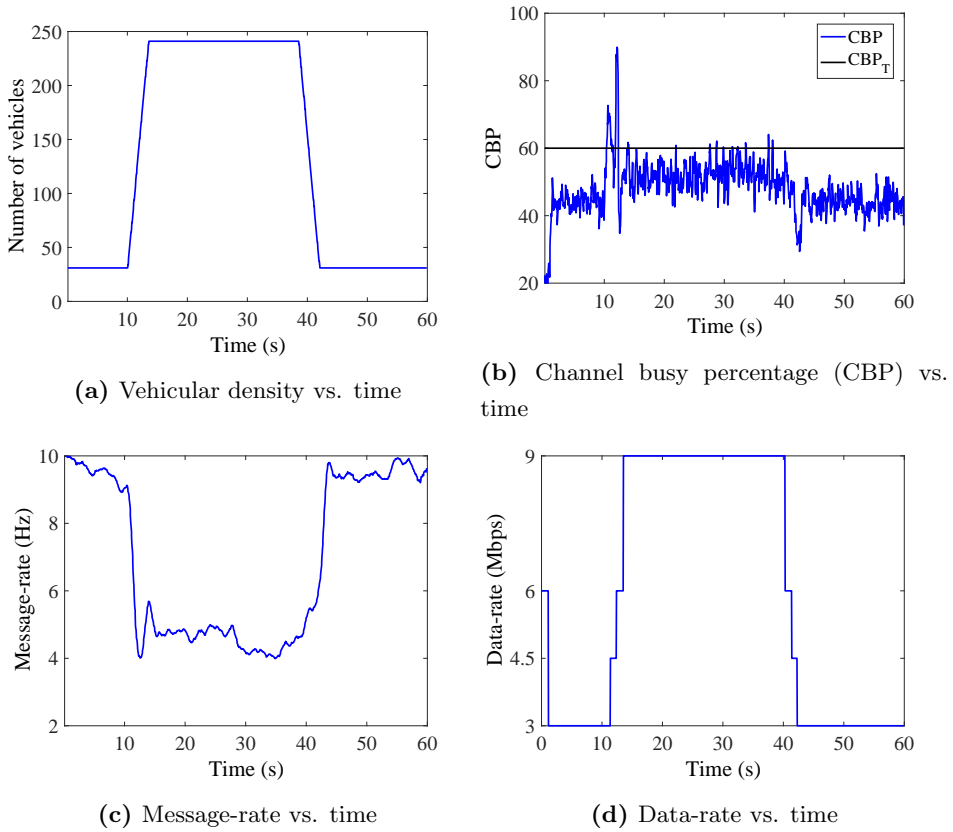


Figure 8.9 – MD-DCC adaptation for abrupt density changes

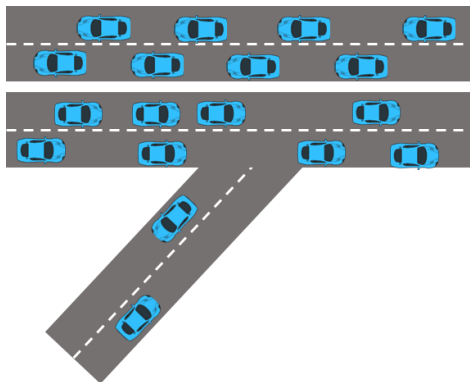


Figure 8.10 – Example scenario for abrupt traffic density changes

to increase the application reliability and awareness range of the application as discussed in Section 6.2.3.

### 8.3.5. Effect of dynamic density changes on the coexistence of MD-DCC and LIMERIC

In a scenario where MD-DCC and LIMERIC coexist, DCC should keep the CBP below the threshold  $CBP_T$ , even when abrupt density changes occur. This was not considered in our coexistence study in Chapter 7. Therefore, in this section we experimentally analyze the effect of abrupt traffic densities changes in case of coexistence of MD-DCC and LIMERIC.

The emulation platform ensures that half of the vehicles run MD-DCC and the other half run LIMERIC. The emulation uses two ENs ( $EN_1, EN_2$ ) and two ONs ( $ON_1, ON_2$ ).  $EN_1$  emulates LIMERIC vehicles, and  $EN_2$  emulates MD-DCC vehicles. Similarly,  $ON_1$  and  $ON_2$  are used to observe LIMERIC and MD-DCC respectively. The MD-DCC algorithm parameters are selected for  $4\text{ Hz } r_{min}$  as discussed in Section 6.3. The parameters of LIMERIC are discussed in Appendix B. The emulation starts with both LIMERIC and MD-DCC vehicles having the default message-rate of  $10\text{ Hz}$  and data-rate of  $6\text{ Mbps}$ .

Figure 8.11 shows the effect of abrupt density changes on the coexistence of MD-DCC and LIMERIC. Figure 8.11a shows how the vehicular density changes over time. It is the same scenario as in the previous section. Figures 8.11b, 8.11c and 8.11d show the CBP, message-rate, and data-rate respectively. These measurements are obtained from the ONs every  $200\text{ ms}$ .

From Figure 8.11b, we observe that MD-DCC and LIMERIC successfully adapt to density changes and both maintain CBP below  $CBP_T$ . Note that the CBP of MD-DCC and LIMERIC are not the same as they are measured at two different ONs which are not calibrated or synchronized.

From Figure 8.11c, we observe that the message-rate of MD-DCC is always greater than the  $4\text{ Hz } r_{min}$  to ensure reliability, and is greater than that of LIMERIC. Furthermore, the data-rate of MD-DCC is always less than or equal to the data-rate of LIMERIC ( $6\text{ Mbps}$ ) as seen in Figure 8.11d.

Figure 8.11e shows the fraction of time spent for beacon transmission over a  $1\text{ s}$  interval by both LIMERIC and MD-DCC. It is calculated every  $1\text{ s}$  and was discussed in Section 4.4. To assure fairness in case of coexistence, the fraction of time spent on beacon transmission for LIMERIC and MD-DCC should be the same. From Figure 8.11e, we observe that the fraction of time spent on beacon transmission for MD-DCC is greater than for LIMERIC. Thus, fairness is not assured when MD-DCC and LIMERIC coexist as MD-DCC tunes both message-rate and data-rate whereas LIMERIC tunes only the message-rate. The difference in fraction of time spent for beacon transmission of LIMERIC and



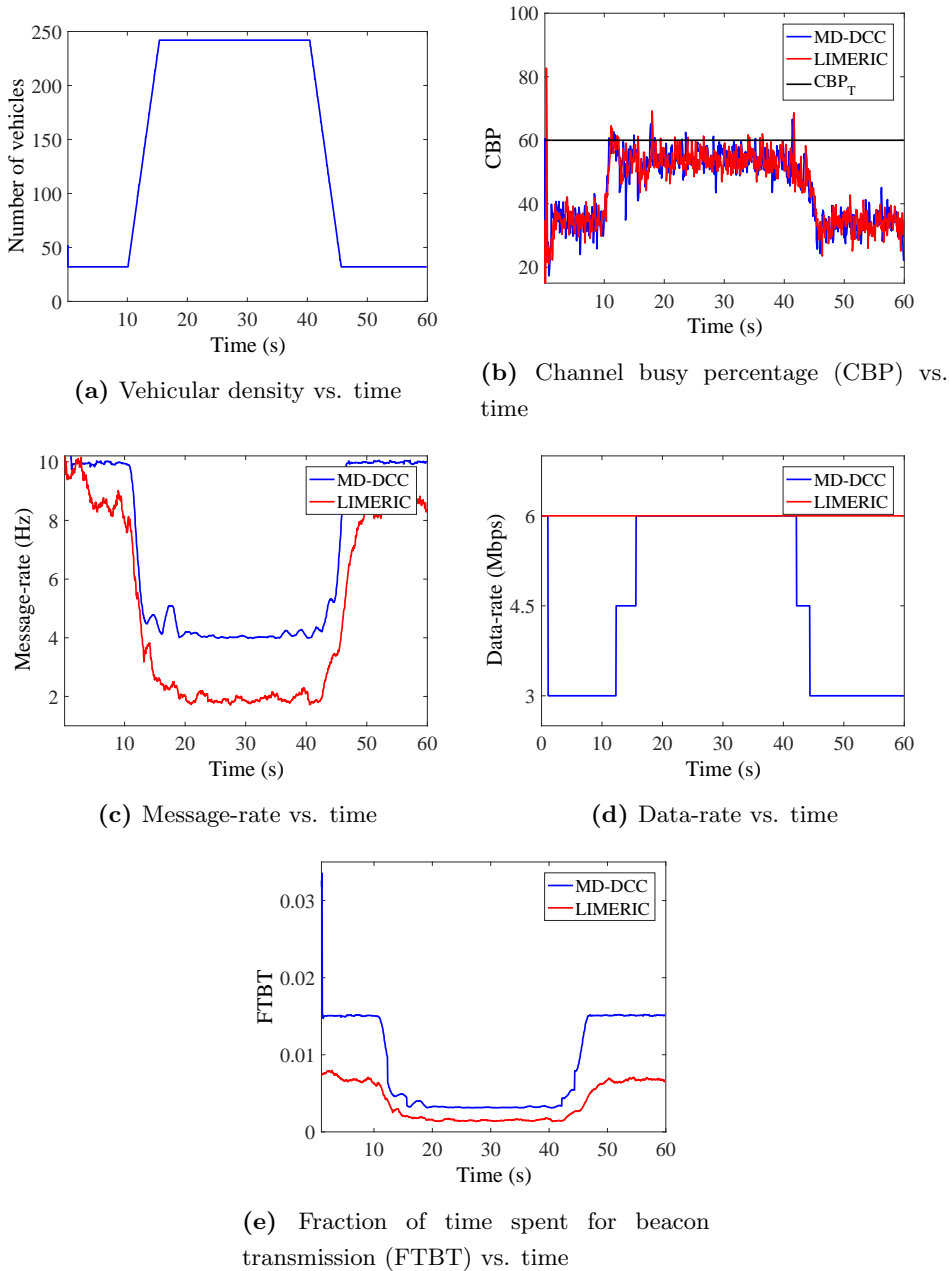


**Figure 8.11** – Effect of abrupt density change in case of coexistence of LIMERIC and MD-DCC

MD-DCC depends on various factors such as vehicular density and mix percentage of LIMERIC and MD-DCC as discussed in Section 7.2.3.

### 8.4. Conclusion

A DCC emulation platform has been implemented on commercial OBUs, in which MD-DCC, PDR-DCC, and LIMERIC were implemented. MD-DCC functionality and performance have been evaluated using the emulation platform.

The experiments have shown that MD-DCC and PDR-DCC implemented on commercial OBUs, adapt message-rate and data-rate as intended and maintain the channel load below the threshold. Furthermore, the results demonstrate that MD-DCC assures fairness and supports around a 2.7 and 10 times larger vehicular density than the message-rate LIMERIC and data-rate PDR-DCC algorithms respectively. In addition, we have shown that MD-DCC successfully adapts the message-rate and data-rate in response to abrupt traffic density changes to maintain the channel load below the threshold. Furthermore, MD-DCC retains its capability to adapt to abrupt traffic density changes even when it coexists with LIMERIC.

The emulation experiments have been performed using a limited number of OBUs and have several limitations. Thus, we have not been able to evaluate the application performance of MD-DCC. Field trials are necessary to evaluate the application performance of MD-DCC under various traffic densities and scenarios such as urban and rural before deployment of MD-DCC.



## Conclusion and future work

In this final chapter, we sum up the overall research findings, pinpointing the most relevant contributions. Furthermore, we discuss some promising future research directions that we foresee in the light of our studies.

### 9.1. Conclusion

Vehicular communication based safety applications rely on exchange of messages between vehicles, to inform their environment, and, foresee and avoid hazardous situations. In this thesis, we focused on ensuring a desirable application performance at high vehicular densities by means of Decentralized Congestion Control (DCC) algorithms. Channel congestion is the major cause for degradation of the application performance at high vehicular densities. DCC algorithms optimize the usage of the channel to avoid congestion which is crucial for a desirable application performance at high vehicular densities. We have systematically investigated the effect of vehicular density on the application performance. Specifically, the contributions are categorized according to the research problems defined in Section 1.4.

#### **Influence of communication parameters on the application performance**

We have analyzed the restrictions imposed on communication parameters, message-rate, data-rate, transmission power, and carrier sensing threshold to maintain the desirable application reliability and awareness range of the application. We have shown that the communication reliability, i.e., the probability of successfully delivering beacon messages, and message-rate of the vehicles determine the application reliability. We have specifically presented a method to determine the minimum message-rate required to maintain the desired application reliability.

**Formulation of the requirements of DCC algorithms to ensure reliable application performance**

We performed state-of-the-art analysis of DCC algorithms and analyzed their effect on the application performance. Based on the inferences from the analysis, we formulated the key design goals of the DCC algorithms to ensure reliable application performance. The proposed DCC algorithms in this thesis address these design goals. In addition, we have shown that unlike transmit power and carrier sensing threshold DCC algorithms, message-rate and data-rate DCC algorithms control the channel load independent of the distribution of the neighbor vehicles. Furthermore, we have shown that data-rate DCC algorithms support a higher number of beacon messages on the channel than transmit power, message-rate, and carrier sensing threshold DCCs.

**Definition analysis and evaluation of data-rate DCC**

We have proposed a data-rate based congestion control algorithm PDR-DCC, to improve application reliability. We have argued that increasing message-rate increases application reliability. Thus, PDR-DCC maintains a message-rate of 10 *Hz* to maximize the application reliability. We have shown that irrespective of application requirements PDR-DCC (data-rate DCC) has better application reliability at near range ( $\leq 200$  *m*) than message-rate (LIMERIC) and transmit power (SUPRA) based DCC algorithms. However, using a fixed 10 *Hz* message-rate for data-rate DCC may lead to lower awareness range than other DCC algorithms. In addition, the study has indicated that a combined message-rate and data-rate congestion control increases the awareness range of the application and the maximum vehicular density supported by DCC algorithms.

**Definition analysis and evaluation of a combined message-rate and data-rate DCC**

We have proposed a combined message-rate and data-rate congestion control MD-DCC that supports large vehicular densities. The essence of MD-DCC is to maintain a message-rate above the minimum required message-rate of the application to ensure the desired application reliability. Furthermore, it selects the minimum data-rate to maximize the awareness range of the application. We have demonstrated that MD-DCC satisfies the key design goals of DCC. We have shown that MD-DCC has better application reliability and awareness range than the earlier proposed PDR-DCC and algorithms suggested in ETSI (LIMERIC) and SAE (SAE-DCC) standardization bodies. DCC algorithms should be capable of supporting multiple application simultaneously. Thus,

we have proposed and demonstrated adaptation of MD-DCC based on the most stringent minimum message-rate requirements of the applications to ensure reliable functioning of multiple applications, which is not the case for other DCC algorithms. Furthermore, we have shown that MD-DCC supports 2.7 and 10 times higher vehicular densities than LIMERIC (message-rate) and PDR-DCC (data-rate) respectively.

### **Study of coexistence of DCC algorithms**

We quantified the effect of coexistence of MD-DCC with the ETSI proposed LIMERIC on application performance. We have demonstrated that MD-DCC retains its support to high vehicular densities even when it coexists with LIMERIC. We have shown that there is no significant degradation of the application performance when MD-DCC coexists with LIMERIC. Furthermore, we have demonstrated that coexistence with MD-DCC improves the application performance of LIMERIC. However, fair allocation of the channel use time during coexistence is not assured. In summary, the coexistence of MD-DCC with LIMERIC avoid congestion without any significant degradation of application performance; however, they may experience fairness issues.

### **Experimental evaluation of DCC algorithms**

We performed a preliminary experimental evaluation of MD-DCC. The experiments were performed using a limited number of IEEE 802.11p On-Board Units (OBUs) used for V2X communication. We implement MD-DCC, LIMERIC and PDR-DCC algorithms on OBUs. Through emulations, we demonstrated that MD-DCC assures fairness. In addition, we demonstrated that MD-DCC quickly adapts to abrupt traffic density (channel load) changes and avoids congestion even while coexisting with LIMERIC. Furthermore, we demonstrated that MD-DCC indeed supports higher vehicular densities than message-rate (LIMERIC) and data-rate (PDR-DCC) algorithm.

We conclude that the maximum vehicular density for which an application is supported reliably is increased by using the algorithms presented in this thesis. Specifically, we demonstrated the advantages of adjusting data-rates at high vehicular densities by means of DCC algorithms. Furthermore, the communication requirements for reliable safety applications and design goals of DCC algorithms provide framework and insights for developing new DCC algorithms scalable to large vehicular densities.

## 9.2. Future work

Based on the insights gained in this thesis, we have identified a number of issues that need to be addressed in the future research.

### Extending MD-DCC

The message-rate adaptation of MD-DCC is performed using LIMERIC. However, other message-rate algorithms such as NORAC [30] can also be utilized for MD-DCC implementation. Furthermore, MD-DCC does not guarantee an optimal combination of message-rate and data-rate which maximizes application reliability and awareness range. Hence, future work needs to be done in these directions.

### Coexistence of MD-DCC

We have investigated the coexistence of MD-DCC with the message-rate based LIMERIC. The problem with the coexistence of MD-DCC with LIMERIC is that it leads to unfair allocation of the channel use time. Therefore, ways to assure fairness during coexistence of MD-DCC and LIMERIC should be investigated. Furthermore, future work is needed to assess MD-DCC coexistence with other message-rate, transmit power, and multi-parameter based congestion control algorithms such as SAE-DCC.

### Field trials

Simulation and emulation studies of the proposed solutions were performed. However, the field trials feature scenarios that can be very different from our studies with respect to wireless signal propagation and vehicle distribution. For example, an intersection may have buildings and experience line-of-sight and non-line-of-sight communication links. To develop a congestion control algorithm that supports application reliably in a wide range of scenarios, the evaluation of the proposed solutions with field trials is necessary. Field trials should consider mobility of vehicles, changing vehicular densities, shadowing, and various scenarios such as rural, urban and highway.

### Joint message-rate, data-rate and transmit power DCC

The limitation of MD-DCC is that it does not guarantee the awareness range requirement of the application. MD-DCC tries to maximize the awareness range for a fixed transmit power. However, applications have a minimum awareness range requirement. Thus, tuning the transmit power to guarantee the desired awareness range along with message-rate and data-rate might further increase the

application performance. The required transmit power for a desired awareness range changes with data-rate. Further studies are necessary to analyze the impact of tuning the data-rate on the selection of the transmit power and vice-versa. We recommend the investigation of DCC algorithms that tune multiple parameters as they can improve the maximum vehicular density supported by the channel.

### **Runtime adaptation of DCC based on channel quality**

Due to the highly dynamic vehicular environment the channel quality changes due to shadowing and scenarios such as rural and urban affecting the packet reception ratio PRR, i.e., probability of beacon message delivery. Changes in PRR may affect the application performance. Thus, to ensure the reliability of applications DCC algorithms should adapt parameters, such as the minimum required message-rate of the application, based on the channel quality on runtime. DCC algorithms such as SAE-DCC [58] use PRR as channel quality indicator and generate additional beacon messages when the PRR decreases below a threshold to ensure reliability. We recommend the investigation of such DCC adaptation mechanisms further.

### **Congestion control for the service channel**

In the future, more demanding applications such as platooning and autonomous driving exchange sensor, trajectory and intentions of the vehicles. This will increase the channel load of the service channel (SCH). The SCH will become congested as the density of vehicles and the number of applications on the service channel increases. The proposed congestion control approaches for control channel (CCH) can be implemented on the SCH. However, there exist multiple SCH channels, and the application requirements are different. Hence, further research is needed to address congestion control challenges on the SCH.

### **DCC for cellular V2X**

In Europe, ETSI mandates DCC for all access technologies which utilize the Cooperative-Intelligent Transportation System (C-ITS) spectrum (5.9 GHz) [148]. Thus, DCC is mandatory for cellular V2X (C-V2X). ETSI is already working on the DCC specifications for C-V2X [149] as earlier ETSI DCC specifications were designed for IEEE 802.11p based ITS-G5 access technology [36]. C-V2X has different MAC and PHY layer compared to ITS-G5. Thus, existing DCC algorithms may not be compatible for C-V2X. Research is needed to develop and evaluate C-V2X DCC algorithms.



**Heterogeneous networks**

Safety applications have application reliability and awareness range requirements. These requirements have to be satisfied by the underlying communication system. To address this challenge, the C-ITS platform can utilize different communication technologies to take advantage of their complementarities. This is commonly referred to as heterogeneous networks [150]. The C-ITS architecture in Europe permits heterogeneous networks [77]. For example, heterogeneous networks can be used to avoid congestion by offloading messages from ITS-G5 to C-V2X access technologies and vice-versa. Further, research is needed to design heterogeneous network communication strategies which can enhance the reliability of C-ITS applications.

## APPENDIX A

### Stability analysis of MD-DCC

In this appendix, we conduct an stability analysis of MD-DCC and explain how  $\beta$  is determined based on  $r_{\min}$ . We do not consider the effect of traffic density changes on MD-DCC in our analysis. We assume that the vehicles are synchronized, and the message-rate and data-rate update of all vehicles are done at the same time. The channel busy percentage  $CBP_C(t)$  of the channel at time  $t$  over a period  $\theta$  can be expressed as shown below:

$$CBP_C(t) = \frac{\sum_{j=1}^L (R_j(t) \times \theta) \times T_D}{\theta} = \sum_{j=1}^L R_j(t) \times T_D \quad (\text{A.1})$$

where  $R_j(t)$  represents the message-rate of the  $j^{\text{th}}$  vehicle at time  $t$ . The  $R_j(t) \times \theta$  is the number of packets transmitted by the  $j^{\text{th}}$  vehicle in  $\theta$  s. Thus, the summation of  $R_j(t)$  represents the number of packets transmitted by all  $L$  vehicles in the communication channel.  $T_D$  is the transmission time of packets with data-rate  $D$ ; we assume all vehicles have the same data-rate  $D$ . The message-rate adaptation of MD-DCC is given by Eq.(A.2). The vector representation of the message-rate of all  $L$  vehicles is shown in Eq.(A.3).

$$R_k(t) = (1 - \alpha) \times R_k(t - \theta) + \beta \times (CBP_T - CBP_k(t - \theta)) \quad (\text{A.2})$$

$$\vec{R}(t) = \left[ R_1(t) \quad R_2(t) \quad \cdots \quad R_L(t) \right]^T \quad (\text{A.3})$$

where  $CBP_T$  represents the channel load threshold, and  $T$  indicates the matrix transpose operator. From Eq.(A.3) and Eq.(A.2), the vector representation of Eq.(A.2) becomes

$$\vec{R}(t) = A \vec{R}(t - 1) + \vec{b} CBP_T \quad (\text{A.4})$$

where  $A = \begin{bmatrix} 1 - \alpha - \beta' & -\beta' & \cdots & -\beta' \\ -\beta' & 1 - \alpha - \beta' & \cdots & -\beta' \\ \vdots & \vdots & \cdots & \vdots \\ -\beta' & -\beta' & \cdots & 1 - \alpha - \beta' \end{bmatrix},$

$$\vec{b} = \begin{bmatrix} \beta \\ \beta \\ \vdots \\ \beta \end{bmatrix},$$

$$\beta' = \beta \times T_D$$

Matrix A has one eigenvalue at  $z = 1 - \alpha - L\beta'$  and  $(L - 1)$  eigenvalues at  $z = 1 - \alpha$ . A set of unnormalized eigenvectors are

$$\begin{bmatrix} 1 \\ 1 \\ 1 \\ 1 \\ \vdots \\ \vdots \end{bmatrix}, \begin{bmatrix} 1 \\ -1 \\ 0 \\ 0 \\ \vdots \\ \vdots \end{bmatrix}, \begin{bmatrix} 1 \\ 1 \\ -2 \\ 0 \\ \vdots \\ \vdots \end{bmatrix}, \begin{bmatrix} 1 \\ 1 \\ 1 \\ -3 \\ \vdots \\ \vdots \end{bmatrix}, \dots$$

with added condition

$$1 - \alpha - L\beta' > -1 \text{ or } \alpha + L\beta' < 2 \quad (\text{A.5})$$

The system represents an asymptotically stable linear discrete time and is stable if Eq.(A.5) is satisfied. We consider a system stable if  $R_k$  converges to a steady-state value.

The dynamics of CBP on the channel is controlled by the eigenvalue at  $z = 1 - \alpha - L\beta'$ . Summing across the individual  $R_k$  in vector Eq.(A.3), multiplying with  $T_D$  and using Eq.(A.1) we get

$$CBP_C(t) = (1 - \alpha - L\beta') \times CBP_C(t - 1) + L\beta' \times CBP_T \quad (\text{A.6})$$

The differential equation can be solved to get

$$CBP_C(t) = CBP_C + (1 - \alpha - L\beta')^t \times (CBP_C(0) - CBP_C) \quad (\text{A.7})$$

where the steady state convergence of CBP is given by

$$CBP_C = \frac{L \times \beta' \times CBP_T}{\alpha + L \times \beta'} \quad (\text{A.8})$$

Returning to the selection of  $\beta$ , we see that  $CBP_C$  converges with the time constant  $1 - \alpha - L\beta'$ . For a given  $L$  and  $\alpha$  as  $\beta'$  increases from 0 to  $\frac{1-\alpha}{L}$ , the time constant is positive with decreasing magnitude, leading to convergence. As  $\beta'$  increases beyond  $\frac{1-\alpha}{L}$ , the time constant is negative, and the magnitude grows. Thus, the value of  $\beta'$  should be less than or equal to  $\frac{1-\alpha}{L}$  for stable converge, which further satisfies the inequality in Eq.(A.5). As seen in Eq.(A.8) for small

---

$CBP_C$  variation, we need higher values of  $\beta'$ . The maximum possible  $\beta$  is selected as follows:

$$\beta = \frac{(1 - \alpha)}{L_{\max} \times T_D} \quad (\text{A.9})$$

where  $L_{\max}$  represents the maximum number of vehicles to be supported by the communication channel.

MD-DCC tunes data-rate, which leads to change in  $T_D$ . Thus  $\beta$  has to be adapted as the data-rate  $D$  changes. To support the application reliably, we propose a  $\beta$  adaptation based on  $r_{\min}$ . The  $L_{\max}$  supported by the channel with  $r_{\min}$  avoiding congestion for a specific data-rate  $D$  is given by:

$$L_{\max} \times r_{\min} \times T_D = CBP_T \quad (\text{A.10})$$

By substituting Eq.(A.10) in Eq.(A.9), the value of  $\beta$  is obtained by

$$\beta = \frac{(1 - \alpha) \times r_{\min}}{CBP_T} \quad (\text{A.11})$$

We observe that  $\beta$  is independent of the data-rate. It is calculated based on  $r_{\min}$  and thus supports the maximum number of vehicles for the corresponding data-rate. For the proposed  $\beta$  selection mechanism, the algorithm is stable as long as the maximum number of vehicles in the communication channel using a data-rate  $D$  is less than or equal to  $L_{\max}$  (Eq.(A.10)). For static values of  $\alpha$  and  $\beta$ , the algorithm is stable as long as the number of vehicles sharing the channel is less than  $L_{\max}$ .

The performed stability analysis does not consider the effect of traffic density changes on MD-DCC. Thus, MD-DCC may become unstable when the traffic density changes are of the order of magnitude of the channel load measurement interval ( $\theta$ ). This is out of the scope of this thesis.



## APPENDIX B

### Description of DCC algorithms

The detailed description of LIMERIC, DR-DCC, SUPRA, and SAE-DCC are discussed in this appendix. LIMERIC, DR-DCC and SUPRA are message-rate, data-rate and transmit power based DCC algorithm respectively. SAE-DCC is a combined message-rate and transmit power based DCC algorithm proposed by the Society of Automotive Engineers (SAE) standardization body.

#### B.1. LIMERIC

LIMERIC is a distributed message-rate control algorithm that forces the channel load to converge to the channel load threshold,  $CBP_T$ . LIMERIC decreases the message-rate as the channel load increases. The message-rate  $R_i(k)$  of vehicle  $i$  is adjusted periodically every  $\theta$  s as follows:

$$R_i(k) = (1 - \alpha) \times R_i(k - 1) + \beta \times (CBP_T - CBP_i(k - 1)) \quad (\text{B.1})$$

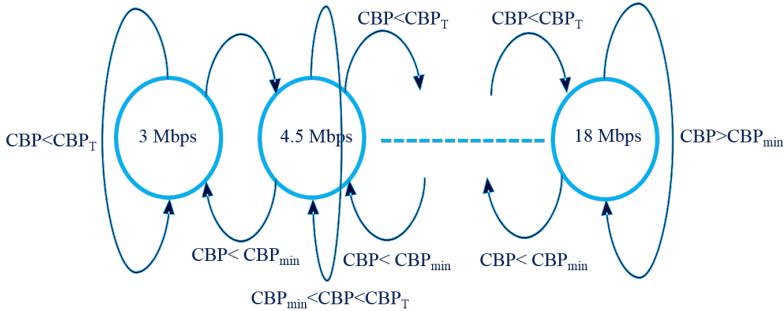
$CBP_i(k-1)$  is an estimate of the global channel load by vehicle  $i$  at  $k-1^{th}$  instance. It is computed by averaging the CBP measurements obtained from neighbor vehicles within the communication range of  $i$ . The speed of convergence of CBP is determined by  $\alpha$ , whereas  $\beta$  ensures stability and steady-state convergence [28]. Furthermore, LIMERIC implements the gain saturation approach discussed in [28]. Gain saturation limits the message-rate update with  $X$  Hz. The parameters of LIMERIC are taken from [28] and are shown in Table B.1.

**Table B.1** – LIMERIC algorithm parameters

Parameter	Value
$\alpha$	0.1
$\beta$	0.029
$X$	1 Hz
$CBP_T$	70%
$\theta$	200 ms

## B.2. DR-DCC

DR-DCC is a data-rate congestion control algorithm similar to PHY-DCC [35] and data-rate DCC proposed by ETSI [36]. Each vehicle adjusts the data-rate based on the CBP measured every  $\theta$  s as shown in Figure B.1. It has an upper CBP threshold  $CBP_T$  and a lower CBP threshold  $CBP_{min}$ . If the CBP is greater than  $CBP_T$ , it increases the data-rate, while, if it is less than  $CBP_{min}$ , it decreases the data-rate. It thus avoids congestion by maintaining CBP below the threshold  $CBP_T$ . DR-DCC uses discrete data-rates 3, 4.5, 6, 9, 12 and 18 Mbps similar to PDR-DCC. The CBP measurements are subjected to some randomness, hence, to avoid unnecessary fluctuations of the data-rate it utilizes a hysteresis as discussed in our work [116]. The parameters of DR-DCC are taken from [116] and are shown in Table B.1.



$CBP$  = Channel busy percentage,  $CBP_T$  = Upper channel load threshold,  $CBP_{min}$  = Lower channel load threshold

**Figure B.1** – DR-DCC algorithm

**Table B.2** – DR-DCC parameters

Parameter	Value
$CBP_{min}$	50%
$CBP_T$	70%
$\theta$	200 ms

## B.3. SUPRA

The stateful Utilization-based Power Adaptation (SUPRA) [33] algorithm is a transmit power based congestion control algorithm. SUPRA maps the CBP to transmit power. It adapts transmit power periodically every  $\theta$  s. The algorithm

uses the maximum transmit power ( $TP_{max}$ ) if the CBP is less than the minimum CBP threshold ( $CBP_{min}$ ). It linearly decreases the transmit power from  $TP_{max}$  and  $TP_{min}$  as the CBP increases from  $CBP_{min}$  to  $CBP_{max}$ . The transmit power  $TP_i(k)$  of vehicle  $i$  at  $k^{th}$  instance is calculated as follows:

$$TP_i(k) = TP_i(k-1) + \eta \times (f(CBP_i(k-1)) - TP_i(k-1)) \quad (B.2)$$

where

$$f(CBP_i(k-1)) = \begin{cases} TP_{max} & CBP_i(k-1) \leq CBP_{min} \\ TP_{max} - \left(\frac{TP_{max} - TP_{min}}{CBP_T - CBP_{min}}\right) \times (CBP_i(k-1) - CBP_{min}) & CBP_{min} < CBP_i(k-1) < CBP_T \\ TP_{min} & CBP_T \leq CBP_i(k-1) \end{cases} \quad (B.3)$$

where  $CBP_i(k-1)$  is the CBP measured by vehicle  $i$  at  $k-1^{th}$  instance,  $f(CBP_i(k-1))$  maps the CBP to the transmit power,  $\eta$  is the gain constant. The values of the parameters are shown in Table B.3.

**Table B.3** – SUPRA parameters

Parameter	Value
$CBP_{min}$	50%
$CBP_T$	70%
$\theta$	200 ms
$TP_{min}$	10 dBm
$TP_{max}$	25 dBm
$\eta$	0.5

#### B.4. SAE-DCC

SAE-DCC considers multiple transmission parameters to control the channel load. The system adjusts the message-rate according to the vehicle density and adjusts the transmit power with respect to the channel load. Besides, the system generates beacon messages immediately and transmits them with maximum transmit power whenever the vehicle dynamics condition is met. The implementation of SAE-DCC was performed together with a master student as a part of his thesis project [151]. A detailed description of this algorithm is provided in the rest of this section.



### B.4.1. Basic packet generation

If no critical events occur, the packet transmission is scheduled based on the maximum inter-transmit time (MAX\_ITT). Max\_ITT is determined based on the number of vehicles within 100 m range  $N(k)$ . Before the calculation of MAX\_ITT, the system firstly computes the smoothed vehicle density in range,  $N_i(k)$ , as presented in Eq.(B.4), in order to obtain a more stable value of Max\_ITT. The weight factor,  $\lambda$ , is introduced to calculate  $N_i(k)$ .

$$N_i(k) = \lambda \times N(k) + (1 - \lambda) \times N_i(k - 1) \quad (\text{B.4})$$

Having calculated the  $N_i(k)$  at the  $k^{\text{th}}$  instance,  $Max\_ITT(k)$ , is determined as shown in Eq.(B.5).  $B$  is the density coefficient, and  $vMax\_ITT$  is the maximum threshold.

$$Max\_ITT(k) = \begin{cases} 100 & N_i(k) \leq B \\ 100 \times \frac{N_i(k)}{B} & B < N_i(k) < \frac{vMax\_ITT}{100} \times B \\ vMax\_ITT & \frac{vMax\_ITT}{B} \times B \leq N_i(k) \end{cases} \quad (\text{B.5})$$

Max\_ITT is calculated every  $vCBPMeasInt$  s. Each vehicle generates the next BSM packet at the interval of the most recently calculated Max\_ITT.

Before the transmission of each newly-generated beacon packet, the transmit power needs to be calculated with respect to the channel busy percent (CBP), which is taken from SUPRA. The  $RawCBP(k)$  is calculated as the ratio of duration indicated as busy over a measurement interval  $vCBPMeasInt$ , as shown below:

$$RawCBP(k) = \frac{100 \times Durationindicatedasbusy}{vCBPMeasInt} \quad (\text{B.6})$$

To filter the measurement noise of CBP, the vehicle also calculates the smooth CBP, as shown in Eq.(B.7), introducing a weight factor  $vCBPWeightFactor$ . The RawCBP and the smooth CBP are calculated every 100 ms and the smooth CBP will be used as an input to determine the transmit power, as shown in Eq.(B.8).

$$CBP(k) = vCBPWeightFactor \times RawCBP(k) + (1 - vCBPWeightFactor) \times CBP(k - 1) \quad (\text{B.7})$$

$$f(CBP) = \begin{cases} TP_{max} & CBP \leq CBP_{min} \\ TP_{max} - \left( \frac{TP_{max} - TP_{min}}{CBP_T - CBP_{min}} \right) \times (CBP - CBP_{min}) & CBP_{min} < CBP < CBP_T \\ TP_{min} & CBP_T \leq CBP \end{cases} \quad (\text{B.8})$$

where  $TP_{max}$  and  $TP_{min}$  are the minimum and the maximum transmit power.  $CBP_{min}$  is the minimum CBP threshold, and  $CBP_T$  is the maximum CBP threshold.

To avoid a sudden jump in the value of the transmit power, the system calculates  $Base\_TP$  based on the previous transmit power  $Previous\_TP$ , as shown below:

$$Base\_TP = Previous\_TP + vSUPRAGain \times (f(CBP) - Previous\_TP) \quad (B.9)$$

where  $vSUPRAGain$  is the stateful utilization based power adaptation gain.

#### B.4.2. Packet generation based on vehicle dynamics

The packet generation based on vehicle dynamics is triggered by the tracking error  $e(k)$ . The reference vehicle is known as the Host Vehicle (HV) and its neighbor vehicles are known as Remote Vehicles (RVs). The tracking error is defined as the difference between the actual position of the HV and the position where HV thinks the RVs estimate the HV is located at the current time. The calculation can be completed following three steps every 100 *ms*:

- (1) Each HV extrapolates its current position based on its latest known status information, defined as HV local estimator, using the 2-D position extrapolation model with a constant speed and heading, as presented in Figure B.2.
- (2) Based on the status information assumed received by the RVs (a detailed description of the assumption of received information can be found in [61]), the HV computes the current position where the RVs believe the HV is located, defined as the HV remote estimator. The HV remote estimator also follows the same mechanism of the position extrapolation as presented in Figure B.2.
- (3) The system calculates  $e(k)$  as the 2-D distance difference between the HV local estimator and the HV remote estimator, which will be used to determine the transmission probability.

The next step is to determine the transmission probability according to the tracking error  $e(k)$ , as presented in Eq.(B.10).

$$p(k) = \begin{cases} 1 - \exp(-75 \times |e(k) - 0.2|)^2 & \text{if } 0.2 \leq e(k) < 0.5 \\ 1 & \text{if } e(k) \geq 0.5 \\ 0 & \text{otherwise} \end{cases} \quad (B.10)$$

The system checks whether the vehicle dynamics condition is met every 100 *ms* by comparing a drawn random number between 0 and 1 with the calculated transmission probability  $p(k)$ . If the random value is less than  $p(k)$  and the time

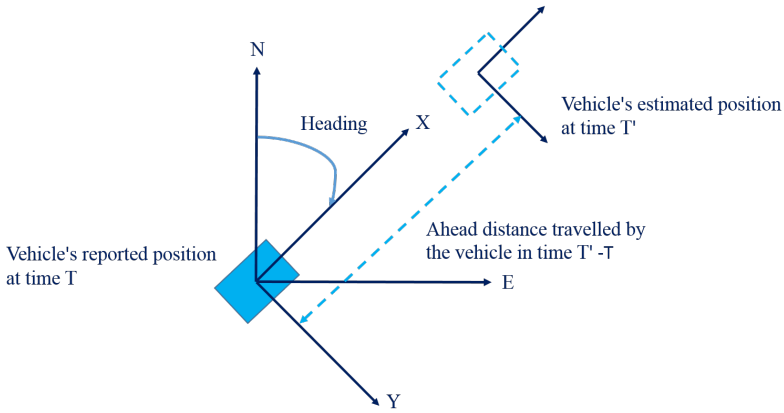


**Figure B.2** – 2D Position Extrapolation [151]

difference between the current time and the time when next packet is scheduled is greater than  $25\text{ ms}$ , the vehicle dynamics condition is met. In this case, the system will cancel the previously scheduled beacon packet generation and will generate and transmit a beacon packet immediately with the maximum allowed transmit power.

The parameters of SAE-DCC are taken from [58] and are shown in Table B.4. Note that the channel load threshold  $CBP_T$  is the same for all four algorithms.

**Table B.4** – SAE-DCC algorithm parameters

Parameter	Value
$\lambda$	0.05
$B$	25
$vMax\_IT$	600 ms
$vCBPMeasInt$	100 ms
$vCBPWeightFactor$	0.5
$TP_{max}$	25 dBm
$TP_{min}$	10 dBm
$CBP_{min}$	50%
$vSUPRAGain$	0.5
$CBP_T$	70%

## C-ITS simulation platform

In this appendix, we discuss the Cooperative Intelligent Transportation System (C-ITS) simulation platform utilized in the thesis. The C-ITS simulator should be capable of simulating both large-scale road traffic and V2X (Vehicle to Everything) communication. In our study, we focus on the V2V (Vehicle to Vehicle) communication performance and its effect on the mobility of the vehicles and vice-versa. We achieve this by incorporating two separate simulators (or simulation engines) for V2V communication and traffic.

### C.1. Network simulator

The simulations of V2V communications are performed using the network simulator ns-3 [46]. ns-3 has been developed to provide an open, extensible simulation platform, for networking research and education. It covers a very large number of applications, protocols, networks and traffic models. It consists of packages which help to build network topologies, the mobility of vehicles, and analyze the network. It helps to perform studies that are more difficult or not easy to perform on the real system. The study can be performed in a controlled manner to analyze the network performance. In brief, ns-3 provides models of how packet data networks work and perform, and provides a simulation engine for users to conduct simulation experiments. In our study, we focus on IEEE 802.11p based systems. The detailed modeling of IEEE 802.11p PHY and MAC layer can be found in [145].

#### C.1.1. Congestion control implementation in ns-3

The focus of the thesis is on the Decentralized Congestion Control (DCC) algorithm. In this section, we discuss the implementation of DCC algorithms in ns-3. The basic architecture of DCC in ns3 is shown in Figure C.1. In ns-3, the basic On-Board Unit for V2V communication is called the node. The node consists of the netdevice (WifiNetdevice [152]), which enables V2V communication. It comprises the IEEE 802.11p physical (WifiPhy [153]), and

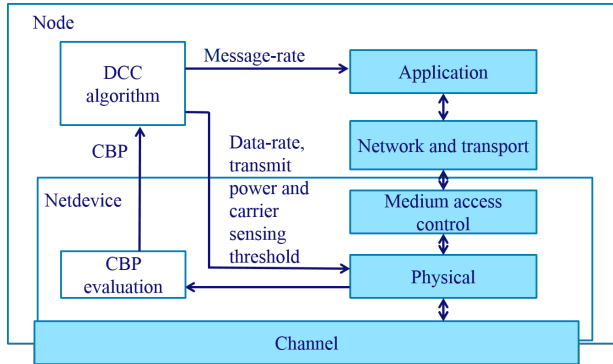


**Figure C.1** – DCC architecture in ns-3

medium access control layers (nqosWAVEMAC [154]). The Channel Busy Percentage (CBP), measurements are performed by each node individually based on how the physical layer senses the channel. The measured CBP is used to implement the decentralized congestion control algorithms using the cross-layer architecture proposed in ETSI [36]. Each node adapts its communication parameters such as message-rate, data-rate, transmit power and carrier sensing threshold individually as proposed by the DCC algorithm. The DCC algorithms perform data-rate, transmit power and carrier sensing threshold adaptation of a node by a physical layer interface. The message-rate adaptation of a node is performed by an application layer interface (Figure C.1).

## C.2. Traffic simulator

The traffic simulations are performed using the Simulation of Urban Mobility, SUMO [47]. It simulates a given traffic demand which consists of vehicles moving through a given road network. It is purely microscopic: each vehicle is modeled explicitly, has an own route, and moves individually through the road network. The modeling of precise vehicular movement similar to human behavior in a traffic simulator is mainly based on the car-following model and lane change model. The car-following model describes the interaction, i.e., the correlation in speed and acceleration, between a vehicle and its leading car in the same lane [146]. The lane-changing model is responsible for determining conditions under which vehicles can change lanes and for executing a lane change [146]. The desired road traffic scenario is simulated using SUMO.

### C.3. C-ITS simulator

Figure C.2 shows the flowchart of the C-ITS simulator. The traffic simulation with the desired road network, number of vehicles, velocity and acceleration of vehicles is modeled using SUMO, which provides the mobility of the vehicles. The trace-file from SUMO provides the position (using the 2-D Cartesian coordinate system), velocity and acceleration of the vehicles for every 100 *ms*. This trace-file is used as an input to ns-3 to implement the mobility of the vehicles. The V2V communication simulations with the desired message-rate, transmit power, channel model, and congestion control are performed in ns-3. Post-processing of the raw data from ns-3 is performed in MATLAB to obtain the performance metrics such as the application reliability, awareness range, and fairness.

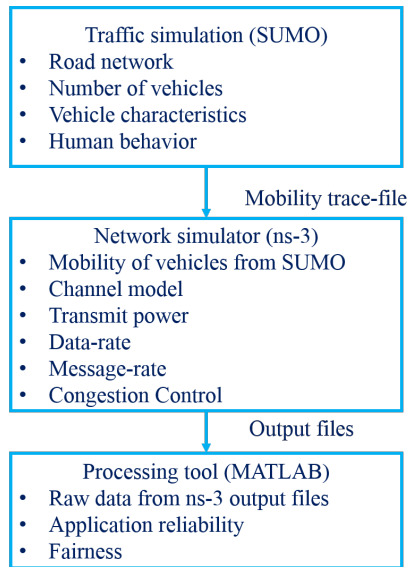


**Figure C.2** – Flowchart of C-ITS simulation and post-processing



## Bibliography

- [1] “Road Safety Annual Report,” International Traffic Safety Data and Analysis Group (IRTAD), Tech. Rep., 2017.
- [2] Association for Safe International Travel. [Online]. Available: <http://asirt.org/Initiatives/Informing-Road-Users/Road-Safety-Facts/Road-Crash-Statistics> [Accessed: March 2018]
- [3] “Annual Accident Report 2015,” European Commission Mobility & Transport Department, Tech. Rep., 2015.
- [4] “Annual Accident Report 2017,” European Commission Mobility & Transport Department, Tech. Rep., 2017.
- [5] World Health Organisation (WHO). [Online]. Available: [http://www.who.int/violence\\_injury\\_prevention/road\\_safety\\_status/2015/TableA2.pdf?ua=1](http://www.who.int/violence_injury_prevention/road_safety_status/2015/TableA2.pdf?ua=1) [Accessed: March 2018]
- [6] “Social costs of road crashes: An international analysis,” Tech. Rep.
- [7] Digital technologies make transport and mobility smarter, safer and greener. [Online]. Available: <https://ec.europa.eu/digital-single-market/en/mobility> [Accessed: March 2018]
- [8] The Self Driving Car Timeline Predictions from the Top 11 Global Automakers. [Online]. Available: <https://www.techemergence.com/self-driving-car-timeline-themselves-top-11-automakers/> [Accessed: June 2018]
- [9] J. Hecht. Lidar for Self-Driving Cars. [Online]. Available: [https://www.osa-opn.org/home/articles/volume.29/january.2018/features/lidar\\_for\\_self-driving\\_cars/](https://www.osa-opn.org/home/articles/volume.29/january.2018/features/lidar_for_self-driving_cars/) [Accessed: March 2018]
- [10] “Human Factors for Connected Vehicles: Effective Warning Interface Research Findings,” U.S. Department of Transportation, National Highway Traffic Safety Administration, Tech. Rep., 2014.
- [11] “Vehicle Safety Communications- Applications,” United States Department of Transportation, Tech. Rep., 2009.
- [12] M. Bagheri, M. Siekkinen, and J. K. Nurminen, “Cellular-based vehicle to pedestrian (V2P) adaptive communication for collision avoidance,” in *2014 International Conference on Connected Vehicles and Expo (ICCVE)*, Nov 2014, pp. 450–456.
- [13] P. Shrivastava, V. Lodhi, and S. V. Vargiya, “Vehicle to vehicle safety device - an ease for safe driving,” in *2015 2nd International Conference on Computing for Sustainable Global Development (INDIACom)*, March 2015, pp. 251–255.
- [14] B. Aygn, “Distributed Adaptation Techniques for Connected Vehicles,” Ph.D. dissertation, Worcester Polytechnic Institute, 2016.
- [15] LTE Release 14. [Online]. Available: <http://www.3gpp.org/release-14> [Accessed: March 2018]
- [16] “IEEE Standard for Information technology– Local and metropolitan area networks– Specific requirements– Part 11: Wireless LAN Medium Access Control (MAC) and Physical



- Layer (PHY) Specifications Amendment 6: Wireless Access in Vehicular Environments,” *IEEE Std 802.11p-2010 (Amendment to IEEE Std 802.11-2007 as amended by IEEE Std 802.11k-2008, IEEE Std 802.11r-2008, IEEE Std 802.11y-2008, IEEE Std 802.11n-2009, and IEEE Std 802.11w-2009)*, pp. 1–51, July 2010.
- [17] A. Filippi, K. Moerman, G. Daalderop, P. D. Alexander, F. Schober, and W. Pfiel. Ready to roll Why 802.11p beats LTE and 5G for V2X. [Online]. Available: <https://www.siemens.com/content/dam/webassetpool/mam/tag-siemens-com/smdb/mobility/road/connected-mobility-solutions/documents/its-g5-ready-to-roll-en.pdf> [Accessed: March 2018]
- [18] “Vehicle Safety Communications Project Task 3 Final Report; Identify Intelligent Vehicle Safety Applications Enabled by DSRC,” United States Department of Transportation, Tech. Rep., 2005.
- [19] SAFESPOT. [Online]. Available: <http://www.safespot-eu.org/> [Accessed: April 2018]
- [20] Cooperative Vehicle Infrastructure Systems. [Online]. Available: <http://www.ecomove-project.eu/links/cvis/> [Accessed: April 2018]
- [21] “IEEE Draft Amendment to IEEE Std 802.11, 1999 Edition (Reaff 2003) Amendment 7: 4.9 GHz to 5 GHz Operation in Japan (As Amended by IEEE Std 802.11a-1999, 802.11b-1999, 802.11b-1999/Cor 1-2001, 802.11d-2001, 802.11g-2003, 802.11h-2003), and 802.11i-2004),” *IEEE Std P802.11j/D1.6*, 2004.
- [22] “Access layer specification for Intelligent Transport Systems operating in the 5 GHz frequency band,” European Telecommunications Standards Institute Intelligent Transport Systems (ITS), Tech. Rep., 2012.
- [23] N. An, T. Gaugel, and H. Hartenstein, “VANET: Is 95% Probability of Packet Reception Safe?” in *ITS Telecommunications (ITST), 2011 11th International Conference on*, 2011.
- [24] Z. Tong, H. Lu, M. Haenggi, and C. Poellabauer, “A Stochastic Geometry Approach to the Modeling of DSRC for Vehicular Safety Communication,” *IEEE Transactions on Intelligent Transportation Systems*, vol. 17, no. 5, pp. 1448–1458, May 2016.
- [25] P. van Wijngaarden, “Frame Capture in IEEE 802.11P Vehicular Networks,” Master’s thesis, University of Twente, 2011.
- [26] K. Sjöberg, E. Uhlemann, and E. G. Strom, “How Severe Is the Hidden Terminal Problem in VANETs When Using CSMA and STDMA?” in *2011 IEEE Vehicular Technology Conference (VTC Fall)*, Sept 2011, pp. 1–5.
- [27] A. Weinfied, J. Kenney, and G. Bansal, “An Adaptive DSRC Message Transmission Interval Control Algorithm,” in *ITS World Congress 2011*, Oct 2011.
- [28] J. B. Kenney, G. Bansal, and C. E. Rohrs, “LIMERIC: A Linear Message Rate Control Algorithm for Vehicular DSRC Systems,” in *Proceedings of the Eighth ACM International Workshop on Vehicular Inter-networking*, ser. VANET ’11, 2011, pp. 21–30.
- [29] G. Bansal, H. Lu, J. B. Kenney, and C. Poellabauer, “EMBARC: Error Model Based Adaptive Rate Control for Vehicle-to-vehicle Communications,” in *Proceeding of the Tenth ACM International Workshop on Vehicular Inter-networking, Systems, and Applications*, ser. VANET ’13. New York, NY, USA: ACM, 2013, pp. 41–50. [Online]. Available: <http://doi.acm.org/10.1145/2482967.2482972>
- [30] F. Goudarzi and H. Asgari, “Non-Cooperative Beacon Rate and Awareness Control for VANETs,” *IEEE Access*, vol. 5, pp. 16 858–16 870, 2017.

- [31] M. Torrent-Moreno, J. Mittag, P. Santi, and H. Hartenstein, "Vehicle-to-Vehicle Communication: Fair Transmit Power Control for Safety-Critical Information," *IEEE Transactions on Vehicular Technology*, vol. 58, no. 7, pp. 3684–3703, Sept 2009.
- [32] J. Mittag, F. Schmidt-Eisenlohr, M. Killat, J. Härrri, and H. Hartenstein, "Analysis and Design of Effective and Low-overhead Transmission Power Control for VANETs," in *Proceedings of the Fifth ACM International Workshop on Vehicular Inter-NETworking*, ser. VANET '08. New York, NY, USA: ACM, 2008, pp. 39–48. [Online]. Available: <http://doi.acm.org/10.1145/1410043.1410051>
- [33] Y. P. Fallah, N. Nasiriani, and H. Krishnan, "Stable and Fair Power Control in Vehicle Safety Networks," *IEEE Transactions on Vehicular Technology*, vol. 65, no. 3, pp. 1662–1675, March 2016.
- [34] L. Yang, J. Guo, and Y. Wu, "Channel Adaptive One Hop Broadcasting for VANETs," in *2008 11th International IEEE Conference on Intelligent Transportation Systems*, Oct 2008, pp. 369–374.
- [35] S. Yang, H. Kim, and S. Kuk, "Less is more: need to simplify ETSI distributed congestion control algorithm," *Electronics Letters*, vol. 50, no. 4, pp. 279–281, 2014.
- [36] "Decentralized Congestion Control Mechanisms for Intelligent Transport Systems operating in the 5 GHz range; Access layer part," European Telecommunications Standards Institute Intelligent Transport Systems (ITS), Tech. Rep., 2011.
- [37] R. K. Schmidt, T. Leinmuller, and G. Schafer, "Adapting the Wireless Carrier Sensing for VANETs," in *6th International Workshop on Intelligent Transportation (WIT)*, 2010.
- [38] R. K. Schmidt, A. Brakemeier, T. Leinmüller, F. Kargl, and G. Schäfer, "Advanced Carrier Sensing to Resolve Local Channel Congestion," in *Proceedings of the Eighth ACM International Workshop on Vehicular Inter-networking*, ser. VANET '11. New York, NY, USA: ACM, 2011, pp. 11–20. [Online]. Available: <http://doi.acm.org/10.1145/2030698.2030701>
- [39] D. J. Deng, H. C. Chen, H. C. Chao, and Y. M. Huang, "A Collision Alleviation Scheme for IEEE 802.11P VANETs," *Wirel. Pers. Commun.*, vol. 56, no. 3, pp. 371–383, Feb. 2011. [Online]. Available: <http://dx.doi.org/10.1007/s11277-010-9977-8>
- [40] R. Reinders, M. van Eenennaam, G. Karagiannis, and G. Heijenk, "Contention window analysis for beaconing in VANETs," in *2011 7th International Wireless Communications and Mobile Computing Conference*, July 2011, pp. 1481–1487.
- [41] E. Egea-Lopez, "Fair distributed Congestion Control with transmit power for vehicular networks," in *2016 IEEE 17th International Symposium on A World of Wireless, Mobile and Multimedia Networks (WoWMoM)*, June 2016, pp. 1–6.
- [42] T. Tielert, D. Jiang, H. Hartenstein, and L. Delgrossi, "Joint Power/Rate Congestion Control Optimizing Packet Reception in Vehicle Safety Communications," in *Proceeding of the Tenth ACM International Workshop on Vehicular Inter-networking, Systems, and Applications*, ser. VANET '13. New York, NY, USA: ACM, 2013, pp. 51–60. [Online]. Available: <http://doi.acm.org/10.1145/2482967.2482968>
- [43] C. L. Huang, Y. P. Fallah, R. Sengupta, and H. Krishnan, "Adaptive intervehicle communication control for cooperative safety systems," *IEEE Network*, vol. 24, no. 1, pp. 6–13, Jan 2010.
- [44] B. Cheng, A. Rostami, M. Gruteser, J. B. Kenney, G. Bansal, and K. Sjoberg, "Performance evaluation of a mixed vehicular network with CAM-DCC and LIMERIC vehicles," in *2015*

- IEEE 16th International Symposium on A World of Wireless, Mobile and Multimedia Networks (WoWMoM)*, June 2015, pp. 1–6.
- [45] T. Lorenzen, “Performance Analysis of the Functional Interaction of Awareness Control and DCC in VANETs,” in *2016 IEEE 84th Vehicular Technology Conference (VTC-Fall)*, Sept 2016, pp. 1–7.
- [46] ns-3 a discrete-event network simulator. [Online]. Available: <https://www.nsnam.org/> [Accessed: April 2018]
- [47] Simulation of urban mobility. [Online]. Available: [http://sumo.dlr.de/userdoc/Sumo\\_at\\_a\\_Glance.html](http://sumo.dlr.de/userdoc/Sumo_at_a_Glance.html) [Accessed: April 2018]
- [48] Cohda Wireless MK5 V2X On Board Unit. [Online]. Available: <http://cohdawireless.com> [Accessed: June 2018]
- [49] “C-ITS Platform Final Report,” C-ITS Deployment Platform of the European Commission, Tech. Rep., Jan 2016.
- [50] “Amendment of the Commission’s Rules Regarding Dedicated Short-Range Communication Services in the 5.850-5.925 GHz Band (5.9 GHz Band),” Federal Communications Commission, Tech. Rep., 2002.
- [51] “Amendment of the Commission’s Rules Regarding Dedicated Short-Range Communication Services in the 5.850-5.925 GHz Band (5.9 GHz Band),” Federal Communications Commission, Tech. Rep., 2006.
- [52] H. Lu, “Improving the Scalability performance of Dedicated Short Range Communications,” Ph.D. dissertation, Notre Dame, 2015.
- [53] “Overview of Harmonization Task Groups 1 & 3,” EU US ITS cooperation, Tech. Rep., 2012.
- [54] “Dedicated Short-Range Communications in Intelligent Transport Systems,” Telecommunications Standards Advisory Committee (TSAC), Tech. Rep., 2017.
- [55] China LTE-V2X spectrum proposal. [Online]. Available: [http://zmhd.miit.gov.cn:8080/opinion/noticedetail.do?method=notice\\_detail\\_show&noticeid=1960](http://zmhd.miit.gov.cn:8080/opinion/noticedetail.do?method=notice_detail_show&noticeid=1960) [Accessed: July 2018]
- [56] “Dedicated Short Range Communications (DSRC) Message Set Dictionary,” SAE, International, Tech. Rep., 2009.
- [57] “Vehicular Communications; Basic Set of Applications; Definitions,” European Telecommunications Standards Institute Intelligent Transport Systems, Tech. Rep., 2009.
- [58] “On-Board System Requirements for V2V Safety Communications,” SAE International, J2945<sup>TM</sup>, Technical Report, Mar. 2016.
- [59] “Vehicular Communications; Basic Set of Applications; Part 2: Specification of Cooperative Awareness Basic Service,” European Telecommunications Standards Institute Intelligent Transport Systems, Tech. Rep., 2014.
- [60] “Vehicular Communications; Basic Set of Applications; Part 3: Specifications of Decentralized Environmental Notification Basic Service,” European Telecommunications Standards Institute Intelligent Transport Systems, Tech. Rep., 2014.
- [61] “Dedicated Short Range Communications (DSRC) Message Set Dictionary,” SAE International, J2735<sup>TM</sup>, Technical Report, Sept 2010.
- [62] “Dedicated Short Range Communications (DSRC) Message Set Dictionary,” Tech. Rep., March 2016. [Online]. Available: [https://doi.org/10.4271/J2735\\_201603](https://doi.org/10.4271/J2735_201603)

- 
- [63] “On-Board System Requirements for V2V Safety Communications,” Tech. Rep., March 2016. [Online]. Available: [https://doi.org/10.4271/J2945/1\\_201603](https://doi.org/10.4271/J2945/1_201603)
- [64] “IEEE Draft Guide for Wireless Access in Vehicular Environments (WAVE) - Architecture,” *IEEE P1609.0/D10, January 2018*, pp. 1–104, Jan 2018.
- [65] “IEEE Standard for Wireless Access in Vehicular Environments–Security Services for Applications and Management Messages - Redline,” *IEEE Std 1609.2-2016 (Revision of IEEE Std 1609.2-2013) - Redline*, pp. 1–884, March 2016.
- [66] “IEEE Standard for Wireless Access in Vehicular Environments (WAVE) – Networking Services,” *IEEE Std 1609.3-2016 (Revision of IEEE Std 1609.3-2010)*, pp. 1–160, April 2016.
- [67] “IEEE Standard for Wireless Access in Vehicular Environments (WAVE) – Multi-Channel Operation - Redline,” *IEEE Std 1609.4-2016 (Revision of IEEE Std 1609.4-2010) - Redline*, pp. 1–206, March 2016.
- [68] “ISO/IEC/IEEE International Standard - Information Technology - Telecommunications and information exchange between systems - Local and metropolitan area networks - Specific requirements - Part 2: Logical link control,” *IEEE Std 8802-2-1994*, pp. 1–174, Dec 1994.
- [69] “Intelligent Transport Systems (ITS); V2X Applications; Part 1: Road Hazard Signalling (RHS) application requirements specification,” European Telecommunications Standards Institute Intelligent Transport Systems (ITS), Tech. Rep., 2013.
- [70] “Intelligent Transport Systems (ITS); V2X Applications; Part 3: Longitudinal Collision Risk Warning (LCRW) application requirements specification,” European Telecommunications Standards Institute Intelligent Transport Systems (ITS), Tech. Rep., 2013.
- [71] “Intelligent Transport Systems (ITS); Vehicular Communications; GeoNetworking; Part 4: Geographical addressing and forwarding for point-to-point and point-to-multipoint communications; Sub-part 1: Media-Independent Functionality,” European Telecommunications Standards Institute Intelligent Transport Systems (ITS), Tech. Rep., 2014.
- [72] “Intelligent Transport Systems (ITS); Vehicular Communications; GeoNetworking; Part 5: Transport Protocols; Sub-part 1: Basic Transport Protocol,” European Telecommunications Standards Institute Intelligent Transport Systems (ITS), Tech. Rep., 2017.
- [73] “Intelligent Transport Systems (ITS); Vehicular Communications; GeoNetworking; Part 6: Internet Integration; Sub-part 1: Transmission of IPv6 Packets over GeoNetworking Protocols,” European Telecommunications Standards Institute Intelligent Transport Systems (ITS), Tech. Rep., 2014.
- [74] “Intelligent Transport Systems (ITS); Security; Security header and certificate formats,” European Telecommunications Standards Institute Intelligent Transport Systems (ITS), Tech. Rep., 2015.
- [75] “Intelligent Transport Systems (ITS); Security; ITS communications security architecture and security management,” European Telecommunications Standards Institute Intelligent Transport Systems (ITS), Tech. Rep., 2016.

- [76] “Intelligent Transport Systems (ITS); Security; Trust and Privacy Management,” European Telecommunications Standards Institute Intelligent Transport Systems (ITS), Tech. Rep., 2012.
- [77] “Intelligent Transport Systems (ITS); Communications Architecture,” European Telecommunications Standards Institute Intelligent Transport Systems (ITS), Tech. Rep., 2010.
- [78] “WLAN 802.11p Measurements for Vehicle to Vehicle (V2V) DSRC,” 2009.
- [79] C. Ziegler. The 2017 Mercedes E Class will steer itself up to 130 miles per hour. [Online]. Available: <https://www.theverge.com/2016/1/10/10746250/mercedes-benz-e-class-announced-detroit-auto-show-2016> [Accessed: March 2018]
- [80] A. J. Hawkins. Cadillac CTS sedans can now talk to each other. [Online]. Available: <https://www.theverge.com/2017/3/9/14869110/cadillac-cts-sedan-v2v-communication-dsrc-gm> [Accessed: March 2018]
- [81] Connected vehicle safety pilot. [Online]. Available: [https://www.its.dot.gov/research\\_archives/safety/safety\\_pilot\\_plan.htm](https://www.its.dot.gov/research_archives/safety/safety_pilot_plan.htm) [Accessed: April 2018]
- [82] “Vehicle-to-Vehicle Communications:Readiness of V2V Technology for Application,” 2014.
- [83] Connected Vehicle Pilot Deployment Program. [Online]. Available: [https://www.its.dot.gov/pilots/pilots\\_overview.htm](https://www.its.dot.gov/pilots/pilots_overview.htm) [Accessed: April 2018]
- [84] Coperatieve ITS Corridor Smart Mobility in Nederland. [Online]. Available: <https://itscorridor.mett.nl/default.aspx> [Accessed: April 2018]
- [85] Wyoming connected vehicle pilot. [Online]. Available: <https://wydotcvp.wyroad.info/> [Accessed: April 2018]
- [86] Tampa connected vehicle pilot. [Online]. Available: <https://www.tampacvpilot.com/> [Accessed: April 2018]
- [87] Preventive and Active Safety Application. [Online]. Available: <https://trimis.ec.europa.eu/project/preventive-and-active-safety-application> [Accessed: April 2018]
- [88] DRIVE C2X Accelerate cooperative mobility. [Online]. Available: <http://www.drive-c2x.eu/project> [Accessed: April 2018]
- [89] Harmonized C-ITS deployments throughout Europe. [Online]. Available: <https://www.c-roads.eu/platform.html> [Accessed: March 2018]
- [90] The following day 1 service implemented on the C ROADS platform. [Online]. Available: <https://www.c-roads.eu/pilots/implemented-services.html> [Accessed: April 2018]
- [91] Accelerating C-ITS Mobility Innovation and depLoyment in Europe (C-MoBiLE). [Online]. Available: <http://c-mobile-project.eu/> [Accessed: March 2018]
- [92] C-ITS Corridor (Netherlands-Germany-Austria). [Online]. Available: <http://intercor-project.eu/> [Accessed: March 2018]
- [93] Project SCOOP. [Online]. Available: [www.scoop.developpement-durable.gouv.fr/en](http://www.scoop.developpement-durable.gouv.fr/en) [Accessed: April 2018]
- [94] Coexistence of automated and conventional vehicle. [Online]. Available: <https://www.h2020-coexist.eu/> [Accessed: March 2018]
- [95] Transition Areas for Infrastructure-Assisted Driving. [Online]. Available: <https://www.transaid.eu/> [Accessed: April 2018]
- [96] “Automated emergency brake systems: technical requirements, costs and benefits,” 2013.
- [97] J. Marais, B. Meunier, and M. Berbineau, “Evaluation of GPS availability for train positioning along a railway line,” in *Vehicular Technology Conference Fall 2000. IEEE*

- VTS Fall VTC2000. 52nd Vehicular Technology Conference (Cat. No.00CH37152)*, vol. 5, 2000, pp. 2060–2067 vol.5.
- [98] R. Kumar and H. Kumar, “Availability and handling of data received through GPS device: In tracking a vehicle,” in *2014 IEEE International Advance Computing Conference (IACC)*, Feb 2014, pp. 245–249.
- [99] R. L. Fante and J. J. Vaccaro, “Ensuring GPS availability in an interference environment,” in *IEEE 2000. Position Location and Navigation Symposium (Cat. No.00CH37062)*, 2000, pp. 37–40.
- [100] M. Ismail, I. Mohamad, and M. A. M. Ali, “Availability of GPS and A-GPS signal in UKM campus for hearability check,” in *2011 IEEE 10th Malaysia International Conference on Communications*, Oct 2011, pp. 59–64.
- [101] I. Mohamad, M. A. M. Ali, and M. Ismail, “Availability, reliability and accuracy of GPS signal in Bandar Baru Bangi for the determination of vehicle position and speed,” in *2009 International Conference on Space Science and Communication*, Oct 2009, pp. 224–229.
- [102] K. Kawamura and T. Tanaka, “Study on the improvement of measurement accuracy in GPS,” in *2006 SICE-ICASE International Joint Conference*, Oct 2006, pp. 1372–1375.
- [103] E. Wang, W. Zhao, and M. Cai, “Research on improving accuracy of GPS positioning based on particle filter,” in *2013 IEEE 8th Conference on Industrial Electronics and Applications (ICIEA)*, June 2013, pp. 1167–1171.
- [104] E. Wang, S. Zhang, and Z. Zhang, “A Study on GPS Signal Performance Analysis Platform Based on LabVIEW,” in *2012 8th International Conference on Wireless Communications, Networking and Mobile Computing*, Sept 2012, pp. 1–4.
- [105] Y. He, H. Yu, and H. Fang, “Study on Improving GPS Measurement Accuracy,” in *2005 IEEE Instrumentation and Measurement Technology Conference Proceedings*, vol. 2, May 2005, pp. 1476–1479.
- [106] T. Matsushita, T. Tanaka, and M. Yonekawa, “Improvement accuracy in measurement of long baseline DGPS,” in *2008 SICE Annual Conference*, Aug 2008, pp. 3504–3508.
- [107] H. S. Eom and M. C. Lee, “Position error correction for DGPS based localization using LSM and Kalman filter,” in *ICCAS 2010*, Oct 2010, pp. 1576–1579.
- [108] J. L. Borresen, C. S. Jensen, and K. Torp, “FoGBAT: Combining Bluetooth and GPS Data for Better Traffic Analytics,” in *2016 17th IEEE International Conference on Mobile Data Management (MDM)*, vol. 1, June 2016, pp. 325–328.
- [109] S. J. Brunson, E. M. Kyle, N. C. Phamdo, and G. R. Preziotti, “Alert Algorithm Development Program NHTSA Rear-End Collision Alert Algorithm Final Report,” National Highway Traffic Safety Administration, Tech. Rep., June 2001.
- [110] T. ElBatt, S. K. Goel, G. Holland, H. Krishnan, and J. Parikh, “Cooperative Collision Warning Using Dedicated Short Range Wireless Communications,” in *Proceedings of the 3rd International Workshop on Vehicular Ad Hoc Networks*, ser. VANET '06. New York, NY, USA: ACM, 2006, pp. 1–9. [Online]. Available: <http://doi.acm.org/10.1145/1161064.1161066>
- [111] F. Bai and H. Krishnan, “Reliability Analysis of DSRC Wireless Communication for Vehicle Safety Applications,” in *Intelligent Transportation Systems Conference, 2006. ITSC '06. IEEE*, Sept 2006, pp. 355–362.

- [112] M. Boban and P. M. d'Orey, "Exploring the Practical Limits of Cooperative Awareness in Vehicular Communications," *IEEE Transactions on Vehicular Technology*, vol. 65, no. 6, pp. 3904–3916, June 2016.
- [113] B. Aygun and M. Boban and A. M. Wyglinski, "ECPR: Environment-and context-aware combined power and rate distributed congestion control for vehicular communications," vol. 93, 2016, pp. 3–16.
- [114] N. Lyamin, A. Vinel, M. Jonsson, and B. Bellalta, "Cooperative Awareness in VANETs: On ETSI EN 302 637-2 Performance," *IEEE Transactions on Vehicular Technology*, vol. 67, no. 1, pp. 17–28, Jan 2018.
- [115] "Federal Motor Vehicle Safety Standards; V2V Communications," National Highway Traffic Safety Administration, Tech. Rep., 2016.
- [116] C. B. Math, A. Ozgur, S. Heemstra de Groot, and H. Li, "Data Rate based Congestion Control in V2V communication for traffic safety applications," in *Communications and Vehicular Technology in the Benelux (SCVT), 2015 IEEE Symposium on*, Nov 2015.
- [117] "Cross Layer DCC Management Entity for operation in the ITS G5A and ITS G5B medium; Report on Cross layer DCC algorithms and performance evaluation," European Telecommunications Standards Institute Intelligent Transport Systems (ITS), Tech. Rep., 2014.
- [118] H. C. Jang and W. C. Feng, "Network Status Detection-Based Dynamic Adaptation of Contention Window in IEEE 802.11p," in *2010 IEEE 71st Vehicular Technology Conference*, May 2010, pp. 1–5.
- [119] C. W. Hsu, C. H. Hsu, and H. R. Tseng, "MAC Channel Congestion Control Mechanism in IEEE 802.11p/WAVE Vehicle Networks," in *2011 IEEE Vehicular Technology Conference (VTC Fall)*, Sept 2011, pp. 1–5.
- [120] Y. Mertens, M. Wellens, and P. Mahonen, "Simulation-Based Performance Evaluation of Enhanced Broadcast Schemes for IEEE 802.11-Based Vehicular Networks," in *VTC Spring 2008 - IEEE Vehicular Technology Conference*, May 2008, pp. 3042–3046.
- [121] M. Minelli and S. Tohm, "The potential of transmit data rate control for channel congestion mitigation in VANET," in *2016 International Wireless Communications and Mobile Computing Conference (IWCMC)*, Sept 2016, pp. 262–267.
- [122] R. Jain, D.-M. Chiu, and W. R. Hawe. (1984) A Quantitative Measure of Fairness and Discrimination for Resource Allocation in Shared Computer System.
- [123] "Cross Layer DCC Management Entity for operation in the ITS G5A and ITS G5B medium; Validation set-up and results," European Telecommunications Standards Institute Intelligent Transport Systems (ITS), Tech. Rep., 2015.
- [124] M. S. Frigau, "Fair Decentralized Congestion and Awareness Control for Vehicular Networks," in *2015 IEEE 21st International Conference on Parallel and Distributed Systems (ICPADS)*, Dec 2015, pp. 172–180.
- [125] M. Sepulcre, J. Gozalvez, O. Altintas, and H. Kremono, "Adaptive beaconing for congestion and awareness control in vehicular networks," in *2014 IEEE Vehicular Networking Conference (VNC)*, Dec 2014, pp. 81–88.
- [126] J. Jose, C. Li, X. Wu, L. Ying, and K. Zhu, "Distributed rate and power control in DSRC," in *2015 IEEE International Symposium on Information Theory (ISIT)*, June 2015, pp. 2822–2826.

- 
- [127] S. Gorinsky and H. Vin, "Additive Increase Appears Inferior," Austin, TX, USA, Tech. Rep., 2000.
- [128] T. Tielert, D. Jiang, Q. Chen, L. Delgrossi, and H. Hartenstein, "Design methodology and evaluation of rate adaptation based congestion control for Vehicle Safety Communications," in *IEEE Vehicular Networking Conference (VNC)*, Nov 2011, pp. 116–123.
- [129] G. Bansal, J. B. Kenney, and C. E. Rohrs, "LIMERIC: A Linear Adaptive Message Rate Algorithm for DSRC Congestion Control," *IEEE Transactions on Vehicular Technology*, vol. 62, no. 9, pp. 4182–4197, Nov 2013.
- [130] A. A. Gmez and C. F. Mecklenbrucker, "Dependability of Decentralized Congestion Control for Varying VANET Density," *IEEE Transactions on Vehicular Technology*, vol. 65, no. 11, pp. 9153–9167, Nov 2016.
- [131] S. Subramanian, M. Werner, S. Liu, J. Jose, R. Lupoai, and X. Wu, "Congestion Control for Vehicular Safety: Synchronous and Asynchronous MAC Algorithms," in *Proceedings of the Ninth ACM International Workshop on Vehicular Inter-networking, Systems, and Applications*, ser. VANET '12. New York, NY, USA: ACM, 2012, pp. 63–72. [Online]. Available: <http://doi.acm.org/10.1145/2307888.2307900>
- [132] R. Stanica, E. Chaput, and A. L. Beylot, "Physical Carrier Sense in Vehicular Ad-Hoc Networks," in *2011 IEEE Eighth International Conference on Mobile Ad-Hoc and Sensor Systems*, Oct 2011, pp. 580–589.
- [133] M. Sepulcre, J. Gozalez, and B. Coll-Perales, "Why 6Mbps is not (always) the Optimum Data Rate for Beaconing in Vehicular Networks," *IEEE Transactions on Mobile Computing*, 2017.
- [134] "Cross Layer DCC Management Entity for operation in the ITS G5A and ITS G5B medium; Validation set-up and results," European Telecommunications Standards Institute Intelligent Transport Systems (ITS), Tech. Rep., 2015.
- [135] D. Jiang, Q. Chen, and L. Delgrossi, "Optimal Data Rate Selection for Vehicle Safety Communications," in *Proceedings of the Fifth ACM International Workshop on Vehicular Inter-NETworking*, ser. VANET '08. New York, NY, USA: ACM, 2008, pp. 30–38.
- [136] Lane. [Online]. Available: <https://en.wikipedia.org/wiki/Lane> [Accessed: April 2018]
- [137] Vehicle sizes. [Online]. Available: [https://en.wikipedia.org/wiki/Vehicle\\_size\\_class](https://en.wikipedia.org/wiki/Vehicle_size_class) [Accessed: April 2018]
- [138] Speed limits by country. [Online]. Available: [https://en.wikipedia.org/wiki/Speed\\_limits\\_by\\_country](https://en.wikipedia.org/wiki/Speed_limits_by_country) [Accessed: April 2018]
- [139] "STDMA Recommended Parameters and Settings for Cooperative ITS; Access Layer Part," European Telecommunications Standards Institute Intelligent Transport Systems, Tech. Rep., 2012.
- [140] P. Alexander, D. Haley, and A. Grant, "Cooperative Intelligent Transport Systems: 5.9-GHz Field Trials," *Proceedings of the IEEE*, vol. 99, no. 7, pp. 1213–1235, July 2011.
- [141] Auto-Talks PANGAEA5 V2X Communication Module. [Online]. Available: <http://www.auto-talks.com> [Accessed: June 2018]
- [142] Unex OBU-201E Specifications. [Online]. Available: <http://unex.com.tw/> [Accessed: June 2018]
- [143] Y. Fallah, C.-L. Huang, R. Sengupta, and H. Krishnan, "Analysis of Information Dissemination in Vehicular Ad-Hoc Networks With Application to Cooperative Vehicle



- Safety Systems,” *Vehicular Technology, IEEE Transactions on*, vol. 60, pp. 233–247, Jan 2011.
- [144] A2 motorway. [Online]. Available: [https://en.wikipedia.org/wiki/A2\\_motorway\\_\(Netherlands\)](https://en.wikipedia.org/wiki/A2_motorway_(Netherlands)) [Accessed: April 2018]
- [145] M. Lamage and T. R. Henderson, “Yet Another Network Simulator,” in *Proceeding from the 2006 Workshop on Ns-2: The IP Network Simulator*, ser. WNS2 '06. New York, NY, USA: ACM, 2006. [Online]. Available: <http://doi.acm.org/10.1145/1190455.1190467>
- [146] D. Krajzewicz, J. Erdmann, M. Behrisch, and L. Bieker, “Recent Development and Applications of SUMO - Simulation of Urban MObility,” *International Journal On Advances in Systems and Measurements*, vol. 5, pp. 128–138, December 2012.
- [147] S. Stefansson, “Experimental Analysis of Data-Rate based Congestion Control Algorithms in V2X Communications,” Master’s thesis, Eindhoven University of Technology, 2018.
- [148] “Intelligent Transport Systems (ITS); Radiocommunications equipment operating in the 5 855 MHz to 5 925 MHz frequency band; Harmonised Standard covering the essential requirements of article 3.2 of Directive 2014/53/EU,” European Telecommunications Standards Institute Intelligent Transport Systems (ITS), Tech. Rep., 2016.
- [149] “Intelligent Transport Systems (ITS); Access layer part; Congestion Control for the Cellular-V2X PC5 interface,” European Telecommunications Standards Institute Intelligent Transport Systems (ITS), Tech. Rep., 2018.
- [150] M. Sepulcre and J. Gozalvez, “Context-aware heterogeneous V2X communications for connected vehicles,” *Computer Networks*, vol. 136, pp. 13 – 21, 2018.
- [151] Y. Wei, “SAE-DCC Evaluation and Comparison with Popular Congestion Control Algorithms of V2X Communication,” Master’s thesis, Eindhoven University of Technology, 2017.
- [152] ns-3 wifi netdevice. [Online]. Available: [https://www.nsnam.org/doxygen/classes3.1.1\\_wifi\\_net\\_device.html](https://www.nsnam.org/doxygen/classes3.1.1_wifi_net_device.html) [Accessed: April 2018]
- [153] ns-3 wifi physical layer. [Online]. Available: [https://www.nsnam.org/doxygen/classes3.1.1\\_wifi\\_phy.html](https://www.nsnam.org/doxygen/classes3.1.1_wifi_phy.html) [Accessed: April 2018]
- [154] ns-3 wifi medium access control layer. [Online]. Available: [https://www.nsnam.org/doxygen/classes3.1.1\\_nqos\\_wave\\_mac\\_helper.html](https://www.nsnam.org/doxygen/classes3.1.1_nqos_wave_mac_helper.html) [Accessed: April 2018]

## Abbreviations

<b>3GPP</b>	3 <sup>rd</sup> Generation Partnership Project
<b>ADAS</b>	Advanced Driver Assistant System
<b>AC</b>	Access Category
<b>AF-API</b>	Application Facilities Application Programming Interface
<b>AIFS</b>	Attributed Inter Frame Space
<b>AIMD</b>	Additive Increase Multiplicative Decrease
<b>BSM</b>	Basic Safety Message
<b>BTP</b>	Basic Transport Protocol
<b>CAM</b>	Cooperative Awareness Message
<b>CBP</b>	Channel Busy Percentage
<b>CCH</b>	Control Channel
<b>CSMA/CA</b>	Carrier Sense Multiple Access Collision Avoidance
<b>CSW</b>	Curve Speed Warning
<b>C2C-CC</b>	Car 2 Car Communication Consortium
<b>C-ITS</b>	Cooperative Intelligent Transportation Systems
<b>C-V2X</b>	Cellular Vehicle to everything
<b>DCC</b>	Decentralized Congestion Control
<b>DENM</b>	Decentralized Environmental Notification Message
<b>DSRC</b>	Dedicated Short-Range Communication
<b>EDCA</b>	Enhanced Distributed Channel Access
<b>EEBL</b>	Emergency Electronic Brake Lights
<b>EN</b>	Emulation Node

## ABBREVIATIONS

---

<b>ETSI</b>	European Telecommunication Standardization Institute
<b>FCC</b>	Federal Communication Commission
<b>FCW</b>	Forward Collision Warning
<b>GLOSA</b>	Green Light Optimization Speed Advisory
<b>GNSS</b>	Global Navigation Satellite System
<b>GPS</b>	Global Positioning System
<b>ICW</b>	Intersection Collision Warning
<b>IEEE</b>	Institute of Electrical and Electronics Engineers
<b>IP</b>	Internet Protocol
<b>IPv6</b>	Internet Protocol version 6
<b>IRT</b>	Inter Reception Time
<b>ITS-G5</b>	Intelligent Transportation System - 5 GHz
<b>I2P</b>	Infrastructure to Pedestrian
<b>I2V</b>	Infrastructure to Vehicle
<b>LCRW</b>	Longitudinal Collision Risk Warning
<b>LCW</b>	Lane Change Warning
<b>LED</b>	Light Emitting Device
<b>LiDAR</b>	Light Detection and Ranging
<b>LIMERIC</b>	Linear Message Rate Integrated Control
<b>LLC</b>	Logic Link Control
<b>LLC-API</b>	Logic Link Control Application Programming Interface
<b>LTA</b>	Left Turn Assistance
<b>LTE</b>	Long Term Evolution
<b>MAC</b>	Medium Access Control
<b>MD-DCC</b>	Message-rate and Data-rate Decentralized Congestion Control
<b>MIIT</b>	Ministry of Industry and Information Technology
<b>NHTSA</b>	National Highway Traffic Safety Administration
<b>NORAC</b>	Non-cooperative Rate and Awareness Control

<b>OBU</b>	On-Board Unit
<b>ON</b>	Observing Node
<b>PCW</b>	Pre Crash Warning
<b>PDR-DCC</b>	Packet Count Decentralized Congestion Control
<b>PHY</b>	Physical
<b>PRR</b>	Packet Reception Ratio
<b>PULSAR</b>	Periodically Updated Load Sensitive Adaptive Rate control
<b>R-DCC</b>	Reactive DCC
<b>RHS</b>	Road Hazard Signaling
<b>RSU</b>	Roadside Unit
<b>RWAW</b>	Road Work Ahead Warning
<b>SAE</b>	Society of Automotive Engineers
<b>SCH</b>	Service Channel
<b>SINR</b>	Signal-to-Interference-plus-Noise-Ratio
<b>SSMA</b>	Stop Sign Movement Assistant
<b>SUPRA</b>	Stateful Utilization-based Power Adaptation
<b>T-DCC</b>	Triggering DCC
<b>TTC</b>	Time to Collision
<b>TCP</b>	Transmission Control Protocol
<b>TSVW</b>	Traffic Signal Violation Warning
<b>UDP</b>	User Datagram Protocol
<b>US</b>	United States of America
<b>USDOT</b>	United States Department of Transportation
<b>V2B</b>	Vehicle to Device
<b>V2P</b>	Vehicle to Pedestrian
<b>V2I</b>	Vehicle to Infrastructure
<b>V2V</b>	Vehicle to Vehicle
<b>V2X</b>	Vehicle to Everything

## ABBREVIATIONS

---

<b>VSC</b>	Vehicle Safety Communication
<b>VSC-A</b>	Vehicle Safety Communication-Applications
<b>WAVE</b>	Wireless Access for Vehicular Environment
<b>WiFi</b>	Wireless Fidelity
<b>WiMAX</b>	Worldwide Interoperability for Microwave Access
<b>WSMP</b>	WAVE Short Message Protocol

## Acknowledgment

This thesis would not have been possible without the assistance, inspiration, and encouragement of many people. I hereby would like to express my sincere thanks to all of them.

First of all, I would like to express my sincere gratitude to my promoter Prof. Sonia Heemstra de Groot for her continuous support, for her patience, motivation, immense knowledge and for helping me to grow as a researcher. Your guidance and support have helped me through the ups and downs of Ph.D.-life. I would like to thank my supervisors Dr.Hong Li and Prof. Ignas Niemegeers for always finding time for me: be it reading my not-so-well-written chapters or participate in our frequent brainstorming sessions. They have given me a lot of suggestions on improving the skills like the reasoning of ideas, writing research papers, etc. They have given me the freedom to pursue various projects without objection. They always motivated and steered me in the right direction. It is an honor to work with them.

My special gratitude goes to my committee members: Prof. Renato Lo Cigno, Prof. Geert Heijenk, Dr. Jeroen Hoebeke and Prof. Twan Basten. Thank you for taking the time to read and provide insightful comments to my work.

I would like to thank my colleagues from NXP Alessio, Arie and Kees for our regular discussions, which kept me up-to-date on various standardization and industrial activities going on around the world. I would like to thank Qing, Roshan and Diptanil who made me feel at home from the moment I started my Ph.D. I thank them for the countless coffee session we had discussing work and many other topics. I would like to thank Gaurav, Apoorva and Snorri for keeping me on my toes with your witty questions on my research. I would like to thank my office-mates: Maria, Haotian, Da, Ailee, Dimitrios, Xuebing, Luis, Mortaza and Mahir with whom I have shared a lot of joyful time.

Last but not least I want to thank my family for their support throughout these years. If I was even able to start a Ph.D., I owe it to my father Basavaraj, my mother Sulakshana, my brother Shravan and my uncle Pradeep for everything they did to get me here. They have always supported me to pursue my goals. To

## ACKNOWLEDGEMENT

---

my beloved daughter Tarini, I would like to express my thanks for always cheering me up. Finally, I want to thank my wife Manasa for all the sacrifices she made to let me free to focus on my Ph.D. She always wanted the best for me, and pushed me further, even when I tried to stop. Thank you for every day, every hour, every minute, and for being the love of my life.

## Curriculum vitae

Chetan Belagal Math was born in Ramdurg, India, on April 14, 1990. He received his B.E. degree on Electronics and Communication Engineering from University Visvesvaraya College of Engineering, Bangalore, India, on 2011. He earned his M.Tech degree on Telecommunication Systems Engineering from Indian Institute of Technology Kharagpur (IIT KGP), India, on 2014. During his M.Tech he was a recipient of the Ministry of Human Resource and Development (MHRD) scholarship.



On July 2014, he started working towards his PhD degree at Electro-Optical Communication (ECO) group at Eindhoven University of Technology (TU/e), under supervision of Prof. Sonia Heemstra de Groot. His research work was funded under TU/e Impuls program, a strategic cooperation between NXP Semiconductors and Eindhoven University of Technology.

During his PhD, Chetan has co-authored over 15 publications (including journals and conferences) and 4 patents (filed), and supervised 6 Master students. His research interests include Intelligent Transportation Systems, Wireless and Vehicular Communications. He is an active member of the scientific community and as served as a reviewer of various international journals and conferences.